

Supplementary File

The Cloud Factory II: Turbulent Line-widths of Resolved Molecular Clouds in a Galactic Potential

Andrés Izquierdo, Rowan Smith

October 2019

Chapter 1

**Potential-dominated → Galaxy Potential, No
Self-Gravity, Random Supernovae**

1.1 Cloud A₀

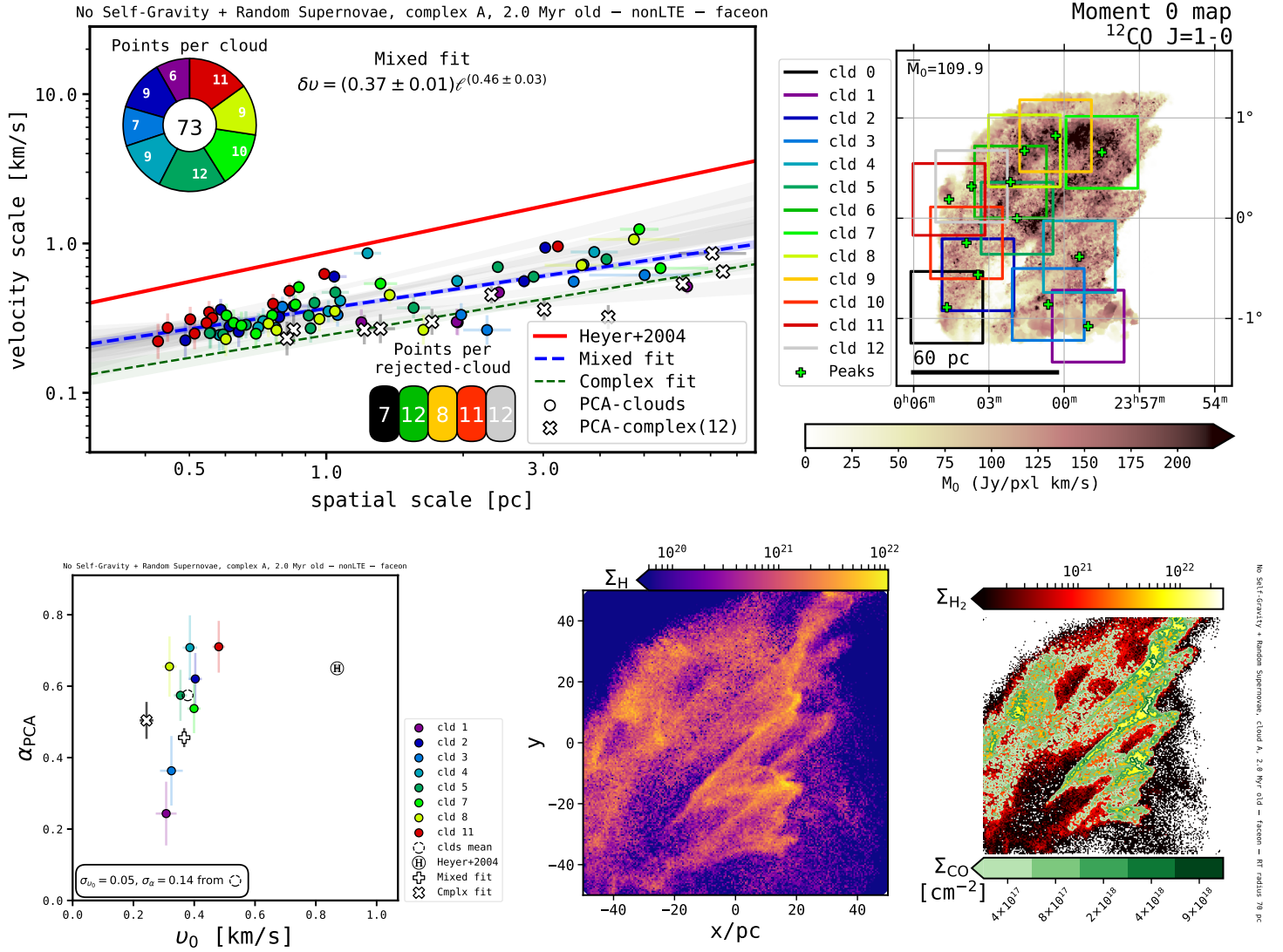


Figure 1.1: Principal component analysis and column densities from Cloud Complex: A₀; physical scenario: Potential-dominated → Galaxy Potential, No Self-Gravity, Random Supernovae; snapshot time: 2.0 Myr; orientation: face-on; RT mode: nonLTE. See full captions in figures on the main manuscript.

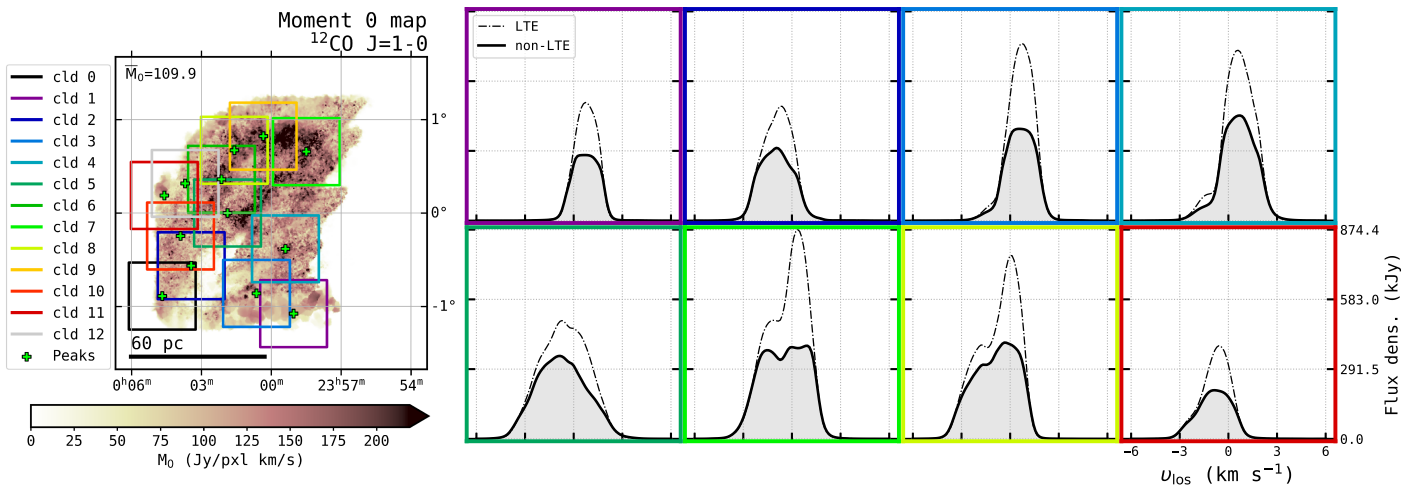


Figure 1.1: (continued) LTE (dashed) and non-LTE (solid) ^{12}CO $J=1-0$ line profiles from non-rejected molecular cloud portions.

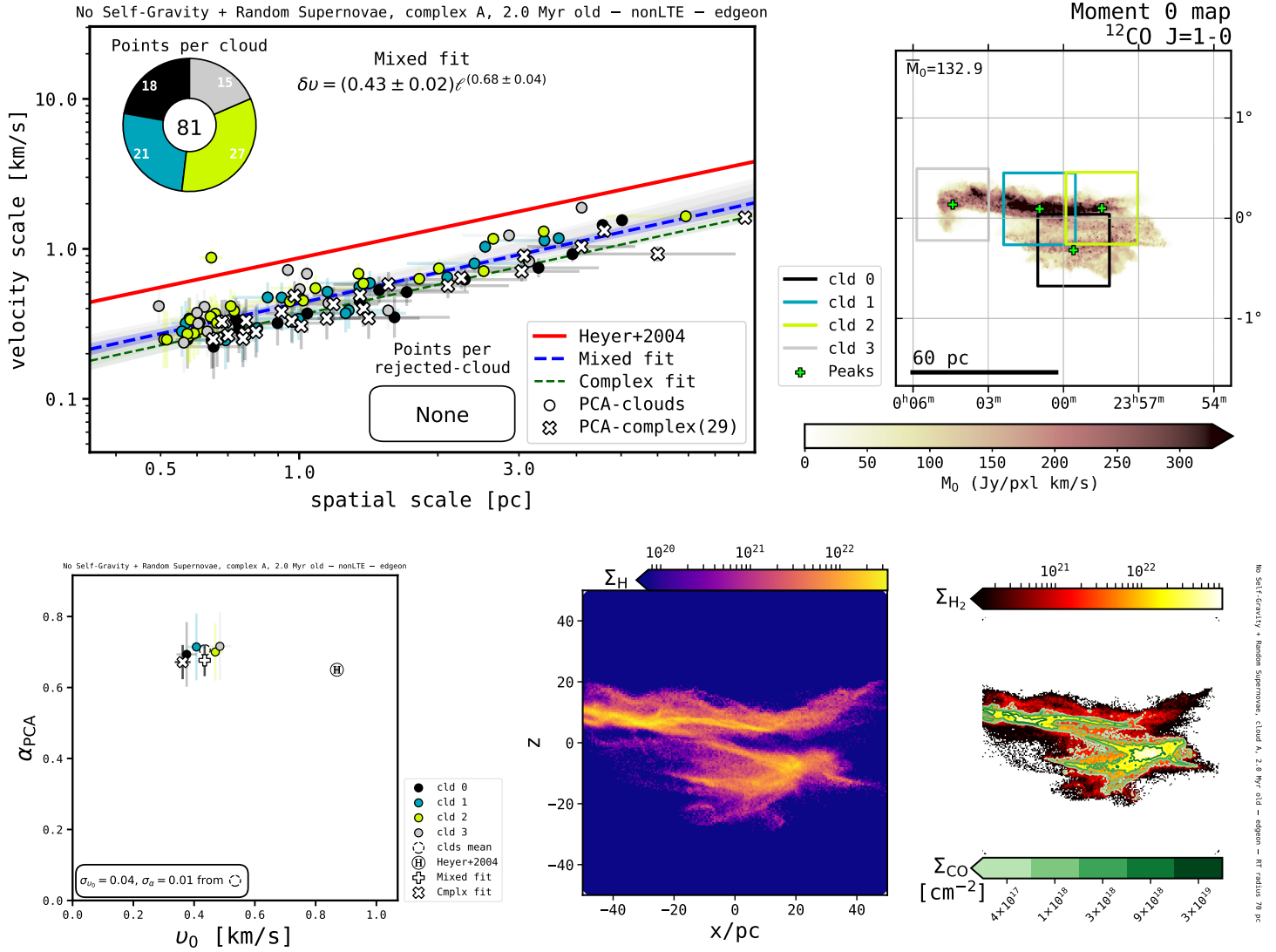


Figure 1.2: Principal component analysis and column densities from Cloud Complex: A₀; physical scenario: Potential-dominated → Galaxy Potential, No Self-Gravity, Random Supernovae; snapshot time: 2.0 Myr; orientation: edge-on $_{\phi=0^\circ}$; RT mode: nonLTE. See full captions in figures on the main manuscript.

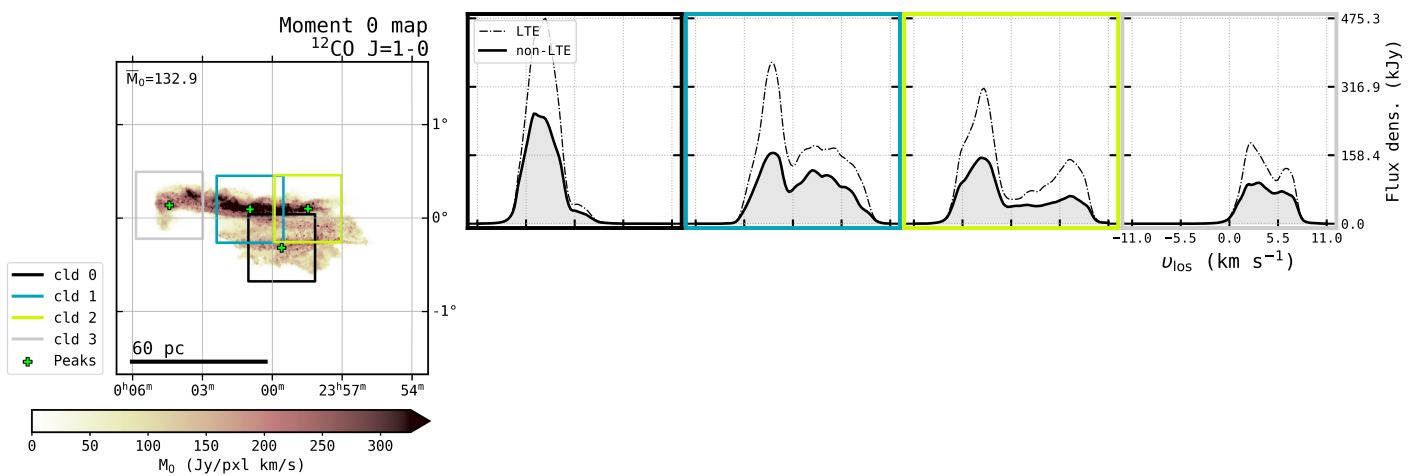


Figure 1.2: (continued) LTE (dashed) and non-LTE (solid) ^{12}CO $J=1-0$ line profiles from non-rejected molecular cloud portions.

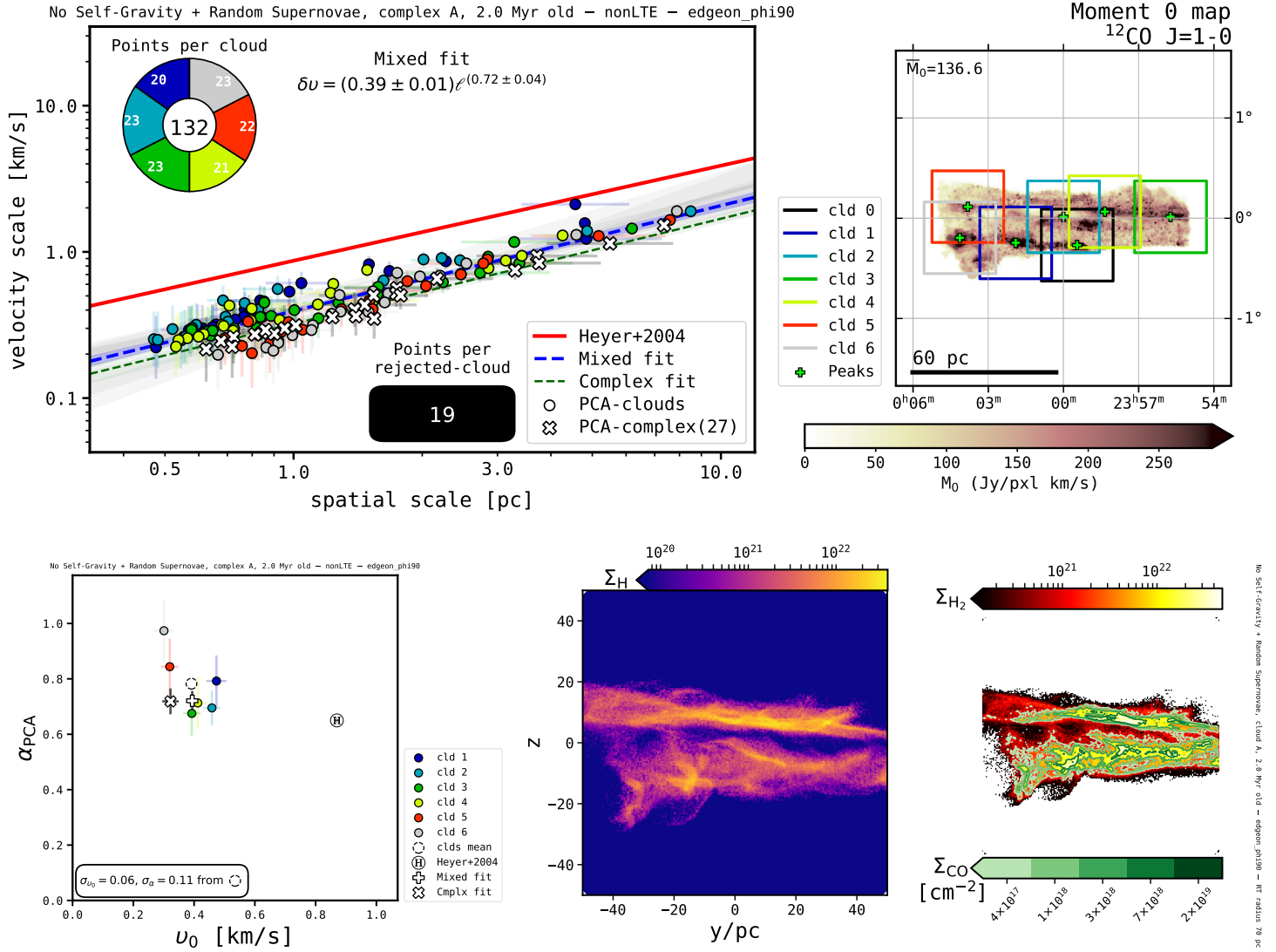


Figure 1.3: Principal component analysis and column densities from Cloud Complex: A_0 ; physical scenario: Potential-dominated \rightarrow Galaxy Potential, No Self-Gravity, Random Supernovae; snapshot time: 2.0 Myr; orientation: edge-on $_{\phi=90^\circ}$; RT mode: nonLTE. See full captions in figures on the main manuscript.

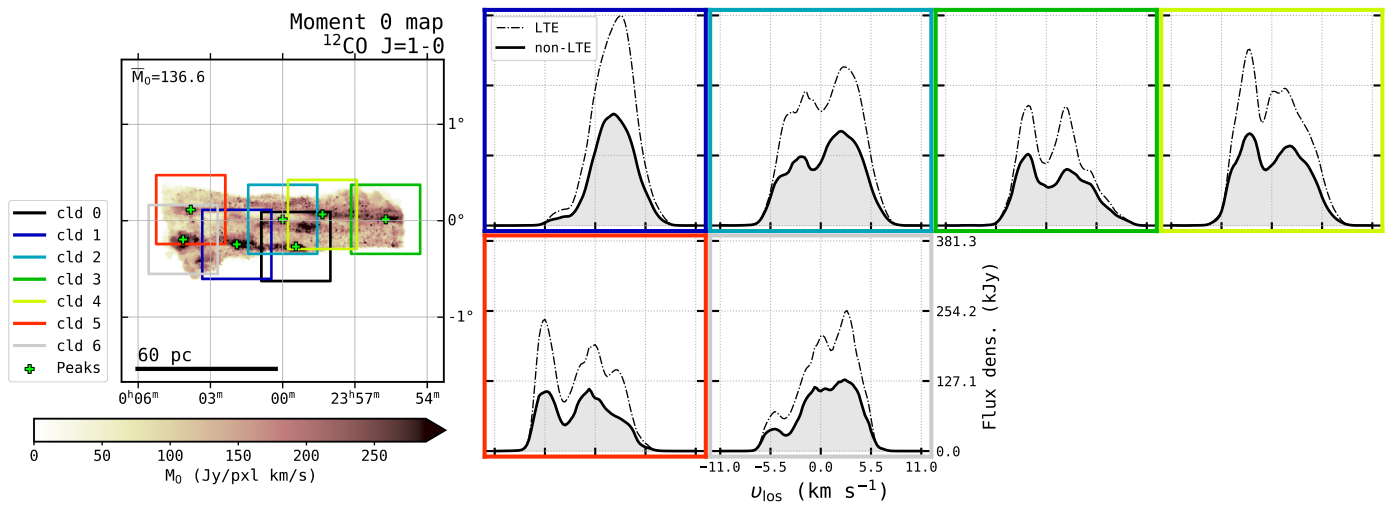


Figure 1.3: (continued) LTE (dashed) and non-LTE (solid) ^{12}CO $J=1-0$ line profiles from non-rejected molecular cloud portions.

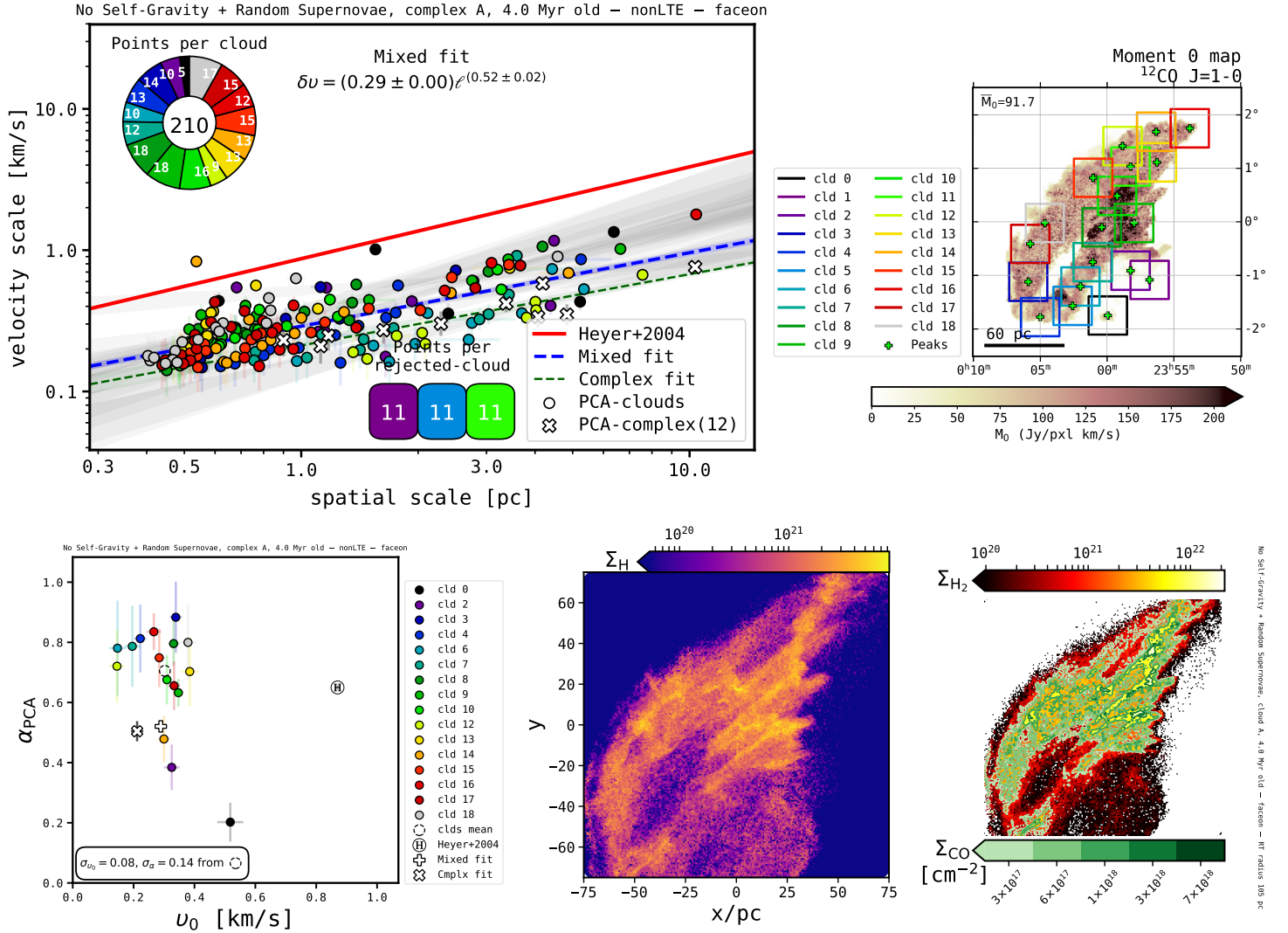


Figure 1.4: Principal component analysis and column densities from Cloud Complex: A₀; physical scenario: Potential-dominated → Galaxy Potential, No Self-Gravity, Random Supernovae; snapshot time: 4.0 Myr; orientation: face-on; RT mode: nonLTE. See full captions in figures on the main manuscript.

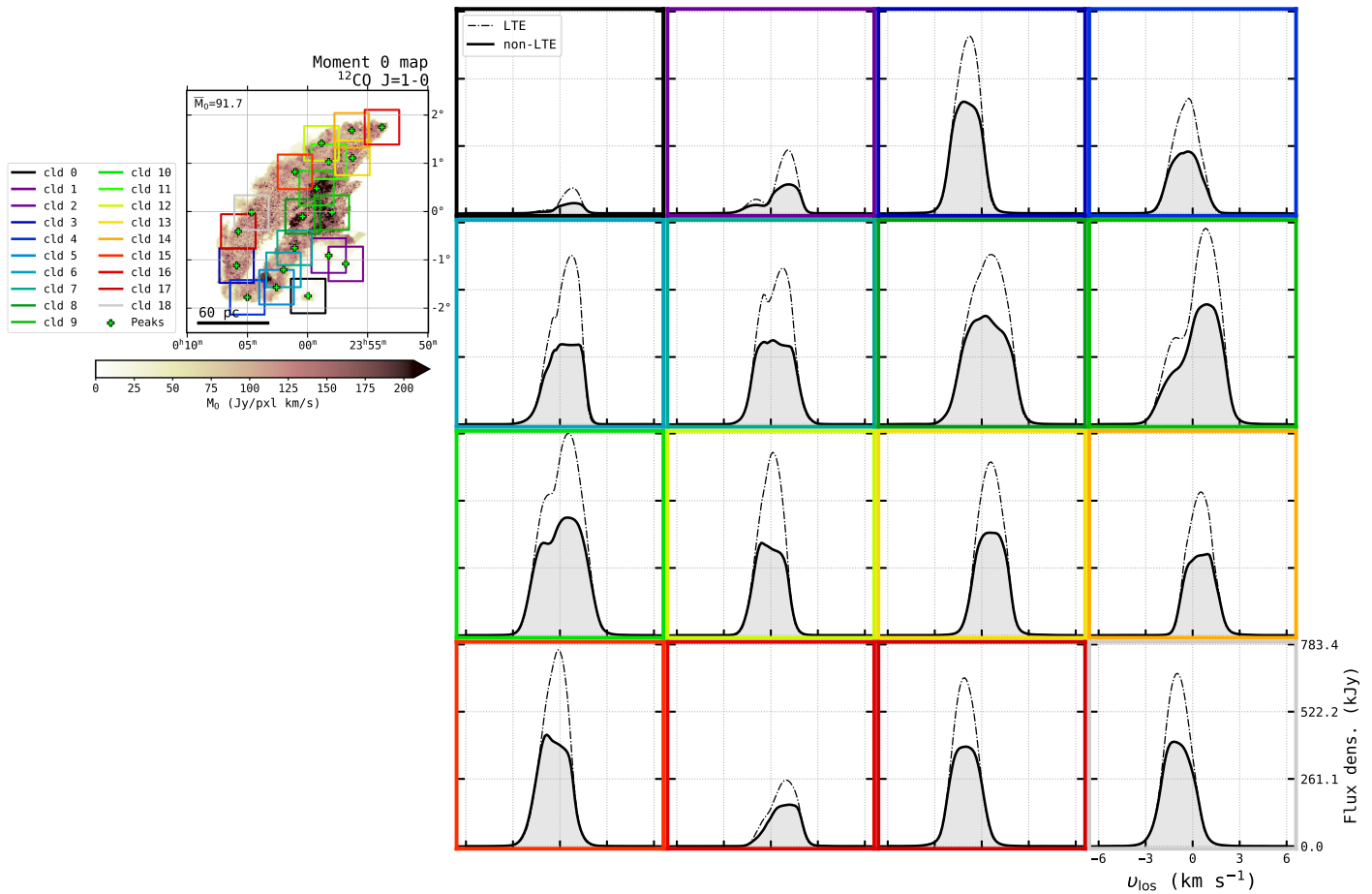


Figure 1.4: (continued) LTE (dashed) and non-LTE (solid) ^{12}CO $J=1-0$ line profiles from non-rejected molecular cloud portions.

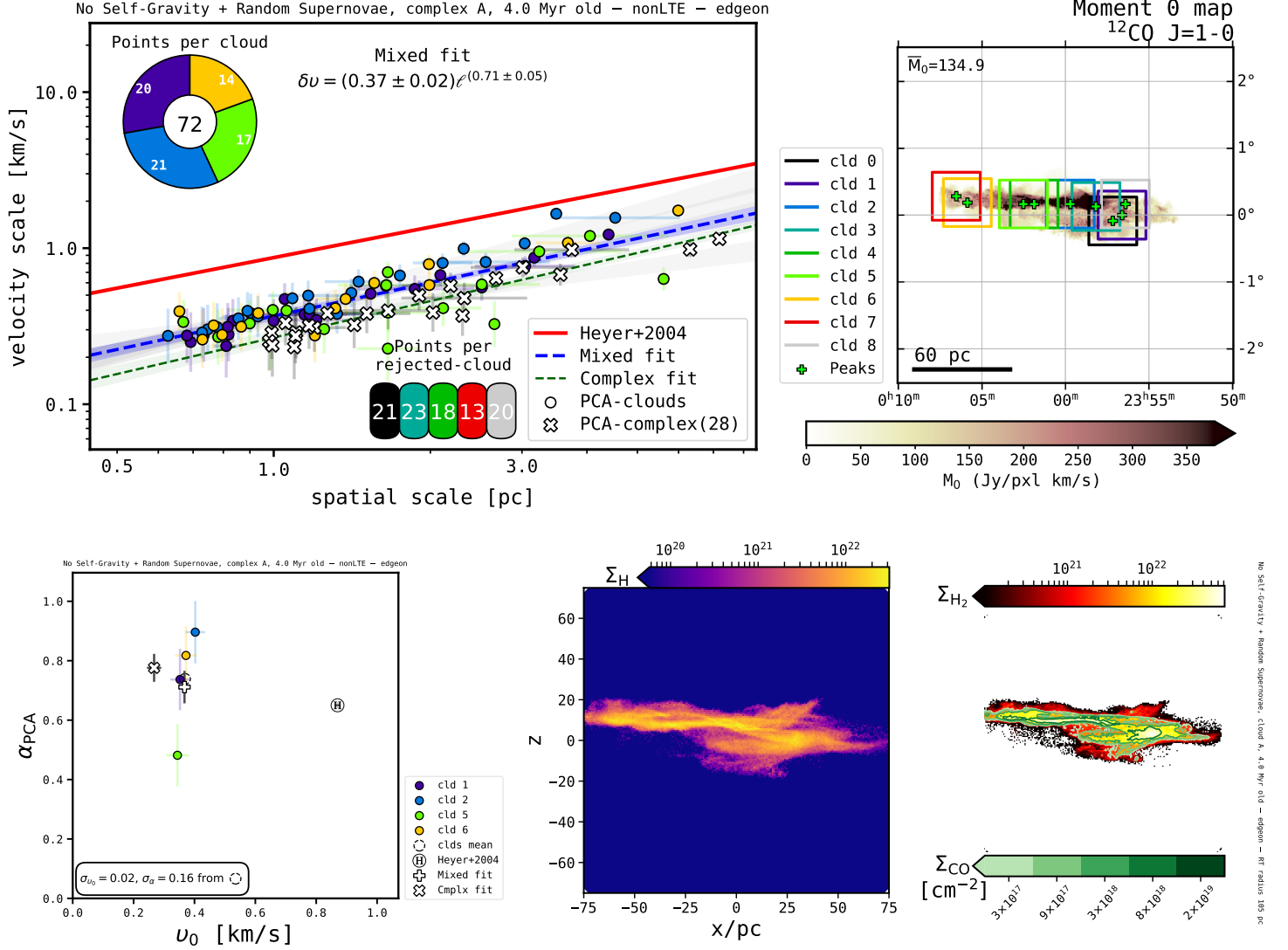


Figure 1.5: Principal component analysis and column densities from Cloud Complex: A₀; physical scenario: Potential-dominated → Galaxy Potential, No Self-Gravity, Random Supernovae; snapshot time: 4.0 Myr; orientation: edge-on $_{\phi=0^\circ}$; RT mode: nonLTE. See full captions in figures on the main manuscript.

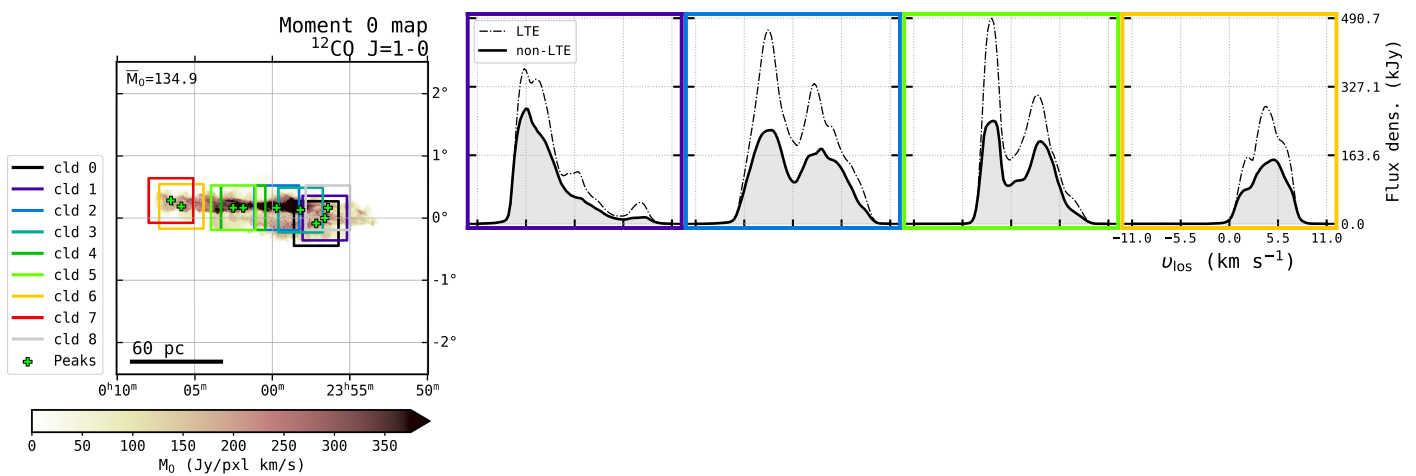


Figure 1.5: (continued) LTE (dashed) and non-LTE (solid) ^{12}CO $J=1-0$ line profiles from non-rejected molecular cloud portions.

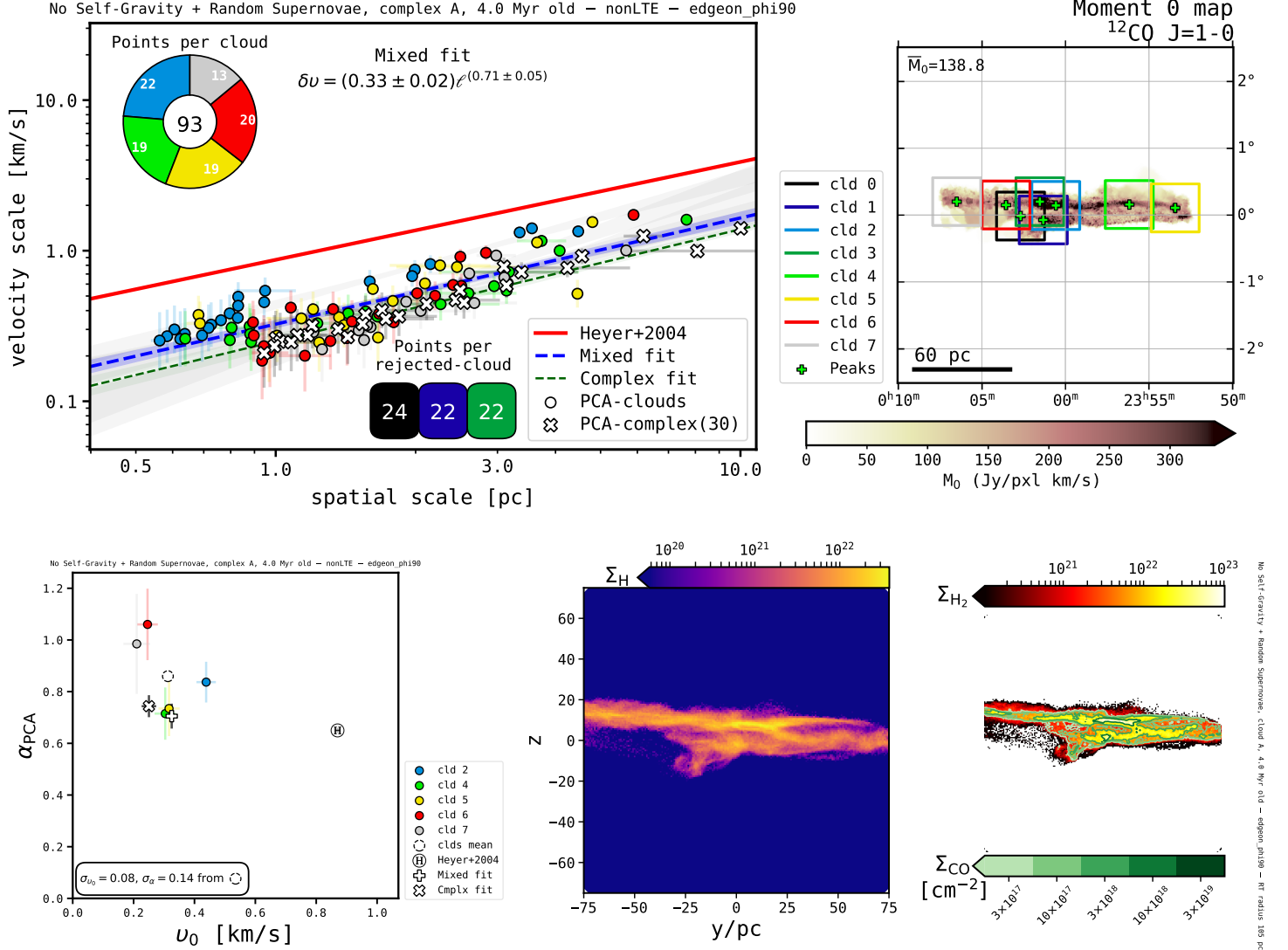


Figure 1.6: Principal component analysis and column densities from Cloud Complex: A₀; physical scenario: Potential-dominated → Galaxy Potential, No Self-Gravity, Random Supernovae; snapshot time: 4.0 Myr; orientation: edge-on $_{\phi=90^\circ}$; RT mode: nonLTE. See full captions in figures on the main manuscript.

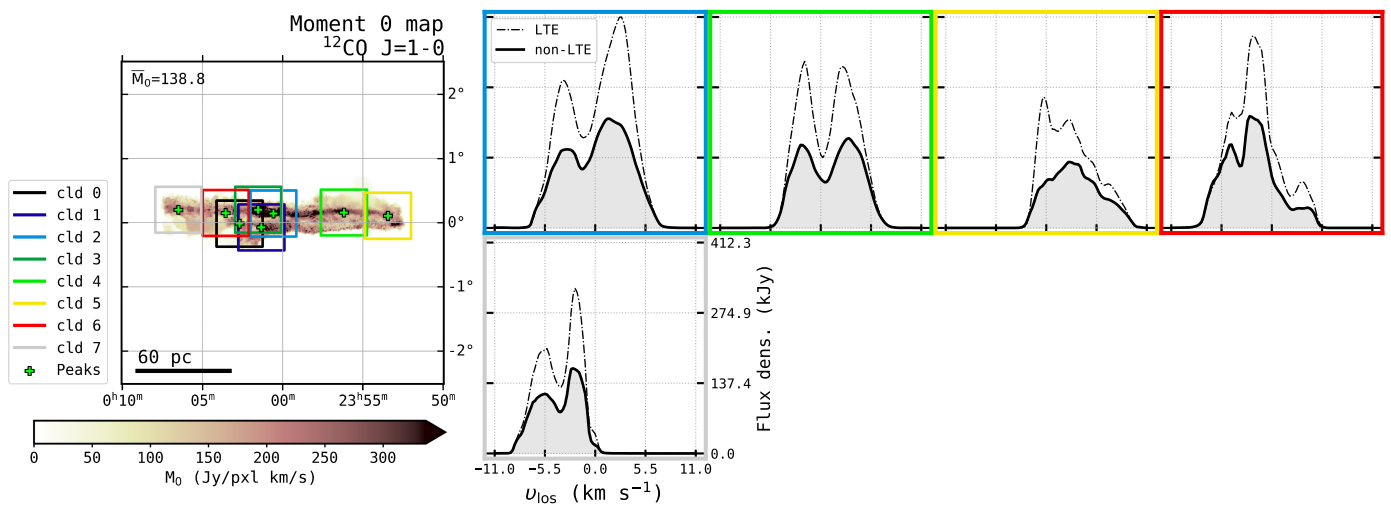


Figure 1.6: (continued) LTE (dashed) and non-LTE (solid) ^{12}CO $J=1-0$ line profiles from non-rejected molecular cloud portions.

1.2 Cloud B_0

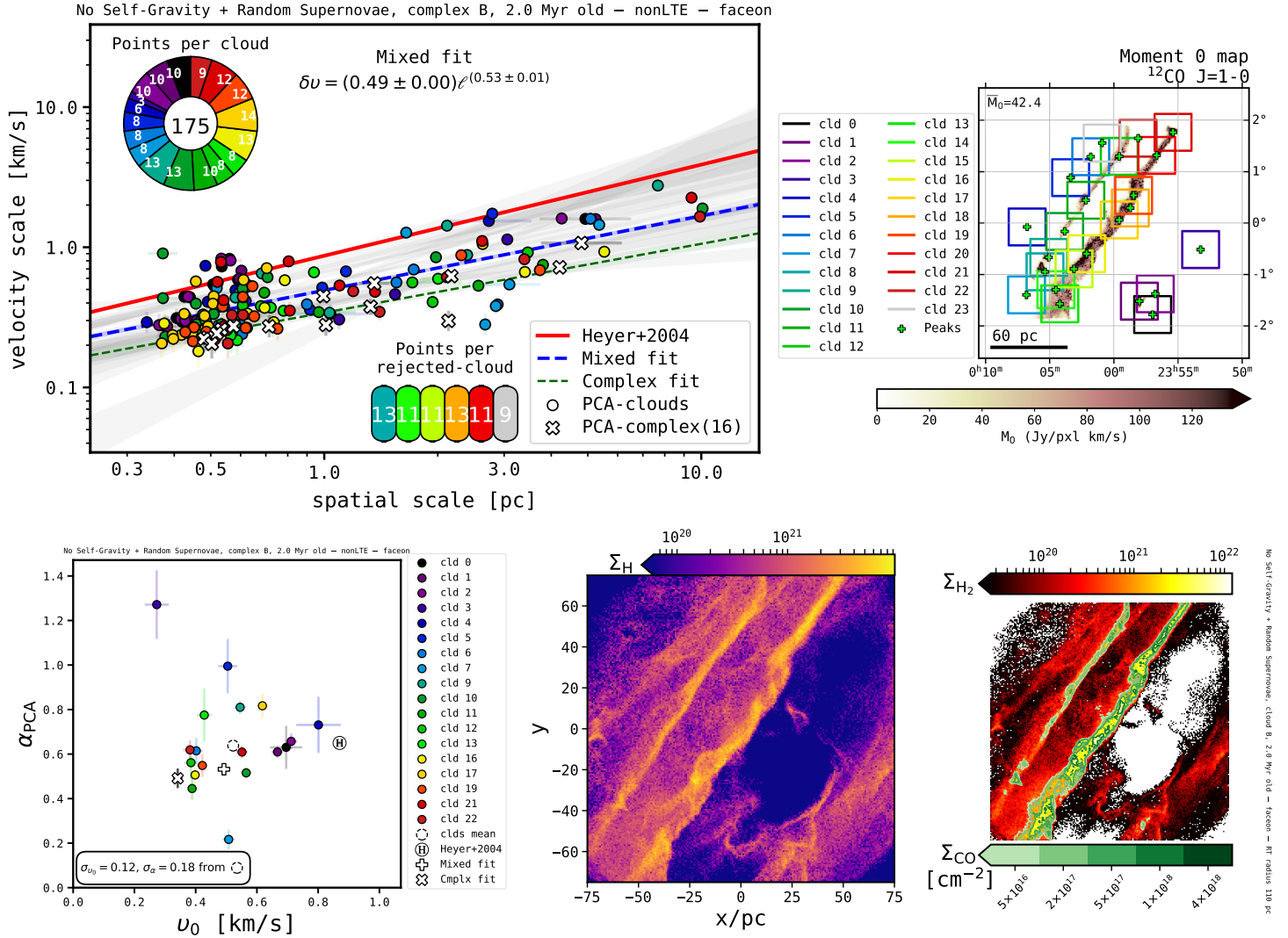


Figure 1.7: Principal component analysis and column densities from Cloud Complex: B₀; physical scenario: Potential-dominated → Galaxy Potential, No Self-Gravity, Random Supernovae; snapshot time: 2.0 Myr; orientation: face-on; RT mode: nonLTE. See full captions in figures on the main manuscript.

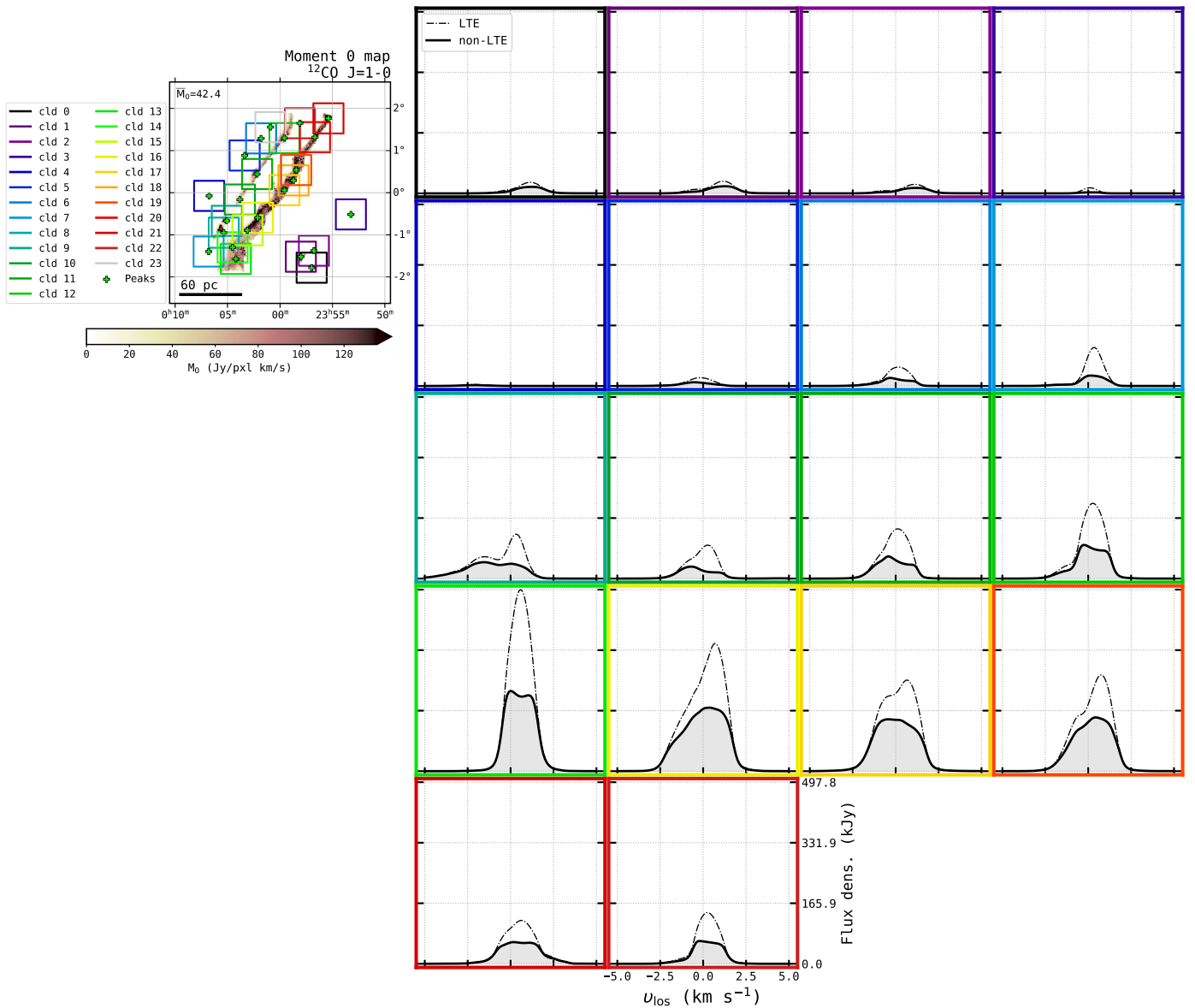


Figure 1.7: (continued) LTE (dashed) and non-LTE (solid) ^{12}CO $J=1-0$ line profiles from non-rejected molecular cloud portions.

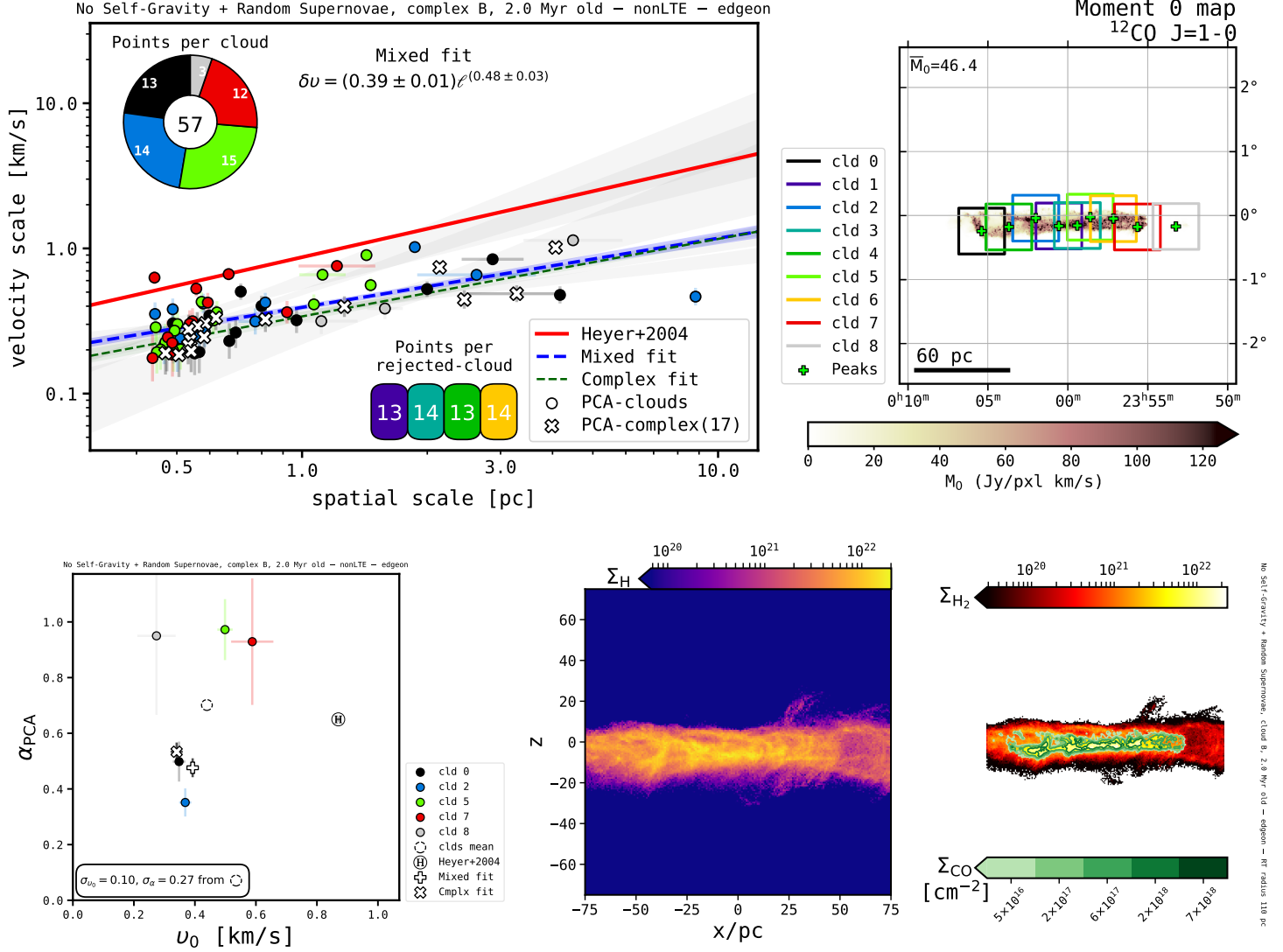


Figure 1.8: Principal component analysis and column densities from Cloud Complex: B₀; physical scenario: Potential-dominated → Galaxy Potential, No Self-Gravity, Random Supernovae; snapshot time: 2.0 Myr; orientation: edge-on $_{\phi=0^\circ}$; RT mode: nonLTE. See full captions in figures on the main manuscript.

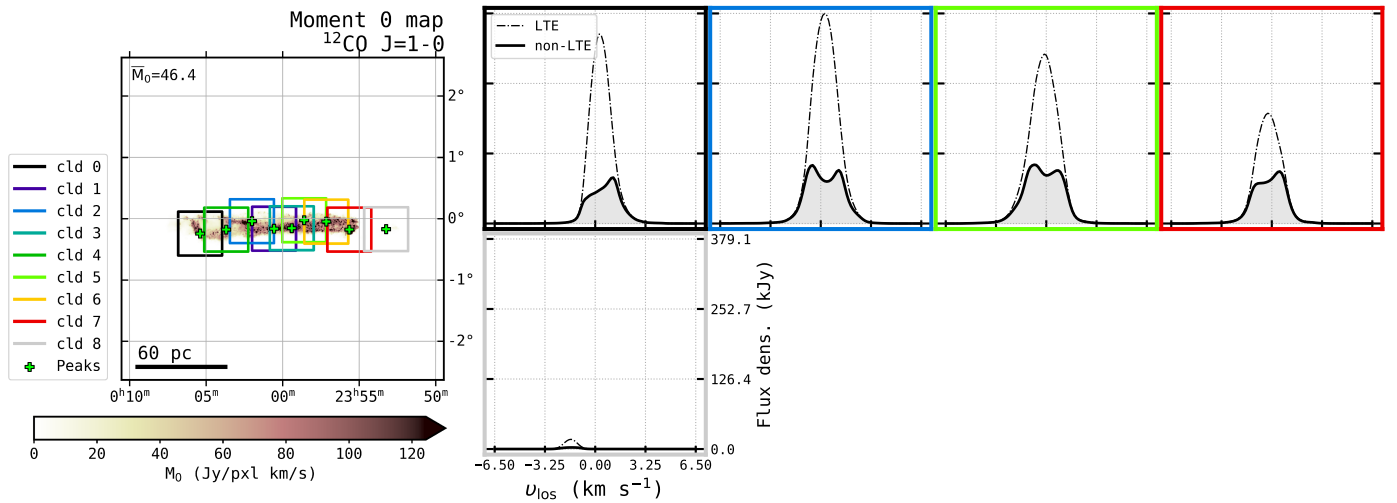


Figure 1.8: (continued) LTE (dashed) and non-LTE (solid) ^{12}CO $J=1-0$ line profiles from non-rejected molecular cloud portions.

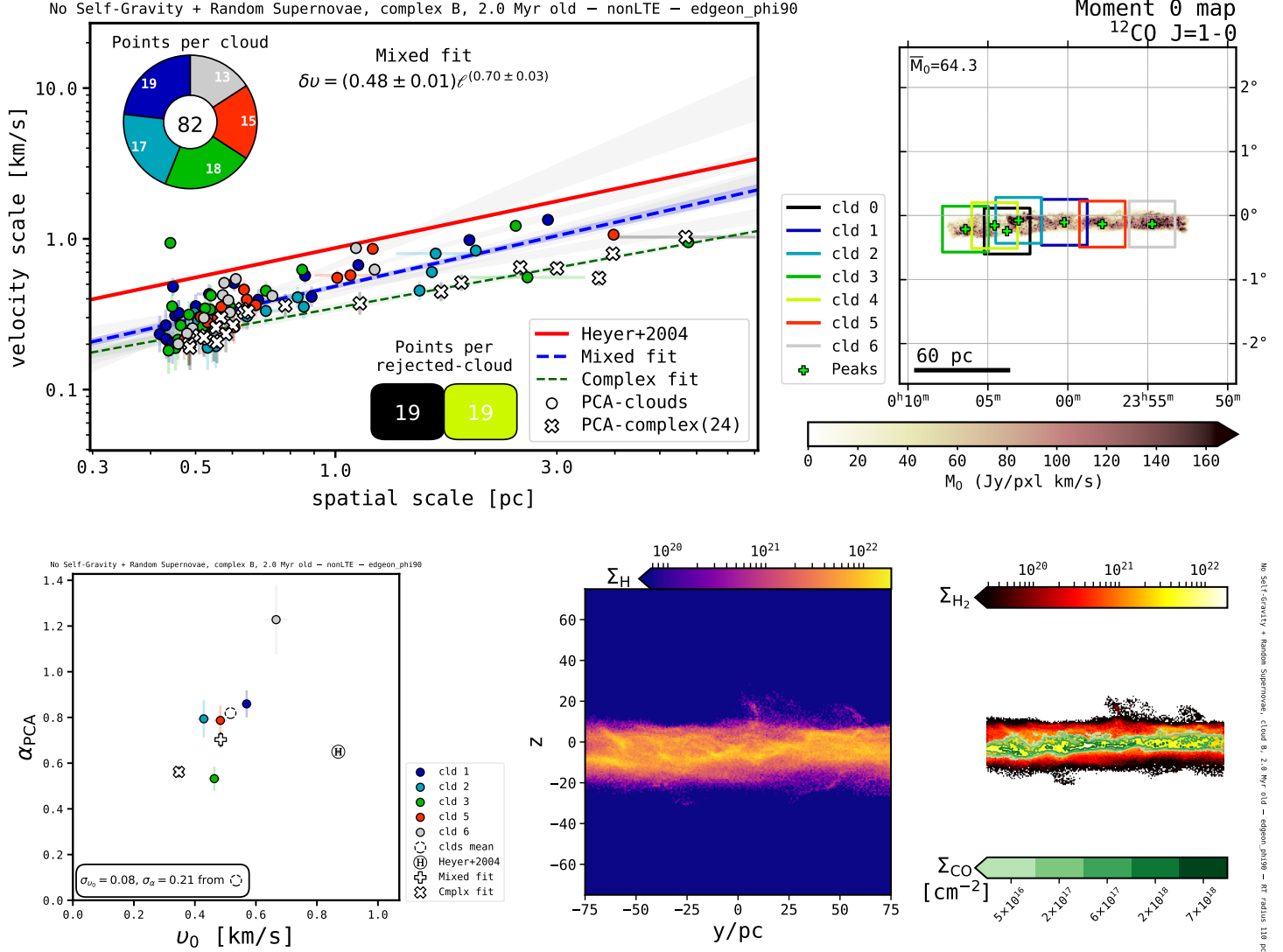


Figure 1.9: Principal component analysis and column densities from Cloud Complex: B₀; physical scenario: Potential-dominated → Galaxy Potential, No Self-Gravity, Random Supernovae; snapshot time: 2.0 Myr; orientation: edge-on $_{\phi=90^\circ}$; RT mode: nonLTE. See full captions in figures on the main manuscript.

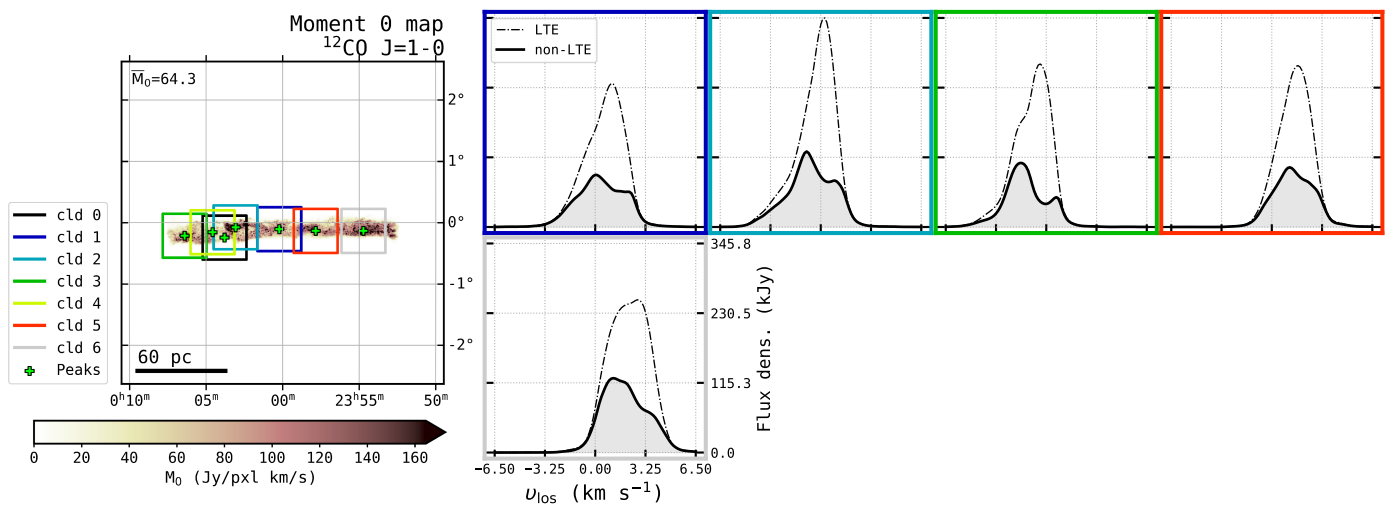


Figure 1.9: (continued) LTE (dashed) and non-LTE (solid) ^{12}CO $J=1-0$ line profiles from non-rejected molecular cloud portions.

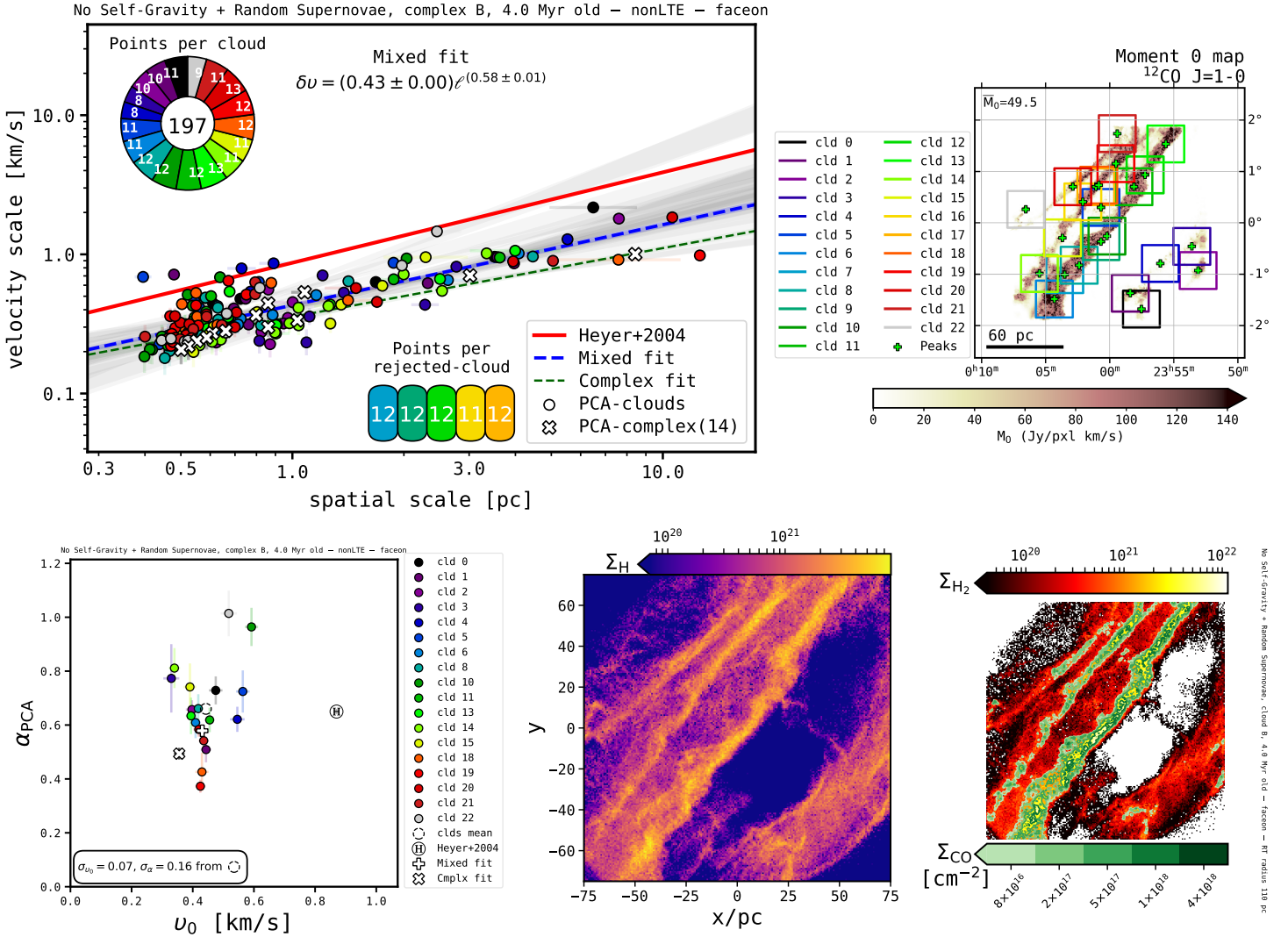


Figure 1.10: Principal component analysis and column densities from Cloud Complex: B₀; physical scenario: Potential-dominated → Galaxy Potential, No Self-Gravity, Random Supernovae; snapshot time: 4.0 Myr; orientation: face-on; RT mode: nonLTE. See full captions in figures on the main manuscript.

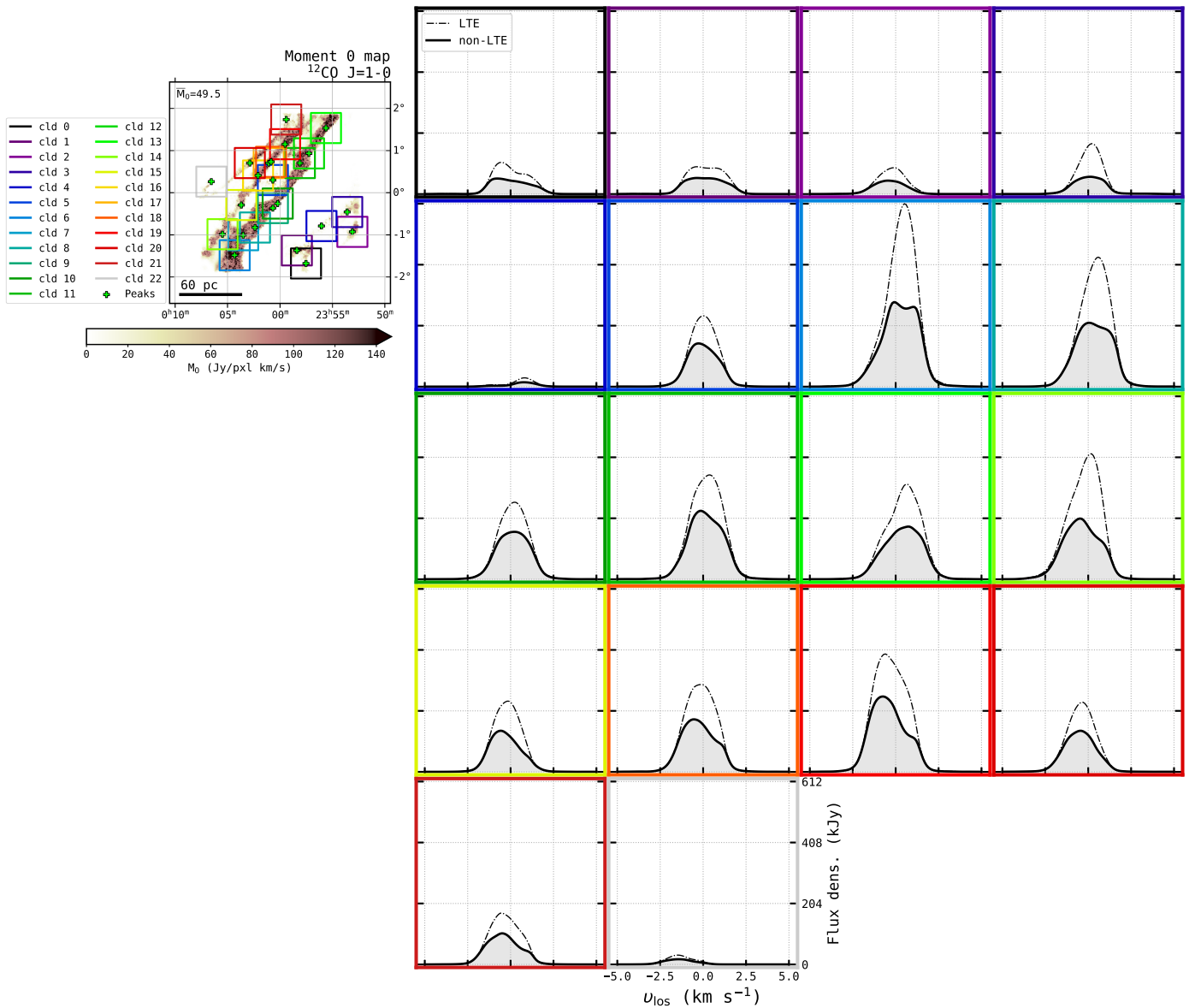


Figure 1.10: (continued) LTE (dashed) and non-LTE (solid) ^{12}CO $J=1-0$ line profiles from non-rejected molecular cloud portions.

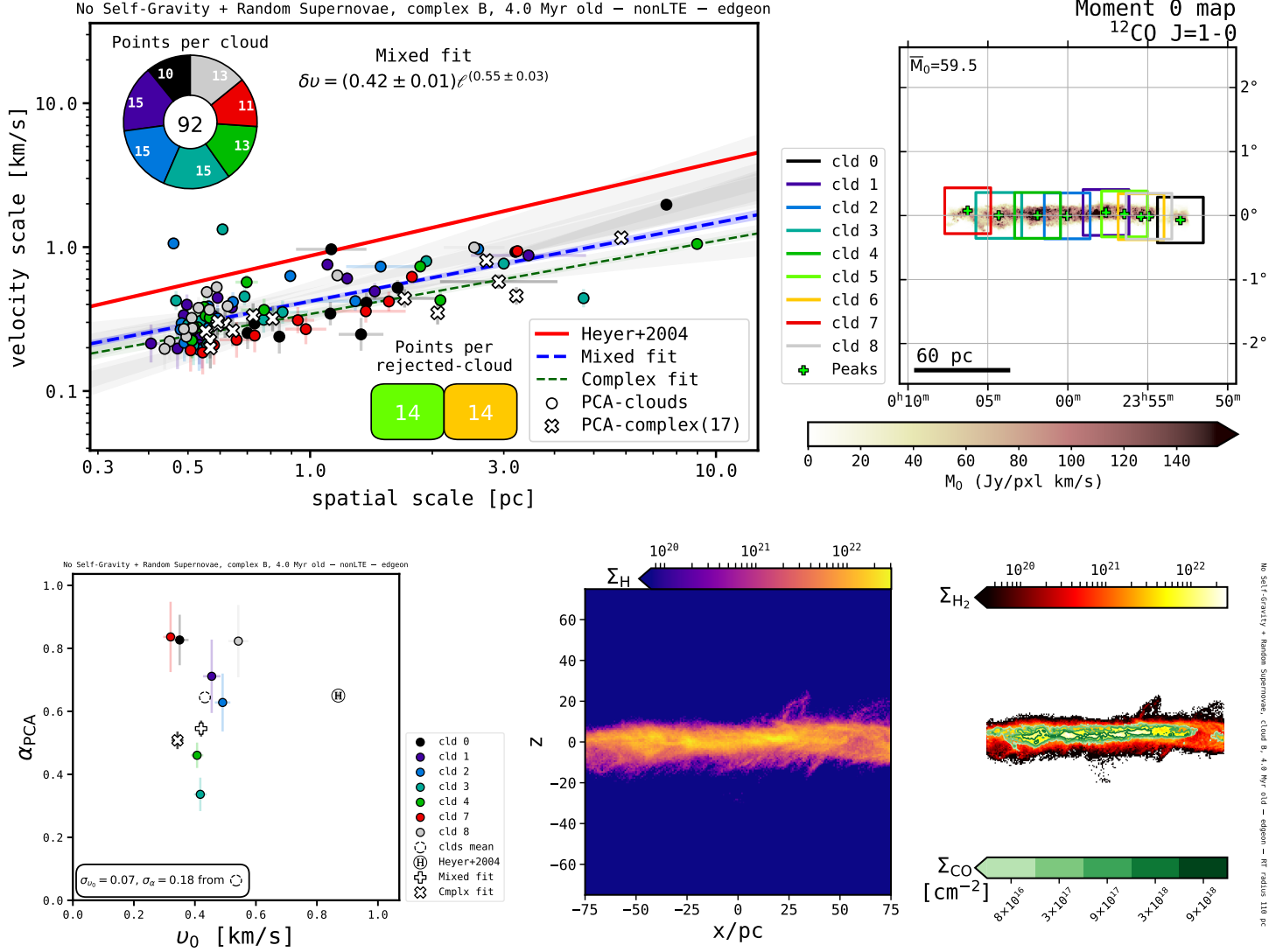


Figure 1.11: Principal component analysis and column densities from Cloud Complex: B₀; physical scenario: Potential-dominated → Galaxy Potential, No Self-Gravity, Random Supernovae; snapshot time: 4.0 Myr; orientation: edge-on_{φ=0°}; RT mode: nonLTE. See full captions in figures on the main manuscript.

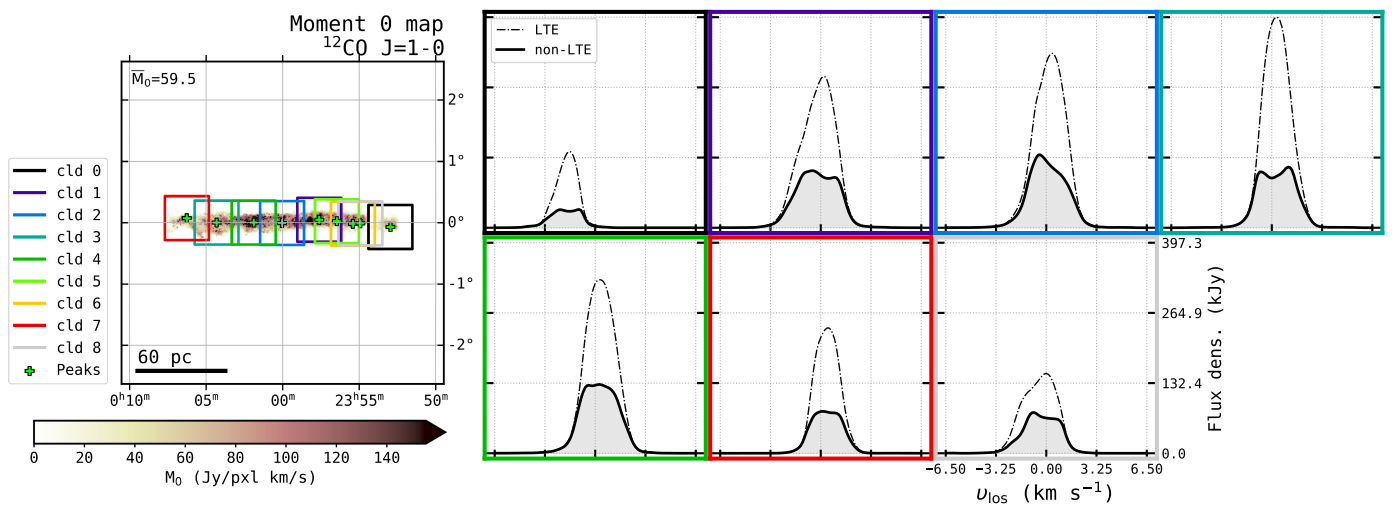


Figure 1.11: (continued) LTE (dashed) and non-LTE (solid) ^{12}CO $J=1-0$ line profiles from non-rejected molecular cloud portions.

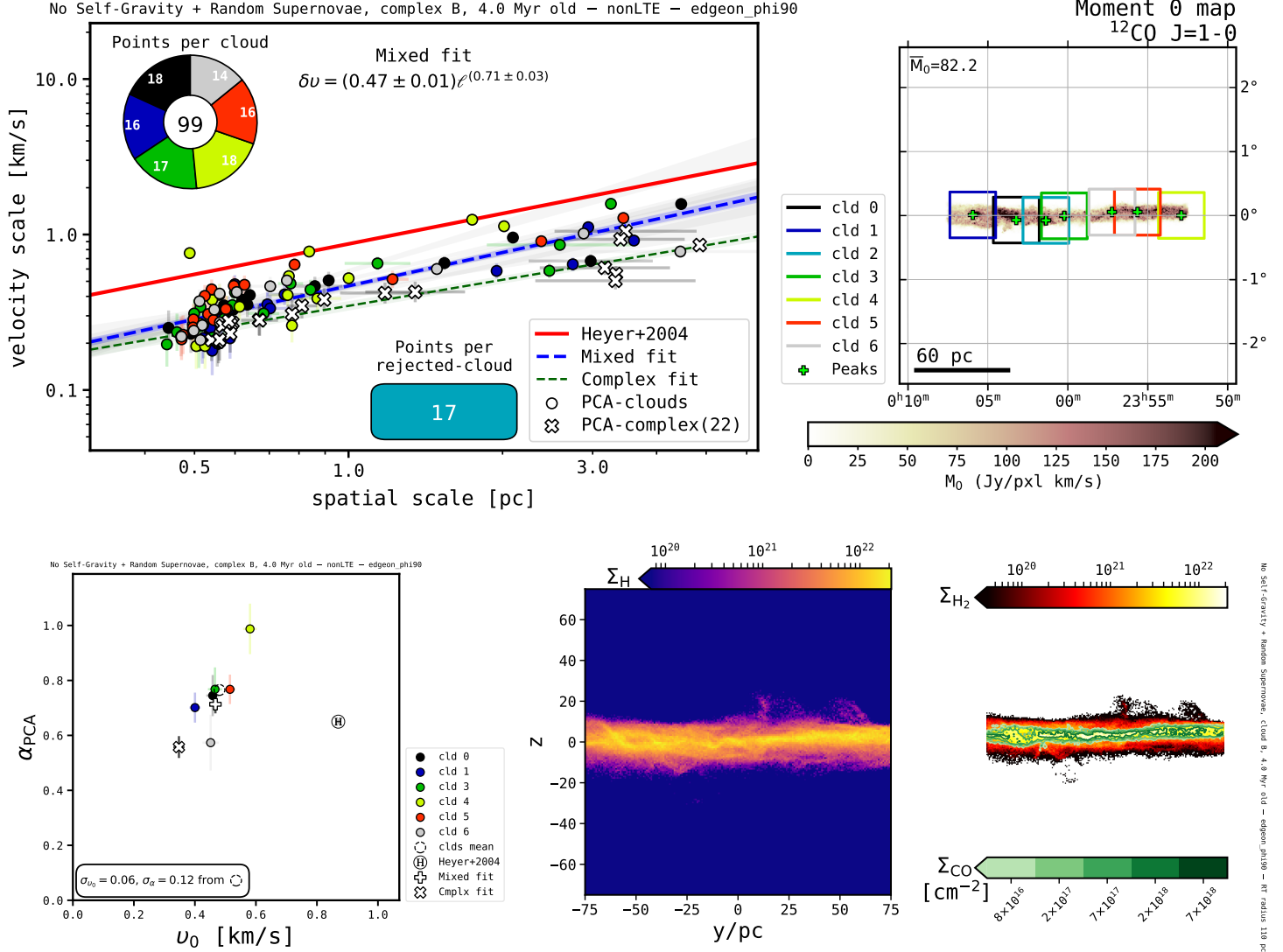


Figure 1.12: Principal component analysis and column densities from Cloud Complex: B₀; physical scenario: Potential-dominated → Galaxy Potential, No Self-Gravity, Random Supernovae; snapshot time: 4.0 Myr; orientation: edge-on $\phi=90^\circ$; RT mode: nonLTE. See full captions in figures on the main manuscript.

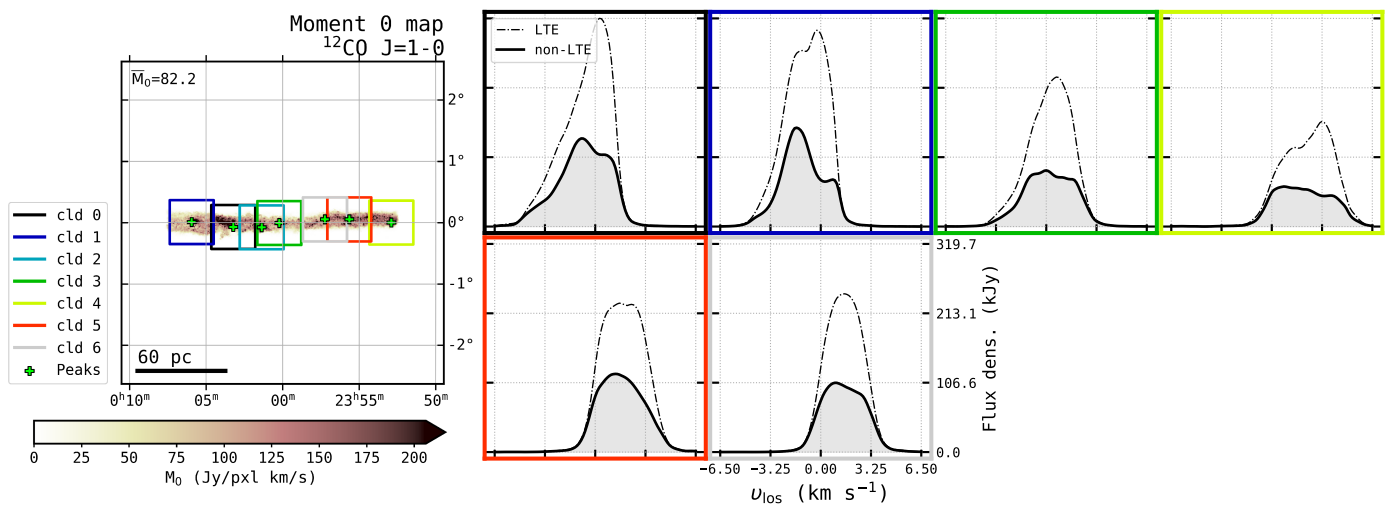


Figure 1.12: (continued) LTE (dashed) and non-LTE (solid) ^{12}CO $J=1-0$ line profiles from non-rejected molecular cloud portions.

Chapter 2

Potential-dominated → Galaxy Potential, Self-Gravity, Random Supernovae

2.1 Cloud A

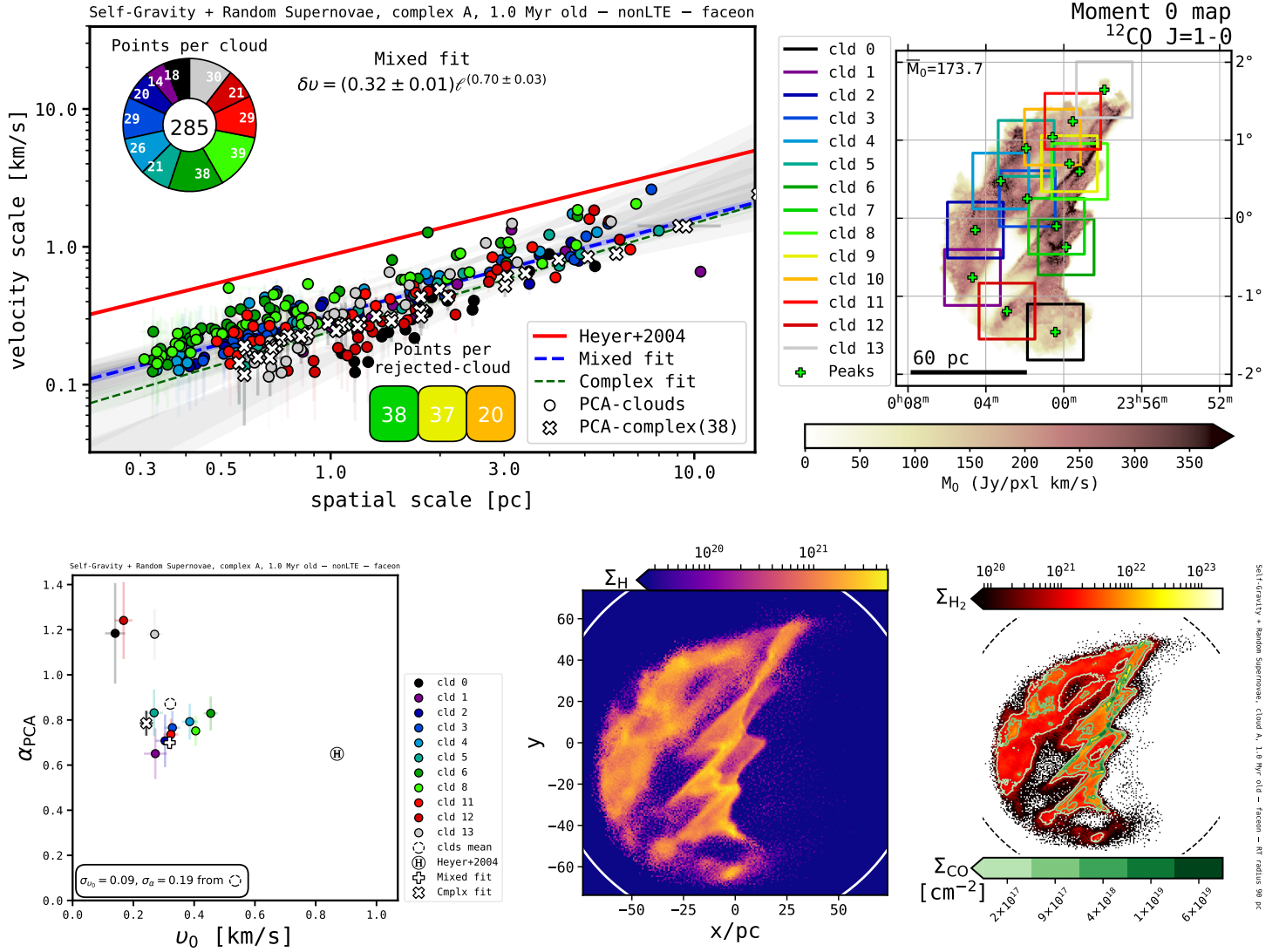


Figure 2.1: Principal component analysis and column densities from Cloud Complex: A; physical scenario: Potential-dominated → Galaxy Potential, Self-Gravity, Random Supernovae; snapshot time: 1.0 Myr; orientation: face-on; RT mode: nonLTE. See full captions in figures on the main manuscript.

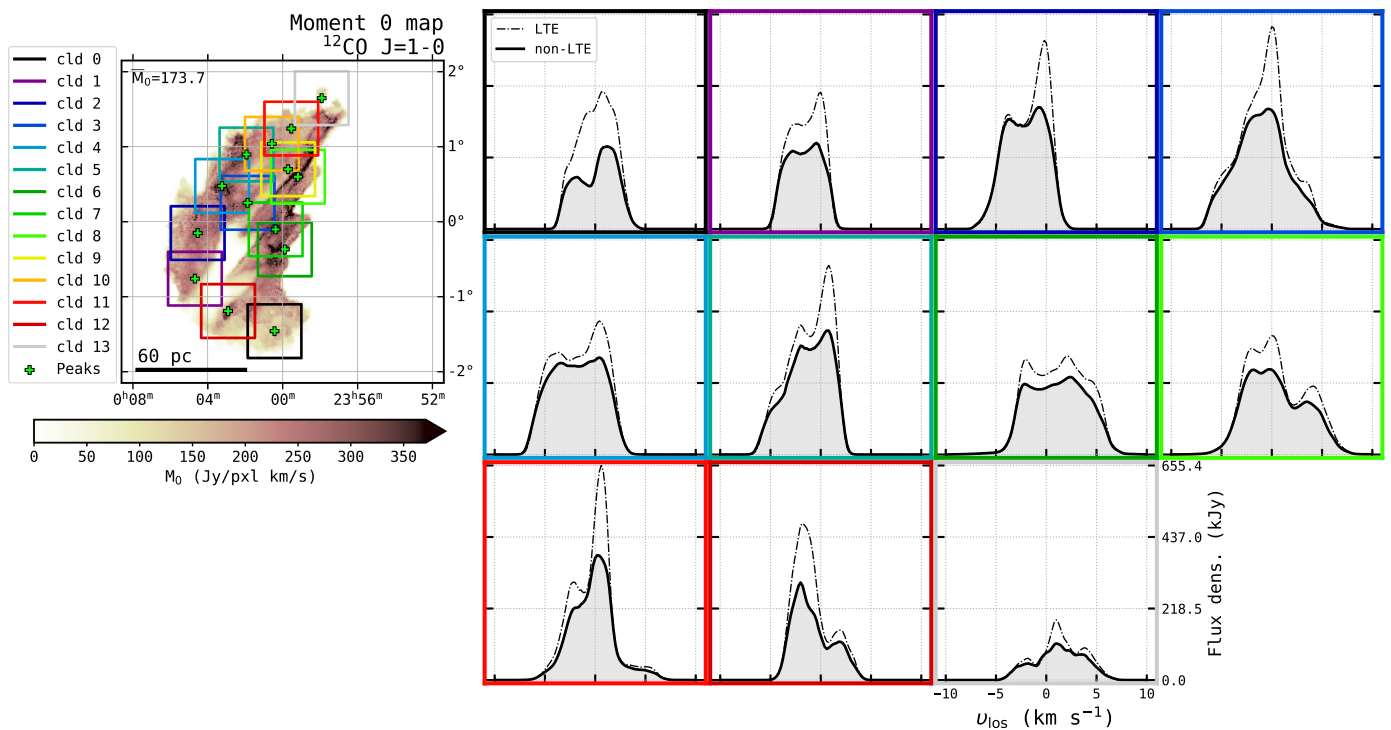


Figure 2.1: (continued) LTE (dashed) and non-LTE (solid) ^{12}CO $J=1-0$ line profiles from non-rejected molecular cloud portions.

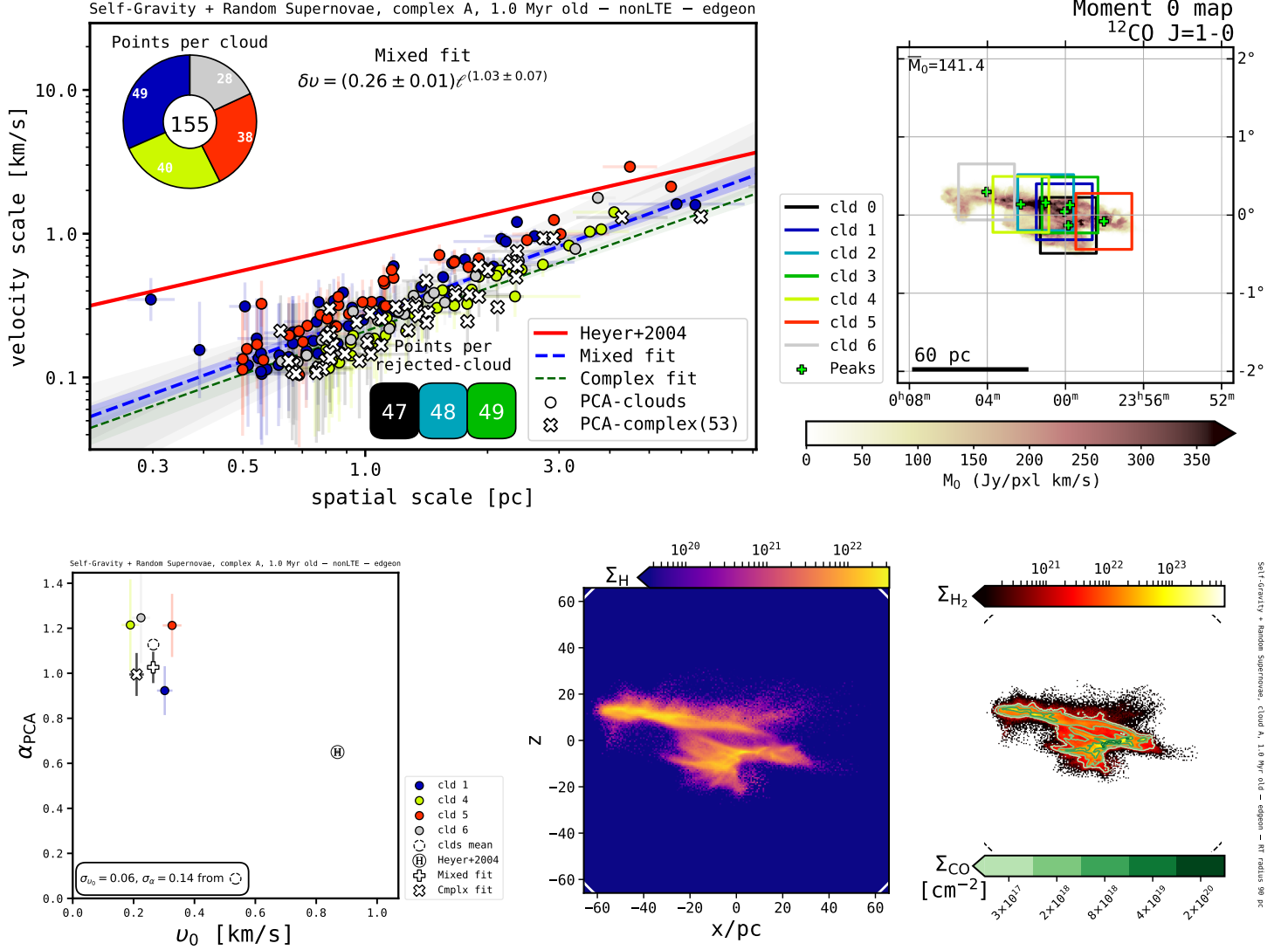


Figure 2.2: Principal component analysis and column densities from Cloud Complex: A; physical scenario: Potential-dominated → Galaxy Potential, Self-Gravity, Random Supernovae; snapshot time: 1.0 Myr; orientation: edge-on $_{\phi=0^\circ}$; RT mode: nonLTE. See full captions in figures on the main manuscript.

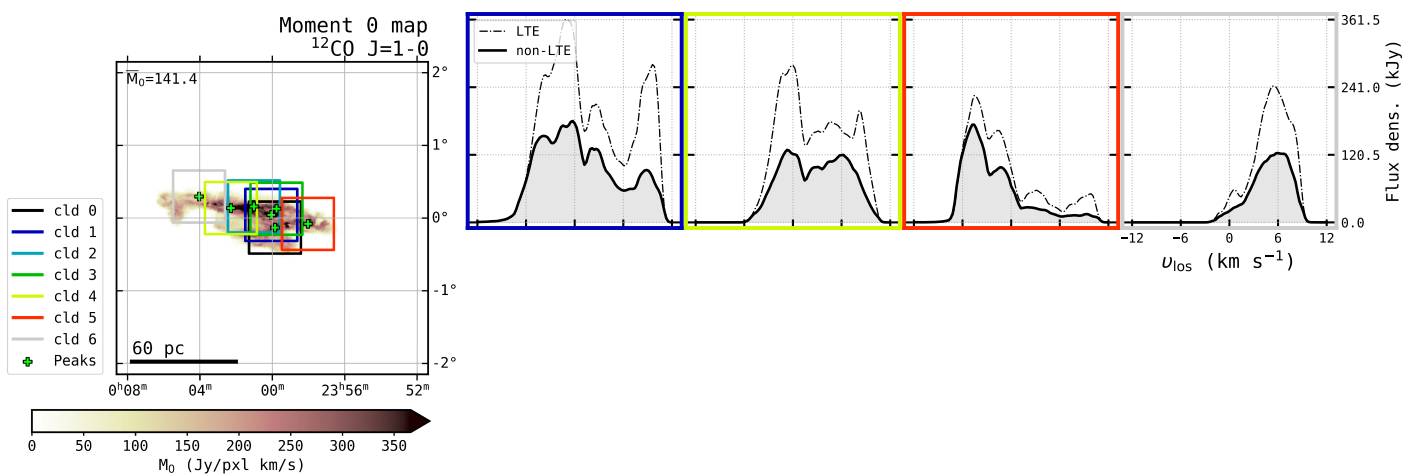


Figure 2.2: (continued) LTE (dashed) and non-LTE (solid) ^{12}CO $J=1-0$ line profiles from non-rejected molecular cloud portions.

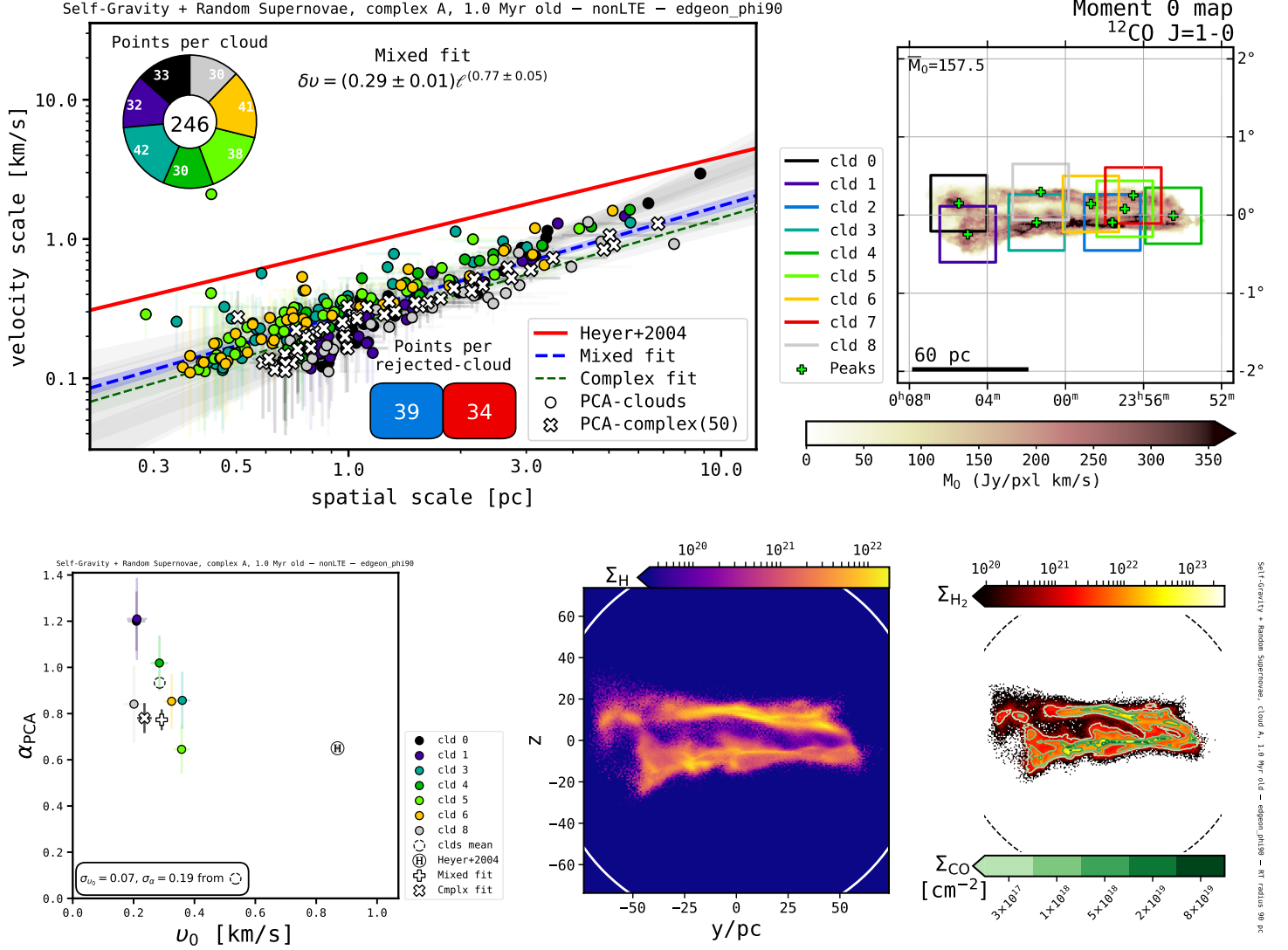


Figure 2.3: Principal component analysis and column densities from Cloud Complex: A; physical scenario: Potential-dominated \rightarrow Galaxy Potential, Self-Gravity, Random Supernovae; snapshot time: 1.0 Myr; orientation: edge-on $\phi=90^\circ$; RT mode: nonLTE. See full captions in figures on the main manuscript.

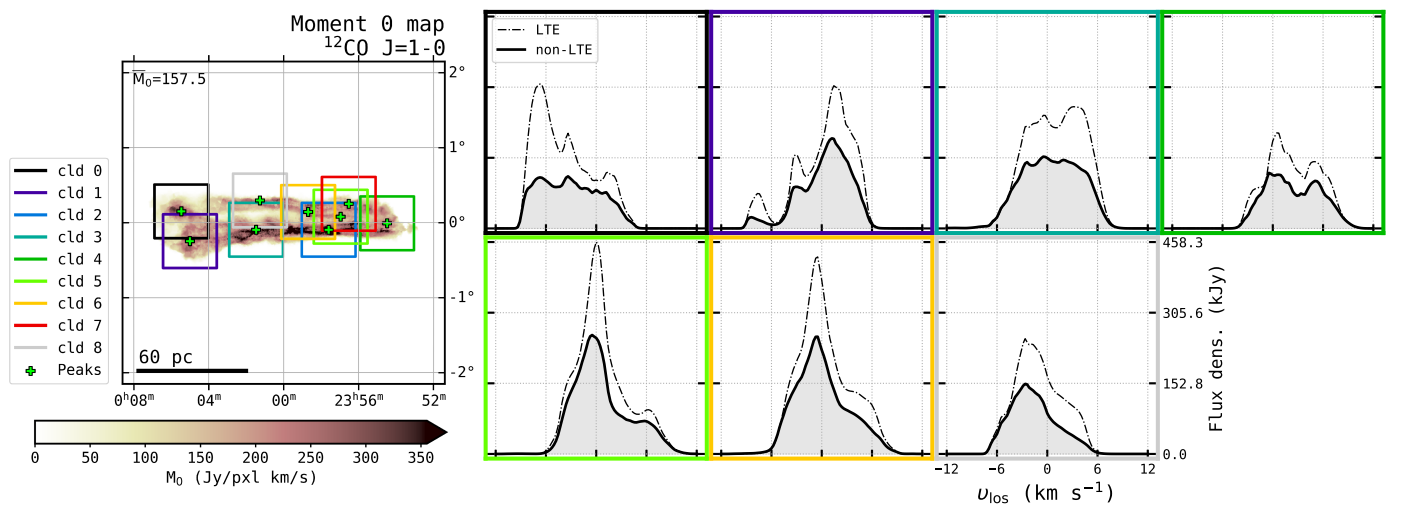


Figure 2.3: (continued) LTE (dashed) and non-LTE (solid) ^{12}CO $J=1-0$ line profiles from non-rejected molecular cloud portions.

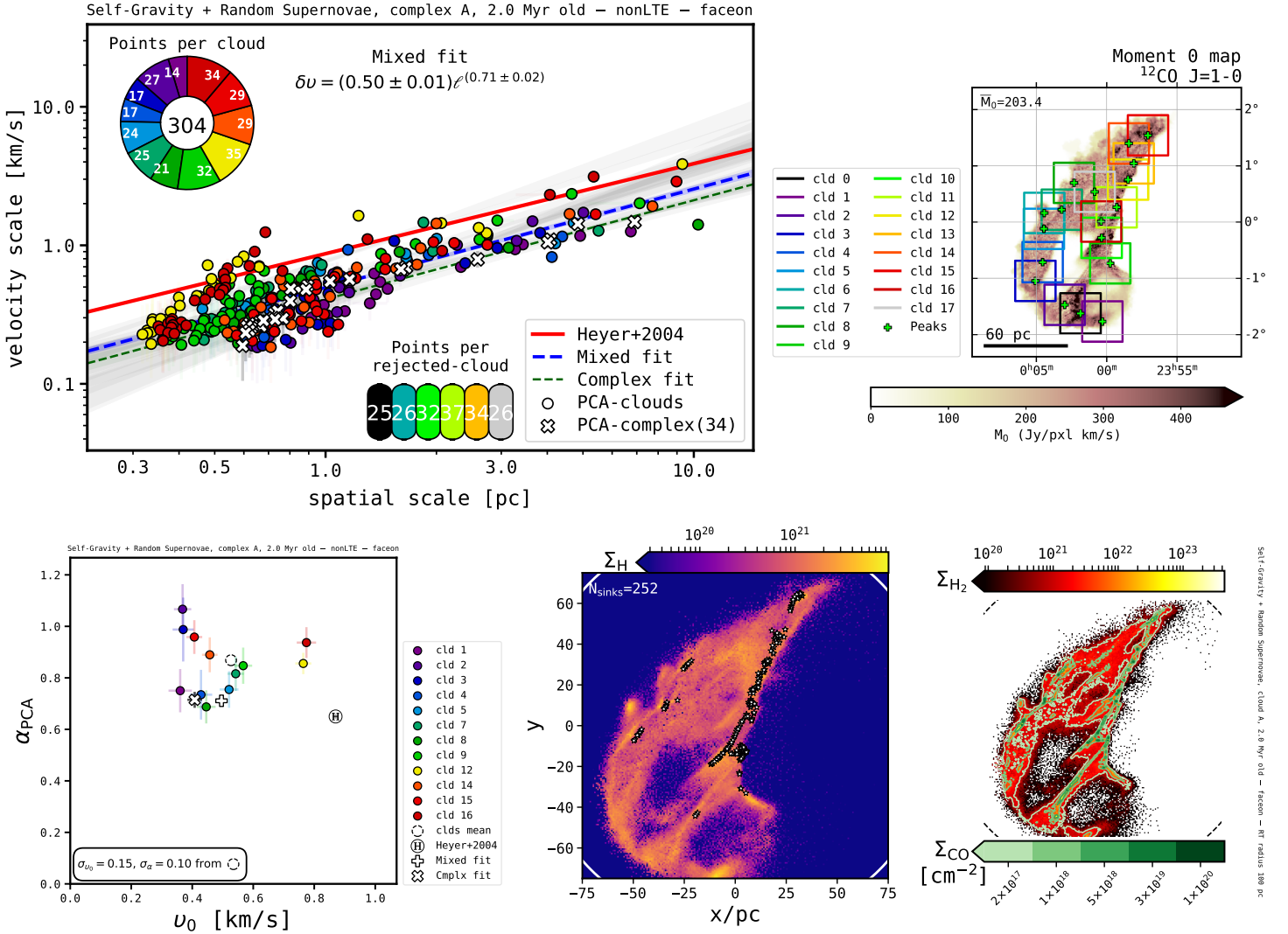


Figure 2.4: Principal component analysis and column densities from Cloud Complex: A; physical scenario: Potential-dominated → Galaxy Potential, Self-Gravity, Random Supernovae; snapshot time: 2.0 Myr; orientation: face-on; RT mode: nonLTE. See full captions in figures on the main manuscript.

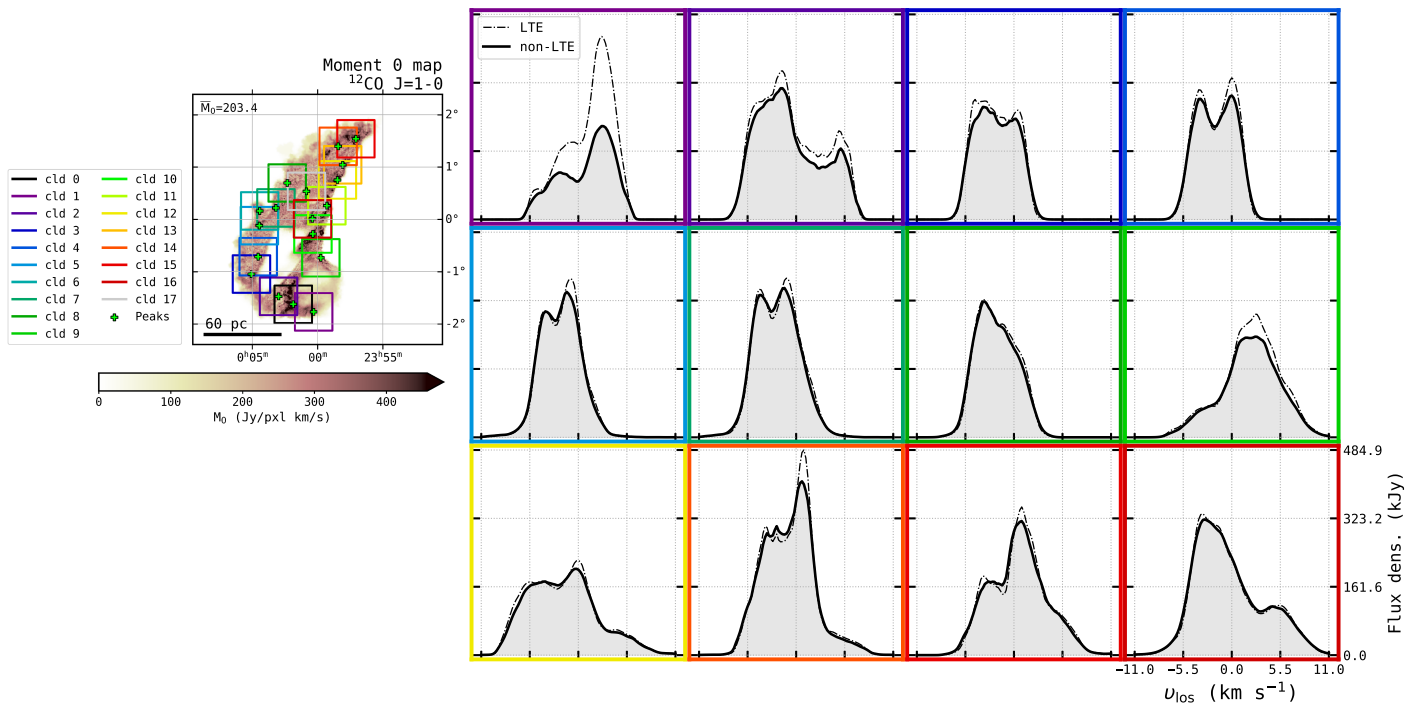


Figure 2.4: (continued) LTE (dashed) and non-LTE (solid) ^{12}CO $J=1-0$ line profiles from non-rejected molecular cloud portions.

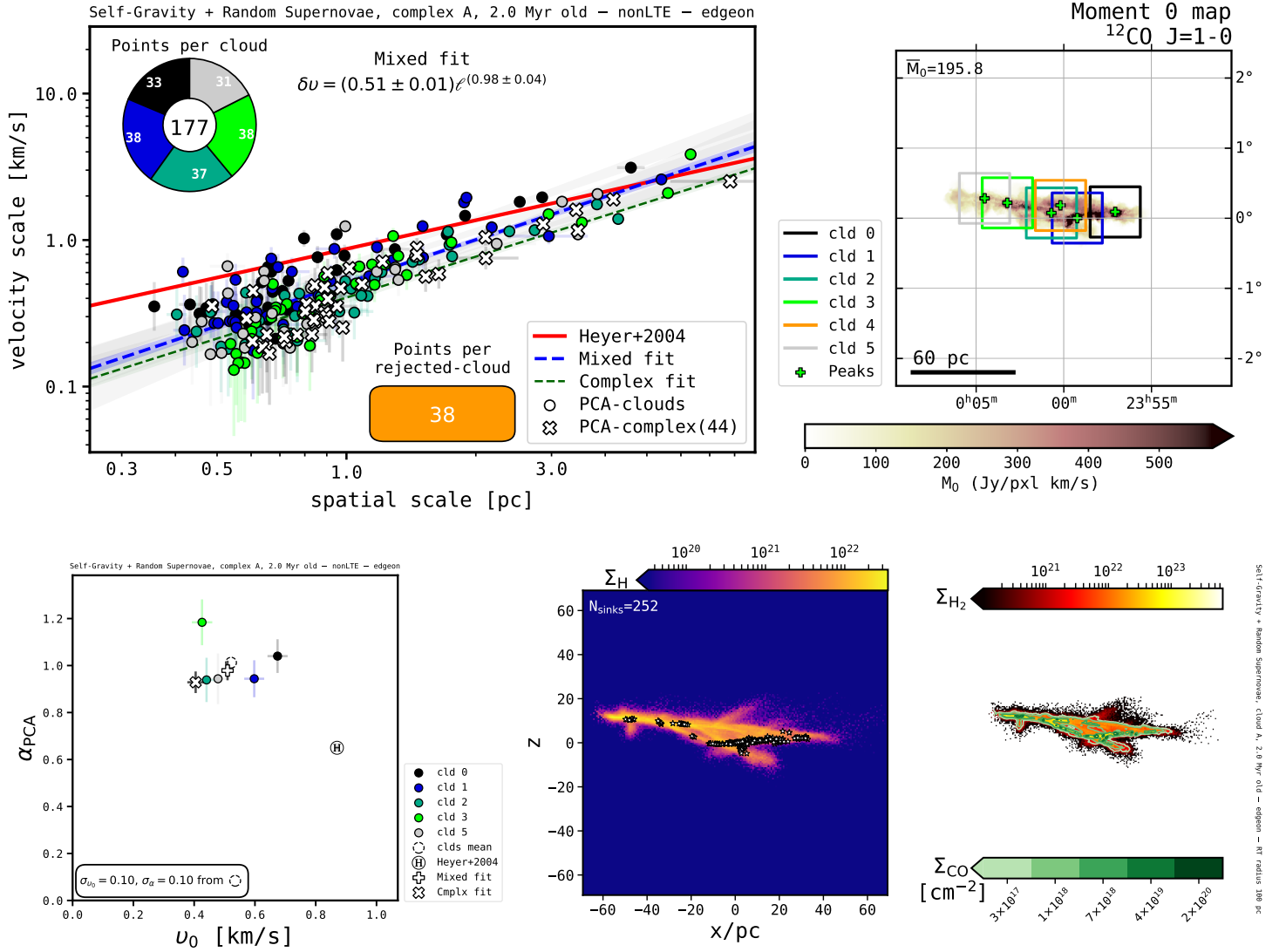


Figure 2.5: Principal component analysis and column densities from Cloud Complex: A; physical scenario: Potential-dominated \rightarrow Galaxy Potential, Self-Gravity, Random Supernovae; snapshot time: 2.0 Myr; orientation: edge-on $\phi=0^\circ$; RT mode: nonLTE. See full captions in figures on the main manuscript.

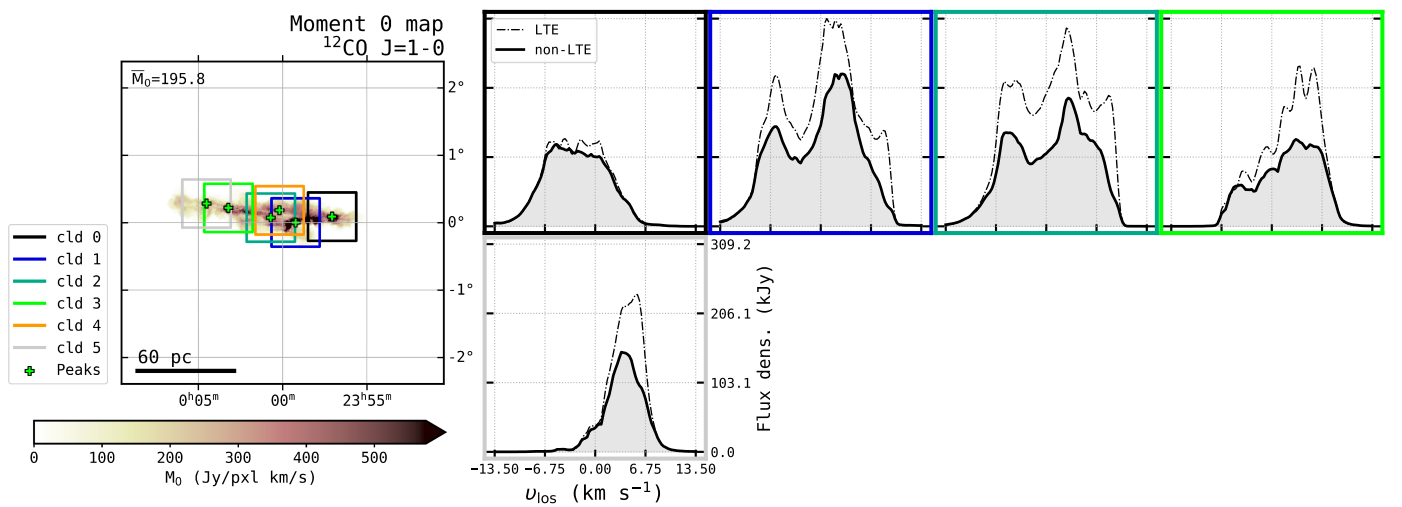


Figure 2.5: (continued) LTE (dashed) and non-LTE (solid) ^{12}CO $J=1-0$ line profiles from non-rejected molecular cloud portions.

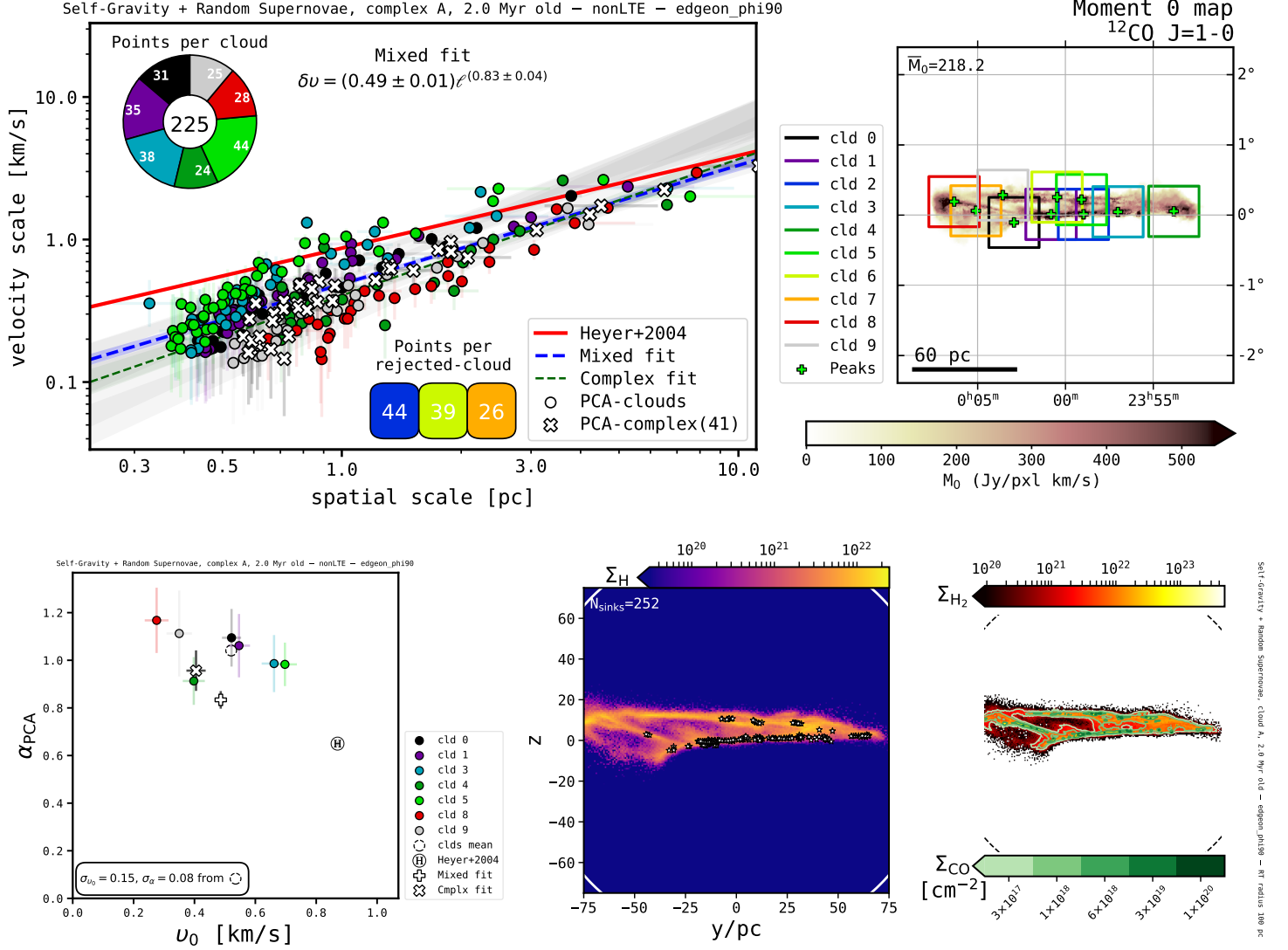


Figure 2.6: Principal component analysis and column densities from Cloud Complex A; physical scenario: Potential-dominated \rightarrow Galaxy Potential, Self-Gravity, Random Supernovae; snapshot time: 2.0 Myr; orientation: edge-on $\phi=90^\circ$; RT mode: nonLTE. See full captions in figures on the main manuscript.

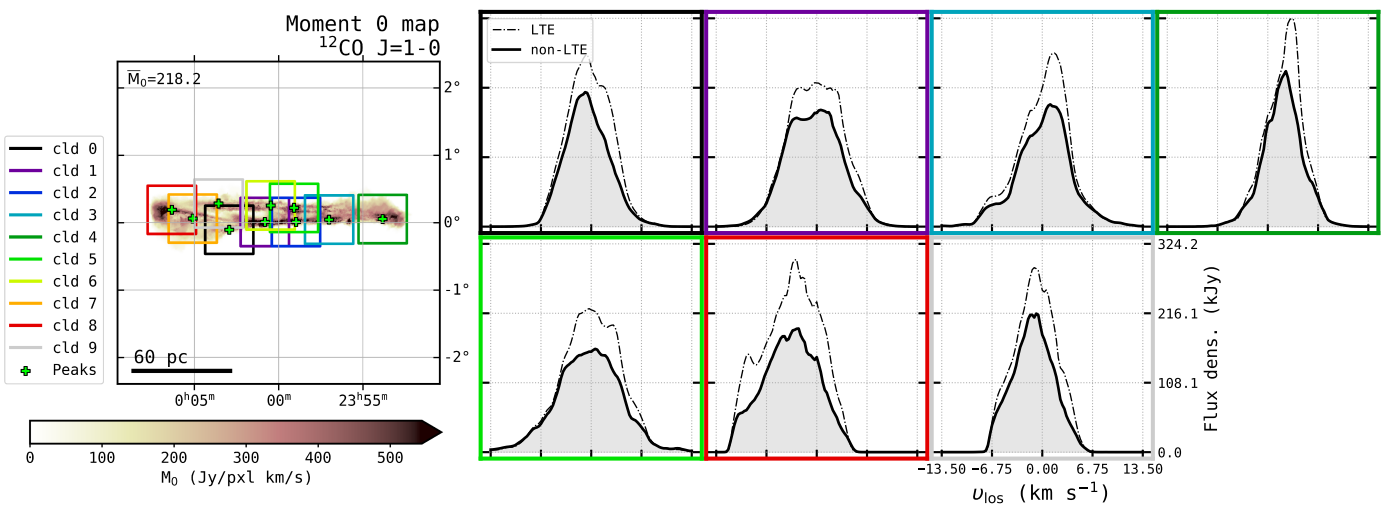


Figure 2.6: (continued) LTE (dashed) and non-LTE (solid) ^{12}CO $J=1-0$ line profiles from non-rejected molecular cloud portions.

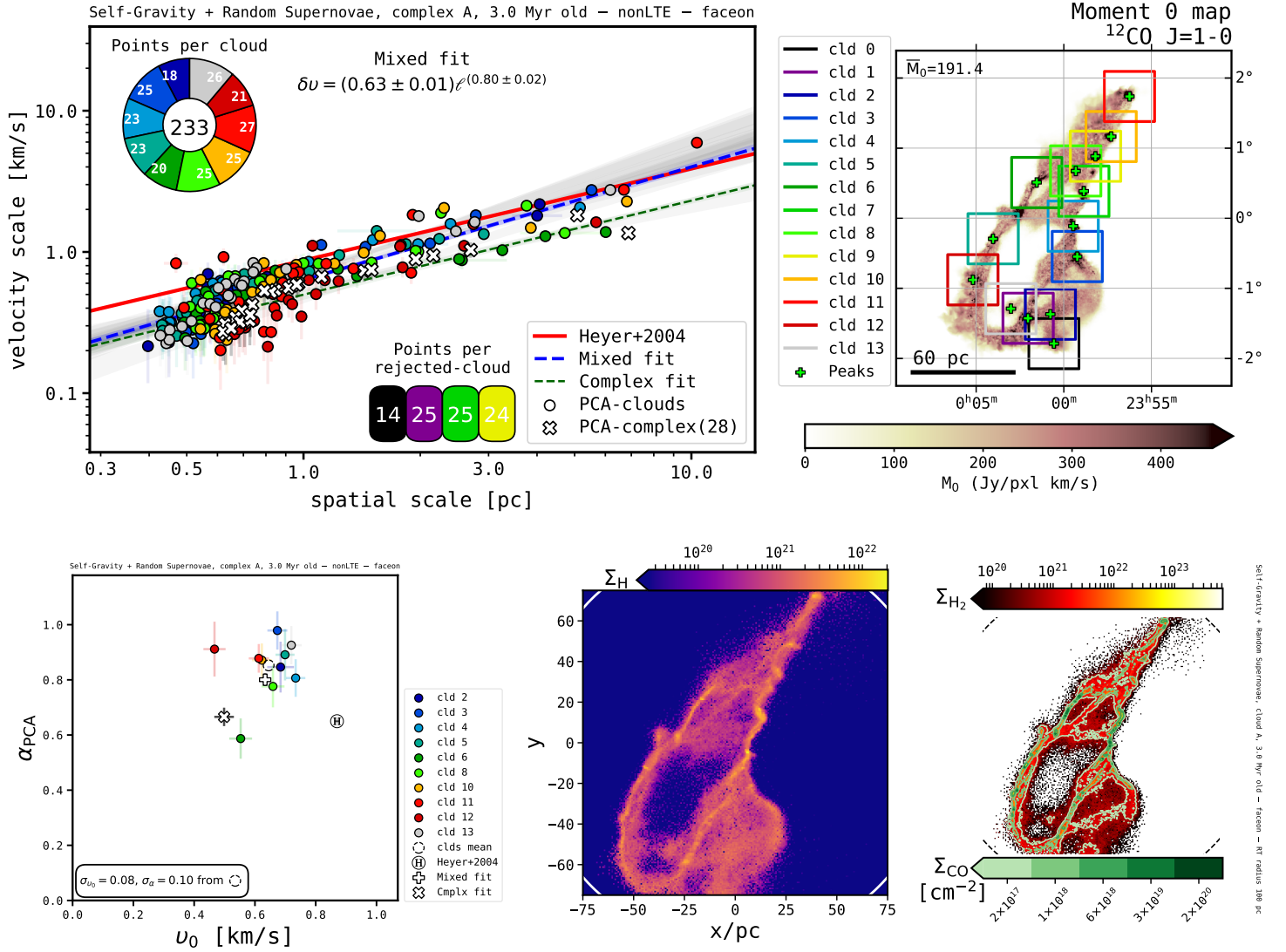


Figure 2.7: Principal component analysis and column densities from Cloud Complex: A; physical scenario: Potential-dominated → Galaxy Potential, Self-Gravity, Random Supernovae; snapshot time: 3.0 Myr; orientation: face-on; RT mode: nonLTE. See full captions in figures on the main manuscript.

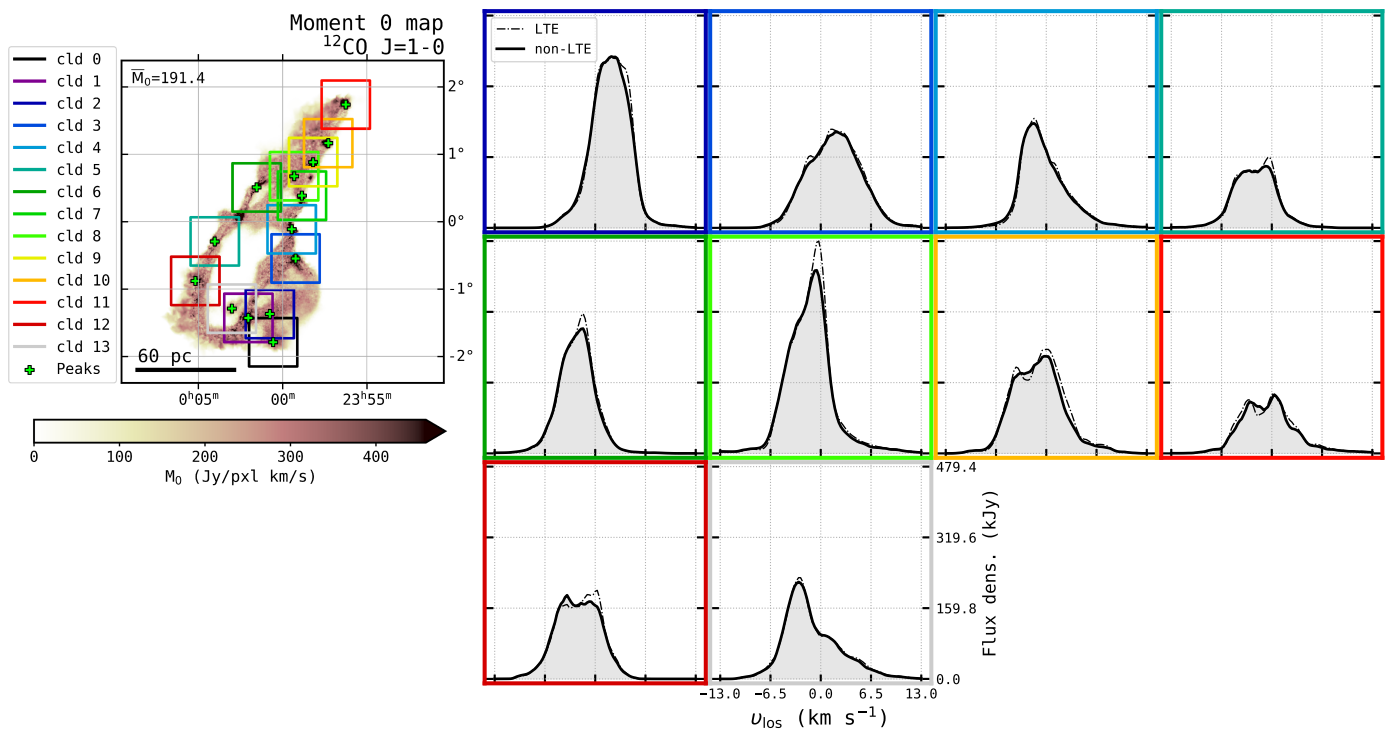


Figure 2.7: (continued) LTE (dashed) and non-LTE (solid) ^{12}CO $J=1-0$ line profiles from non-rejected molecular cloud portions.

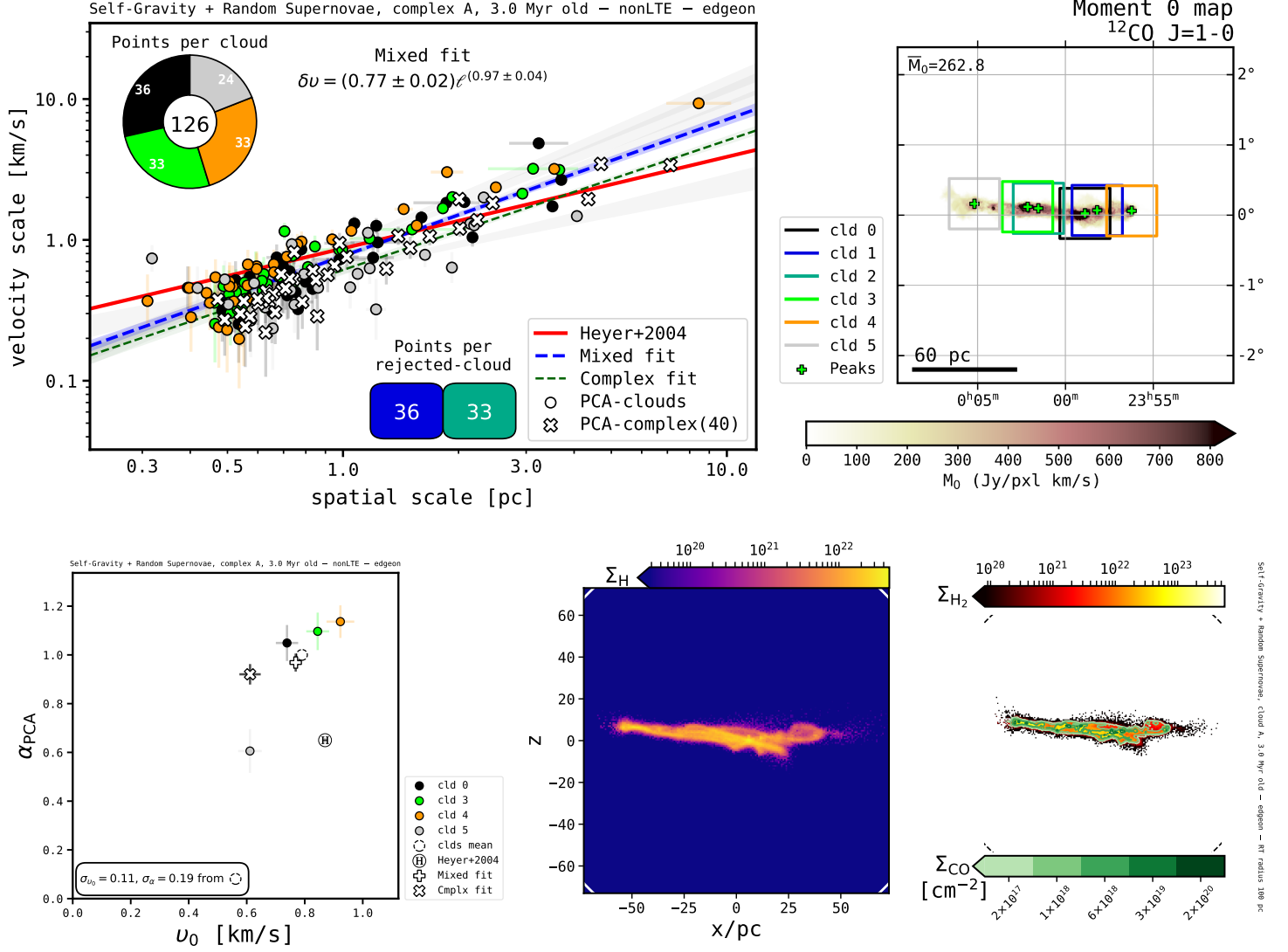


Figure 2.8: Principal component analysis and column densities from Cloud Complex: A; physical scenario: Potential-dominated \rightarrow Galaxy Potential, Self-Gravity, Random Supernovae; snapshot time: 3.0 Myr; orientation: edge-on $\phi=0^\circ$; RT mode: nonLTE. See full captions in figures on the main manuscript.

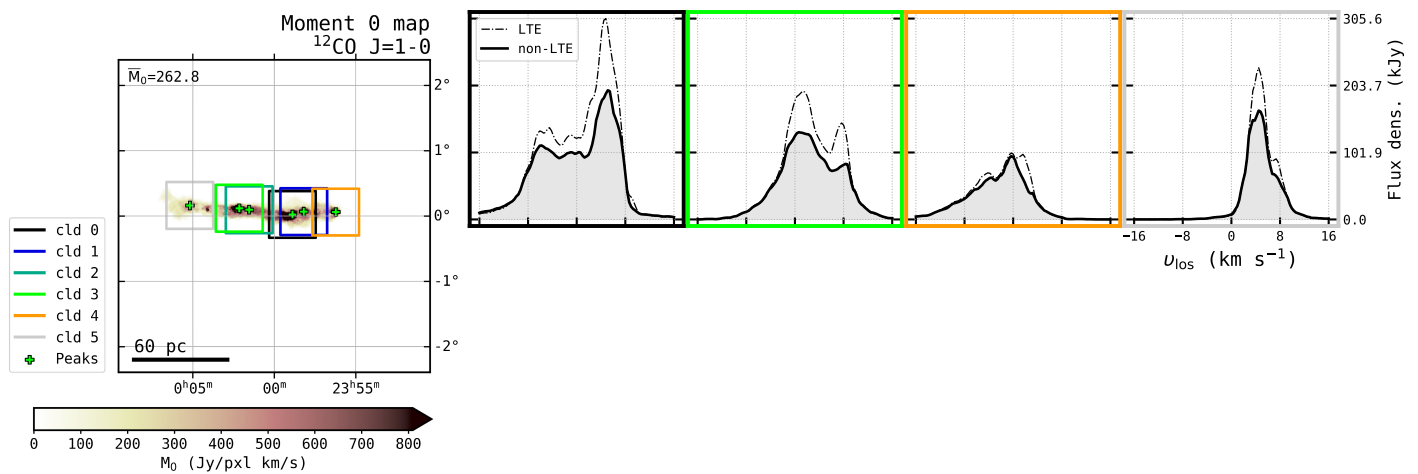


Figure 2.8: (continued) LTE (dashed) and non-LTE (solid) ^{12}CO $J=1-0$ line profiles from non-rejected molecular cloud portions.

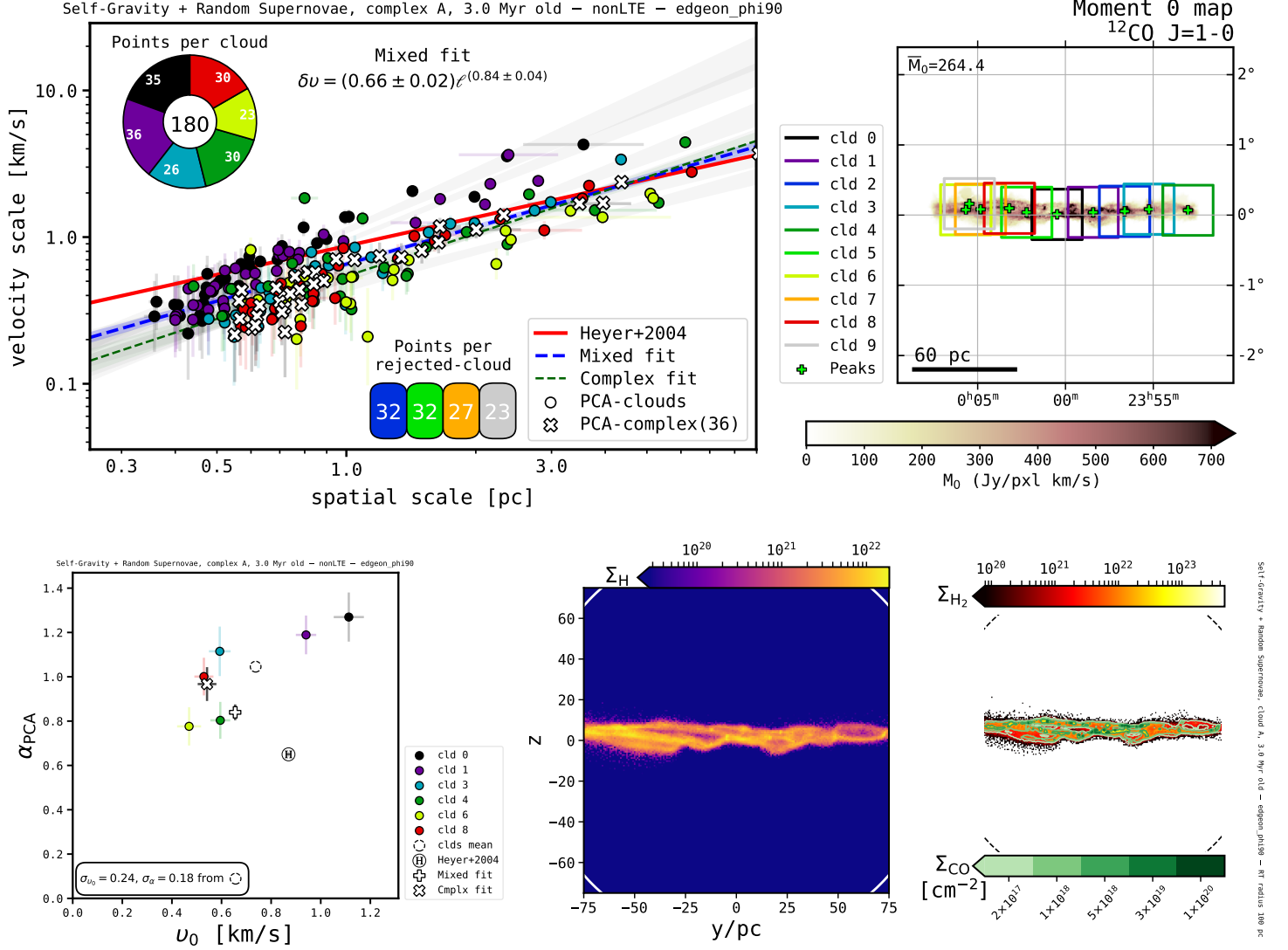


Figure 2.9: Principal component analysis and column densities from Cloud Complex A; physical scenario: Potential-dominated \rightarrow Galaxy Potential, Self-Gravity, Random Supernovae; snapshot time: 3.0 Myr; orientation: edge-on $\phi=90^\circ$; RT mode: nonLTE. See full captions in figures on the main manuscript.

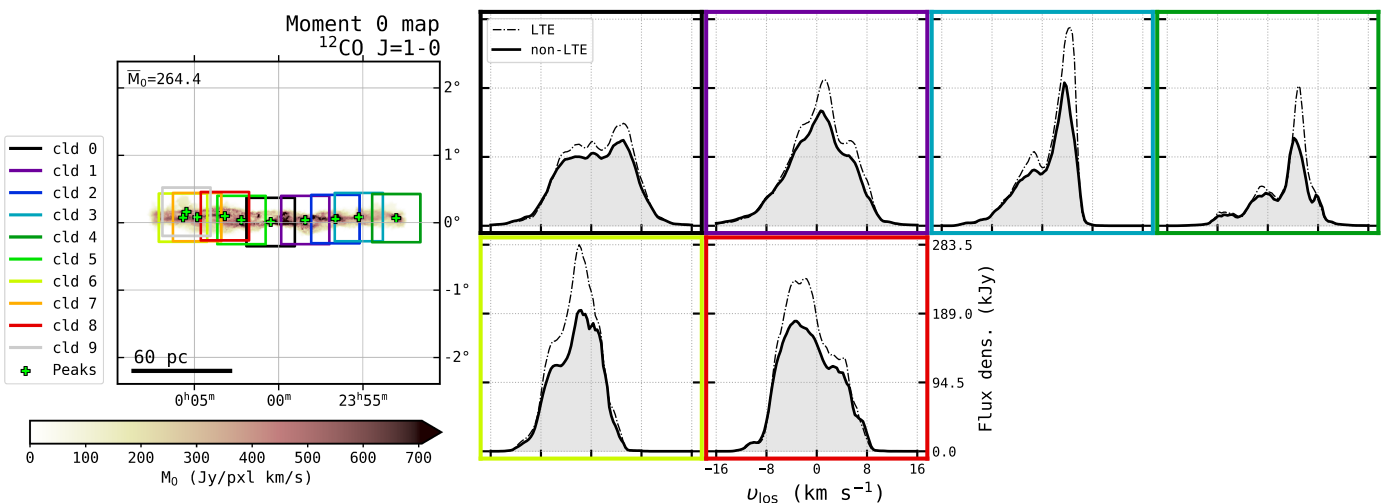


Figure 2.9: (continued) LTE (dashed) and non-LTE (solid) ^{12}CO $J=1-0$ line profiles from non-rejected molecular cloud portions.

2.2 Cloud B

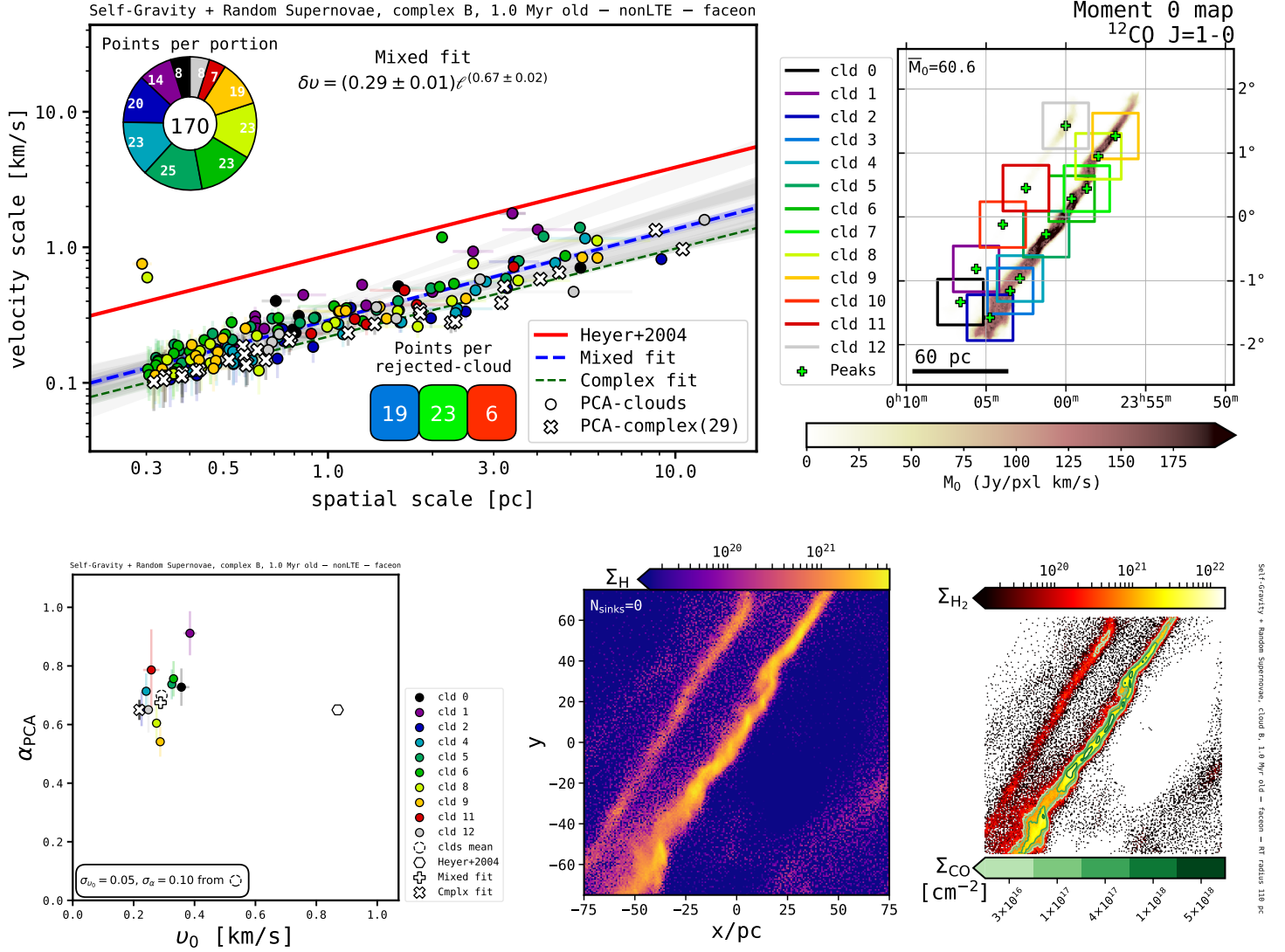


Figure 2.10: Principal component analysis and column densities from Cloud Complex: B; physical scenario: Potential-dominated → Galaxy Potential, Self-Gravity, Random Supernovae; snapshot time: 1.0 Myr; orientation: face-on; RT mode: nonLTE. See full captions in figures on the main manuscript.

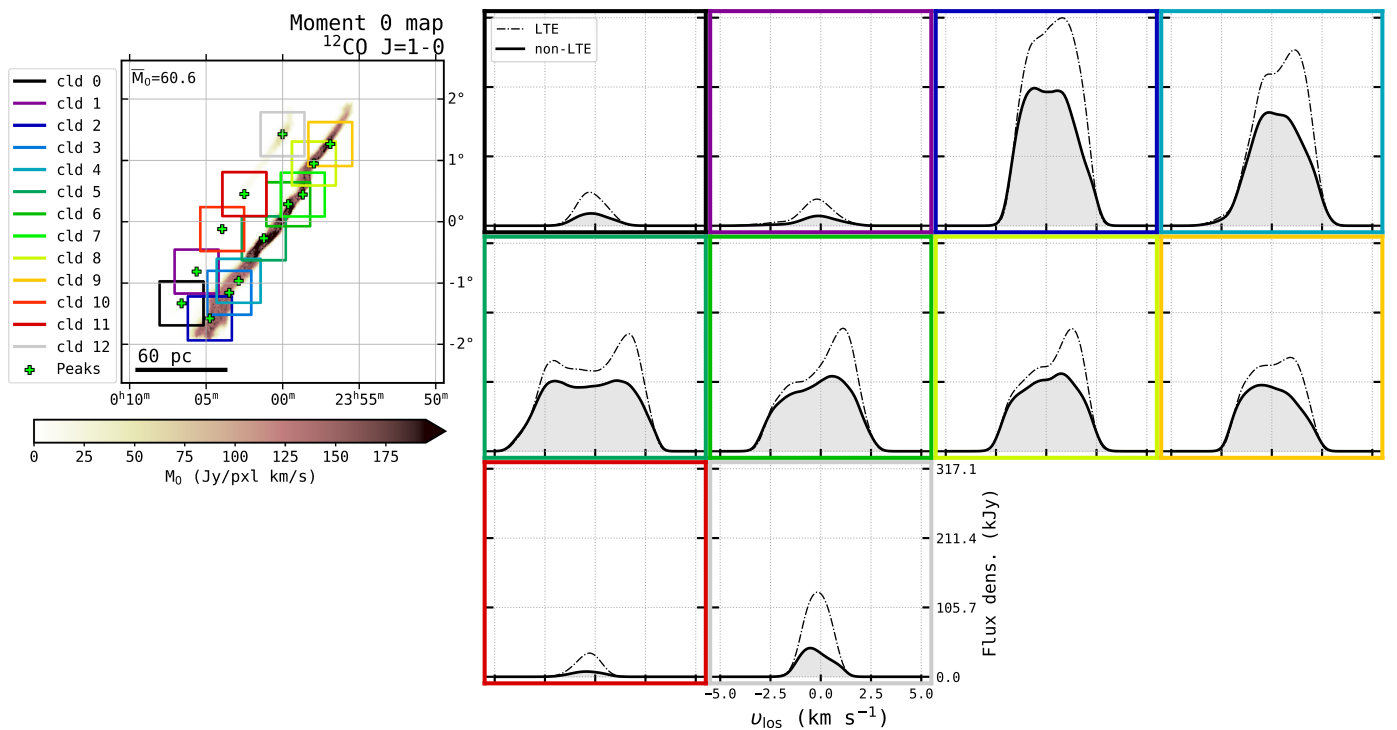


Figure 2.10: (continued) LTE (dashed) and non-LTE (solid) ^{12}CO $J=1-0$ line profiles from non-rejected molecular cloud portions.

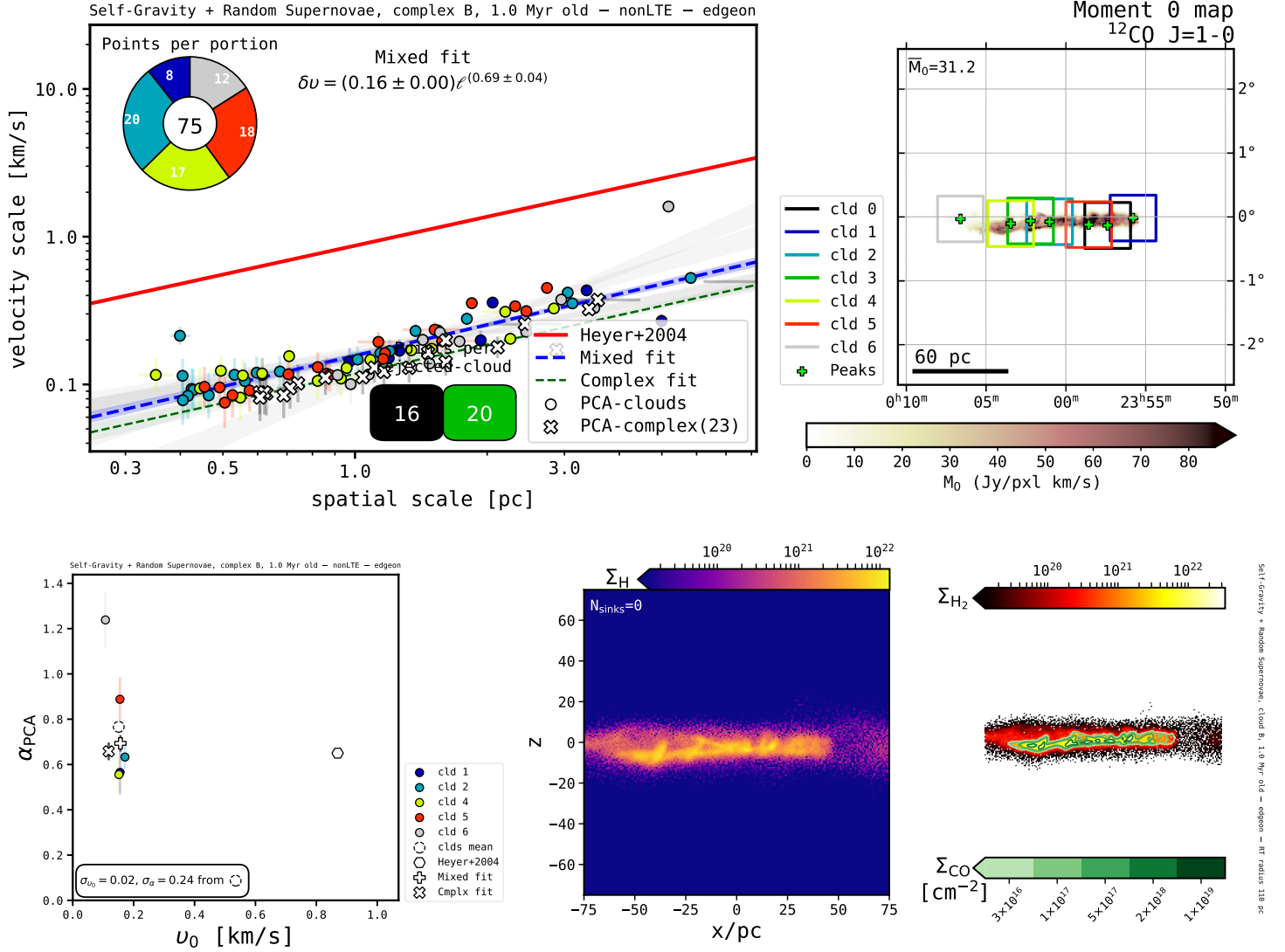


Figure 2.11: Principal component analysis and column densities from Cloud Complex: B; physical scenario: Potential-dominated → Galaxy Potential, Self-Gravity, Random Supernovae; snapshot time: 1.0 Myr; orientation: edge-on $\phi=0^\circ$; RT mode: nonLTE. See full captions in figures on the main manuscript.

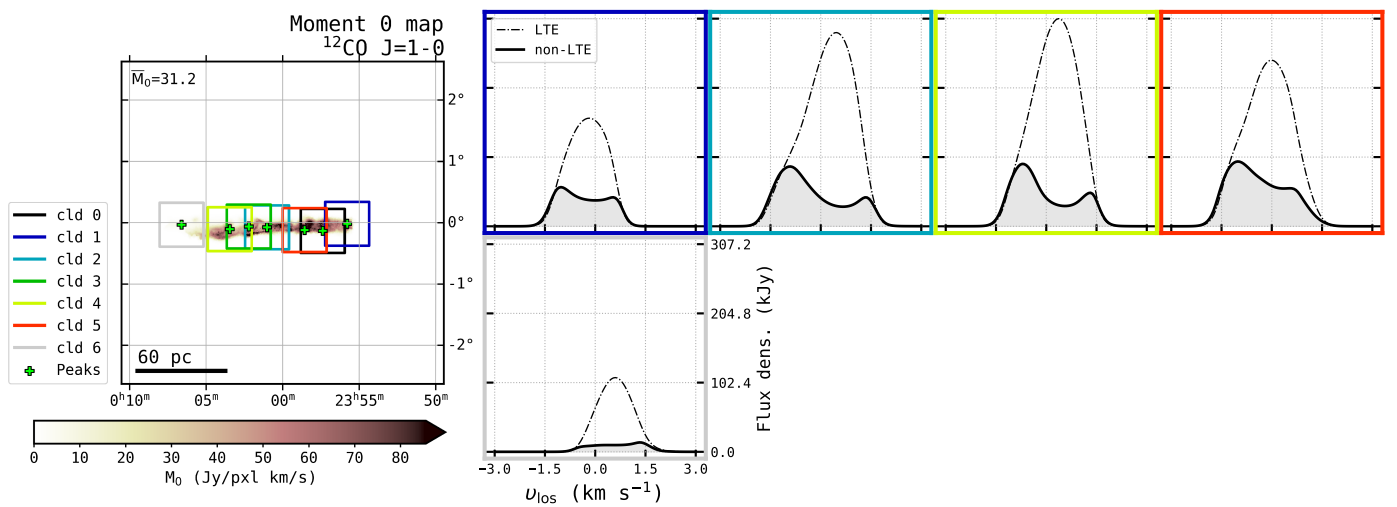


Figure 2.11: (continued) LTE (dashed) and non-LTE (solid) ^{12}CO $J=1-0$ line profiles from non-rejected molecular cloud portions.

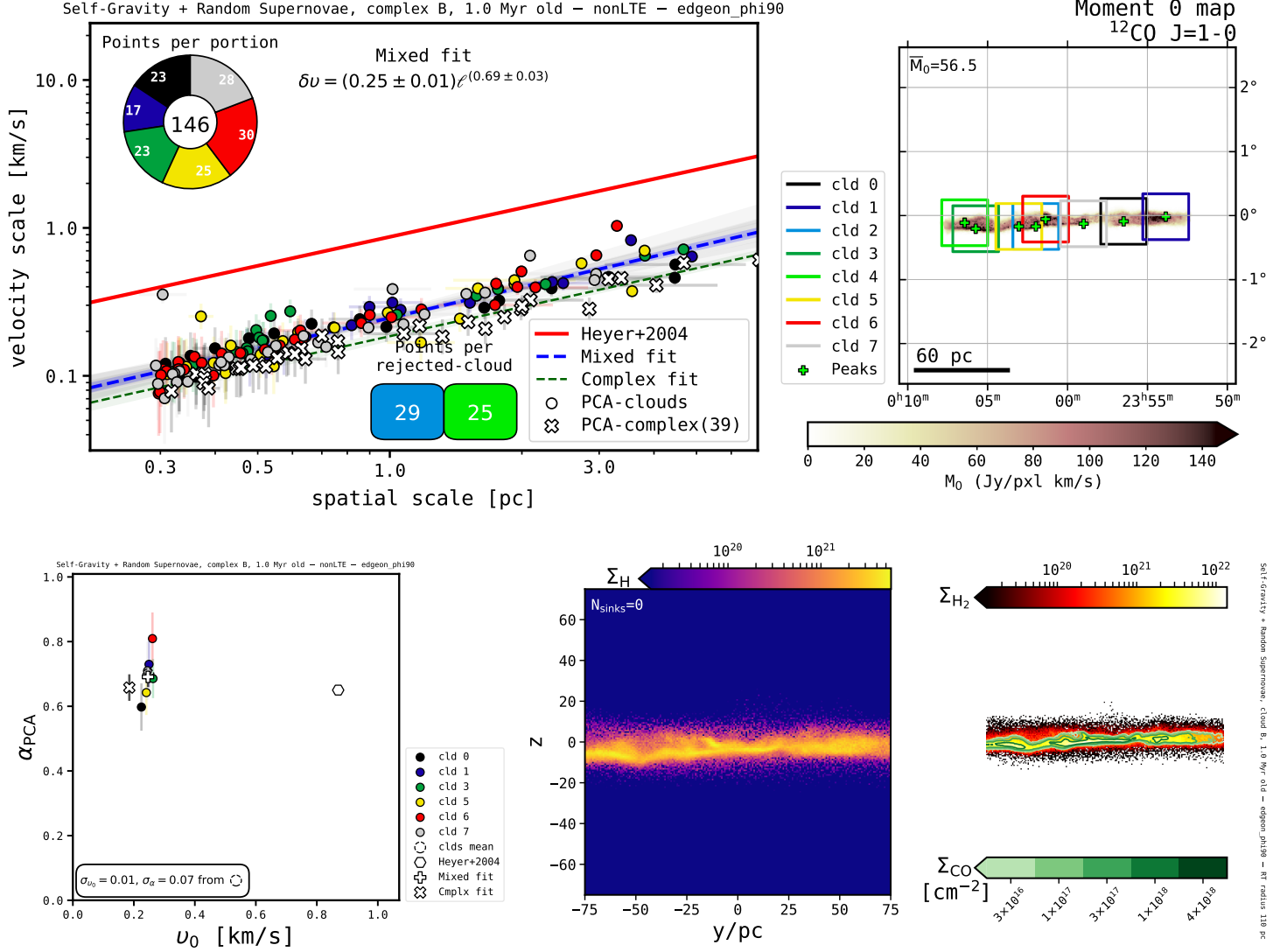


Figure 2.12: Principal component analysis and column densities from Cloud Complex: B; physical scenario: Potential-dominated → Galaxy Potential, Self-Gravity, Random Supernovae; snapshot time: 1.0 Myr; orientation: edge-on $_{\phi=90^\circ}$; RT mode: nonLTE. See full captions in figures on the main manuscript.

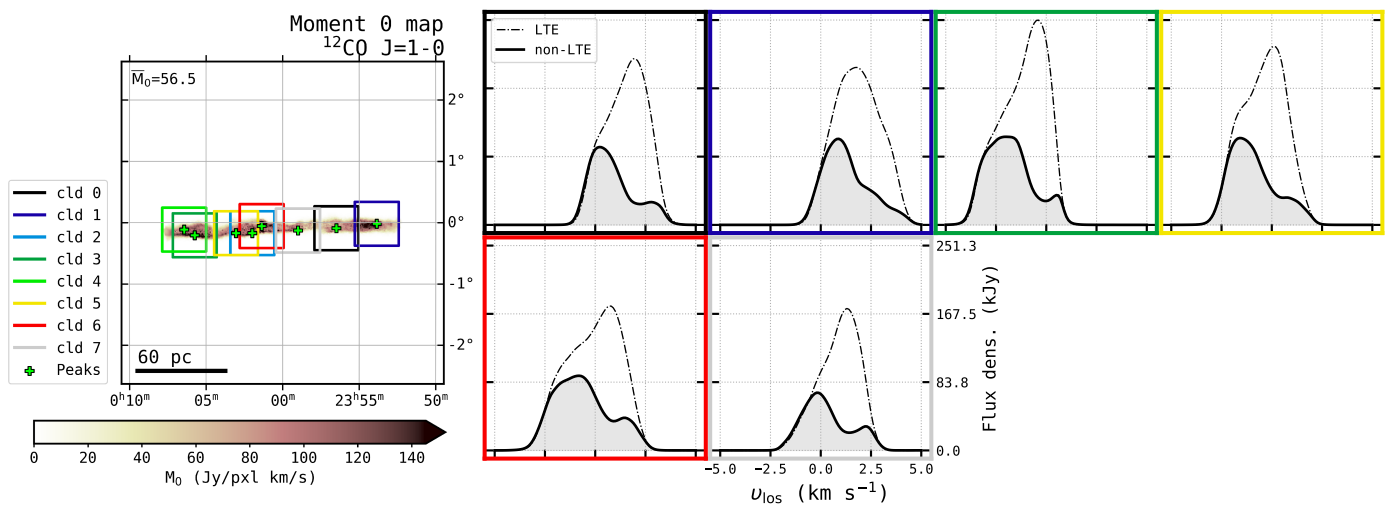


Figure 2.12: (continued) LTE (dashed) and non-LTE (solid) ^{12}CO $J=1-0$ line profiles from non-rejected molecular cloud portions.

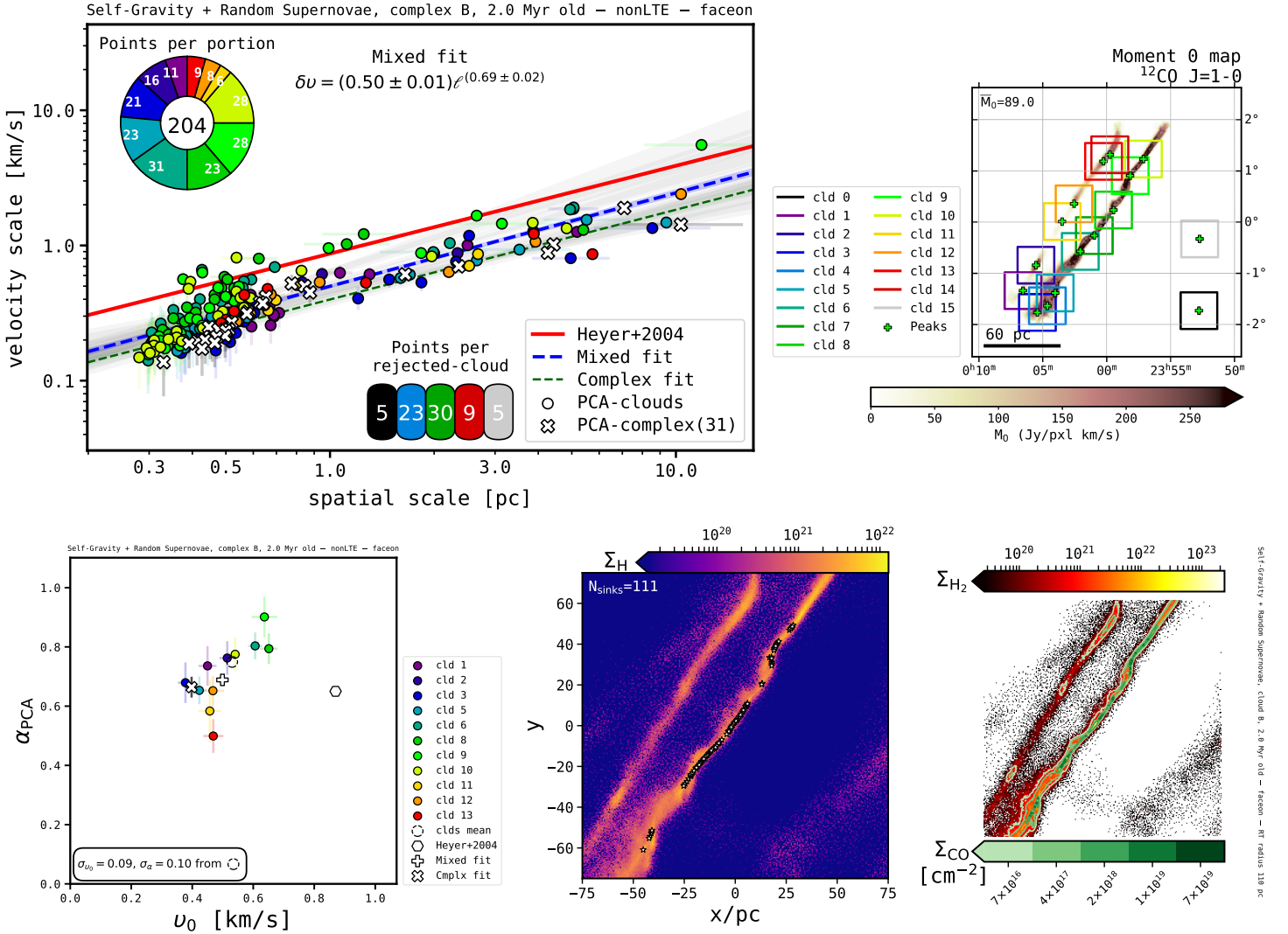


Figure 2.13: Principal component analysis and column densities from Cloud Complex: B; physical scenario: Potential-dominated → Galaxy Potential, Self-Gravity, Random Supernovae; snapshot time: 2.0 Myr; orientation: face-on; RT mode: nonLTE. See full captions in figures on the main manuscript.

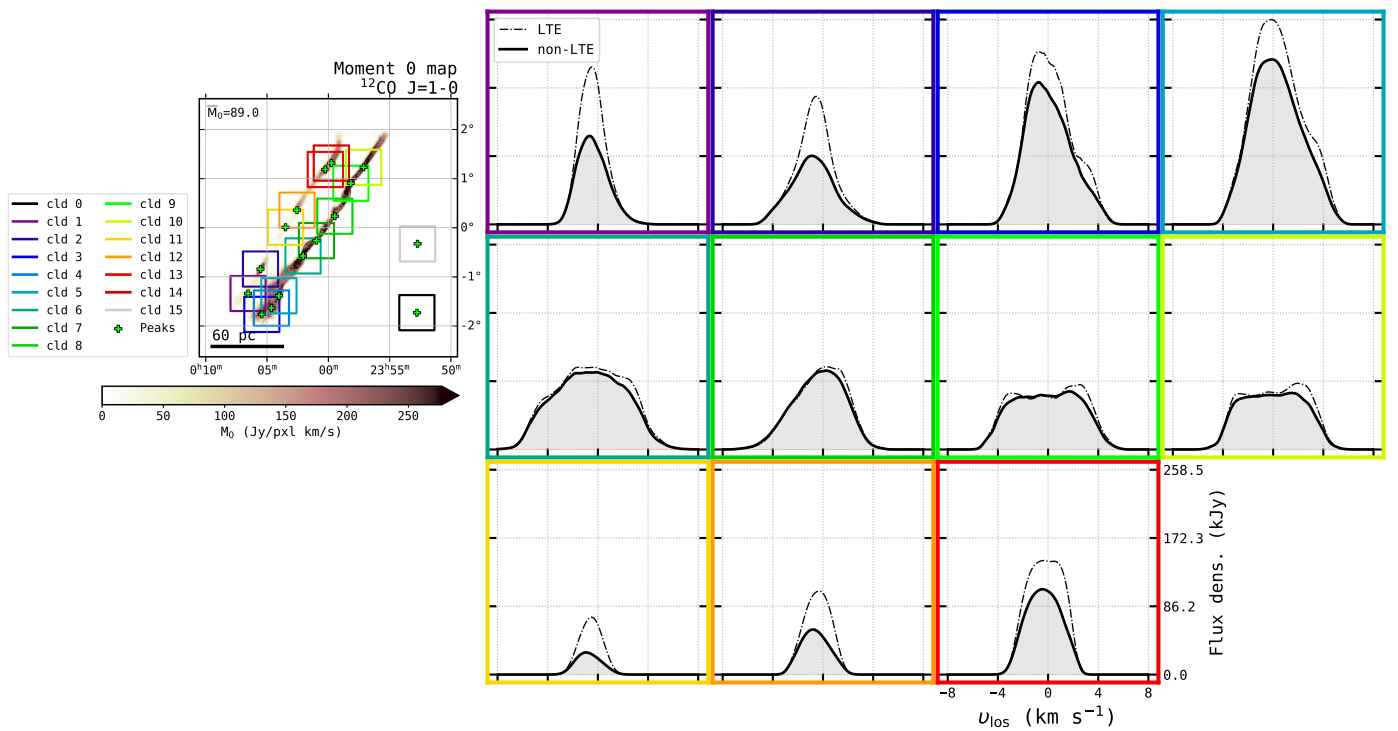


Figure 2.13: (continued) LTE (dashed) and non-LTE (solid) ^{12}CO $J=1-0$ line profiles from non-rejected molecular cloud portions.

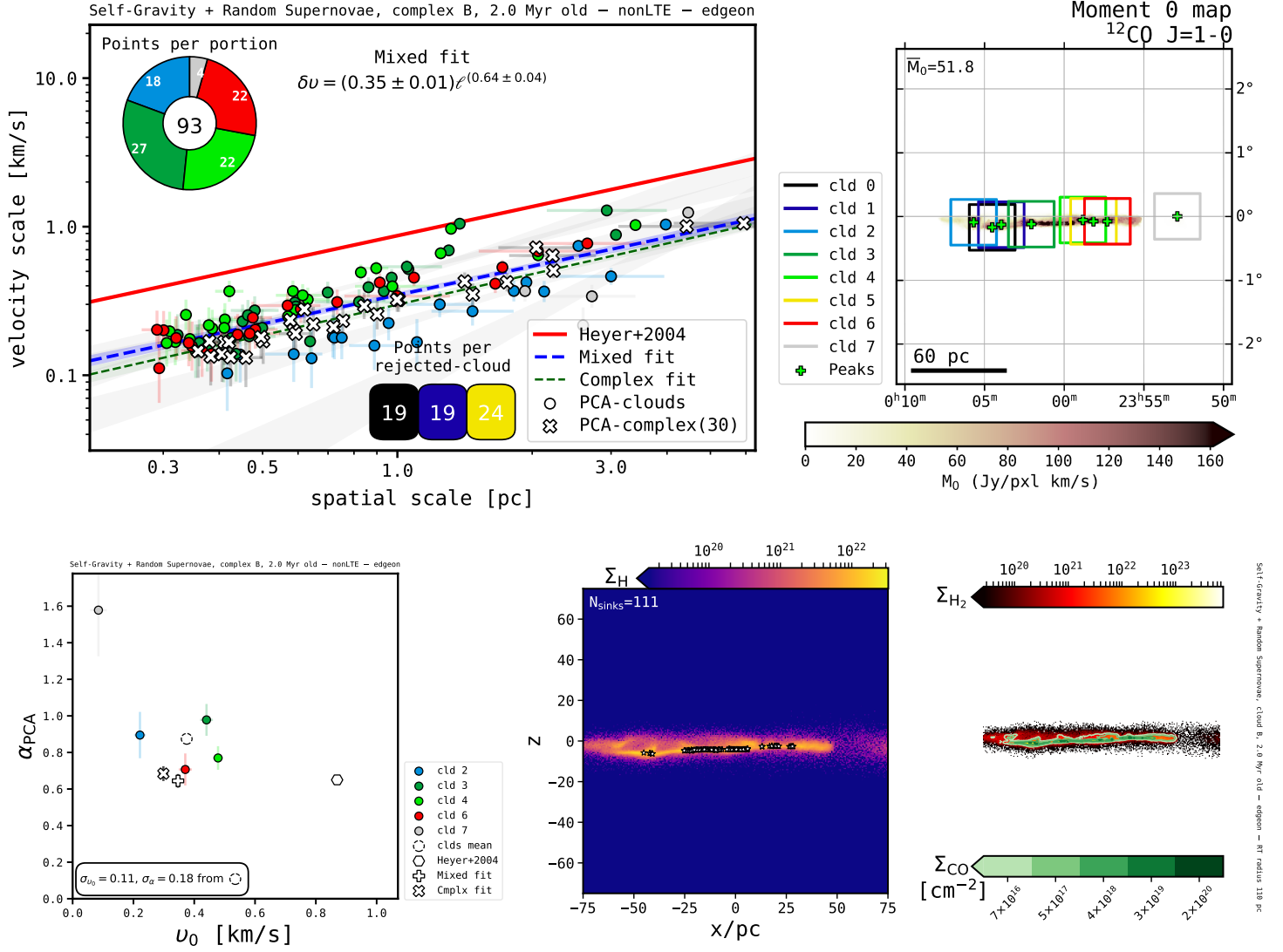


Figure 2.14: Principal component analysis and column densities from Cloud Complex: B; physical scenario: Potential-dominated → Galaxy Potential, Self-Gravity, Random Supernovae; snapshot time: 2.0 Myr; orientation: edge-on $\phi=0^\circ$; RT mode: nonLTE. See full captions in figures on the main manuscript.

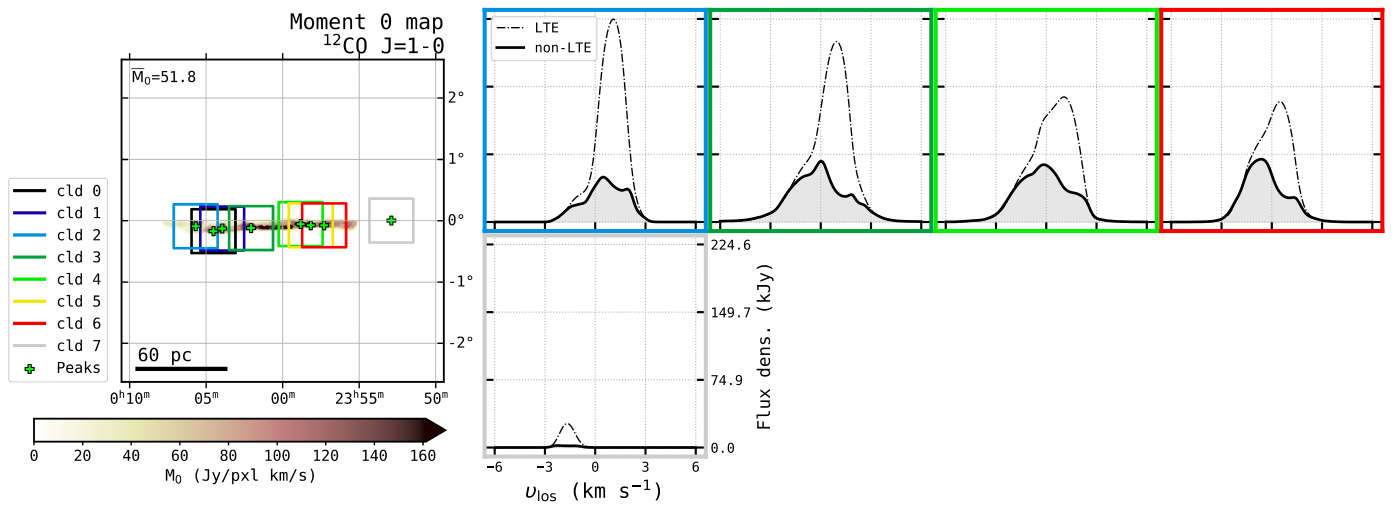


Figure 2.14: (continued) LTE (dashed) and non-LTE (solid) ^{12}CO $J=1-0$ line profiles from non-rejected molecular cloud portions.

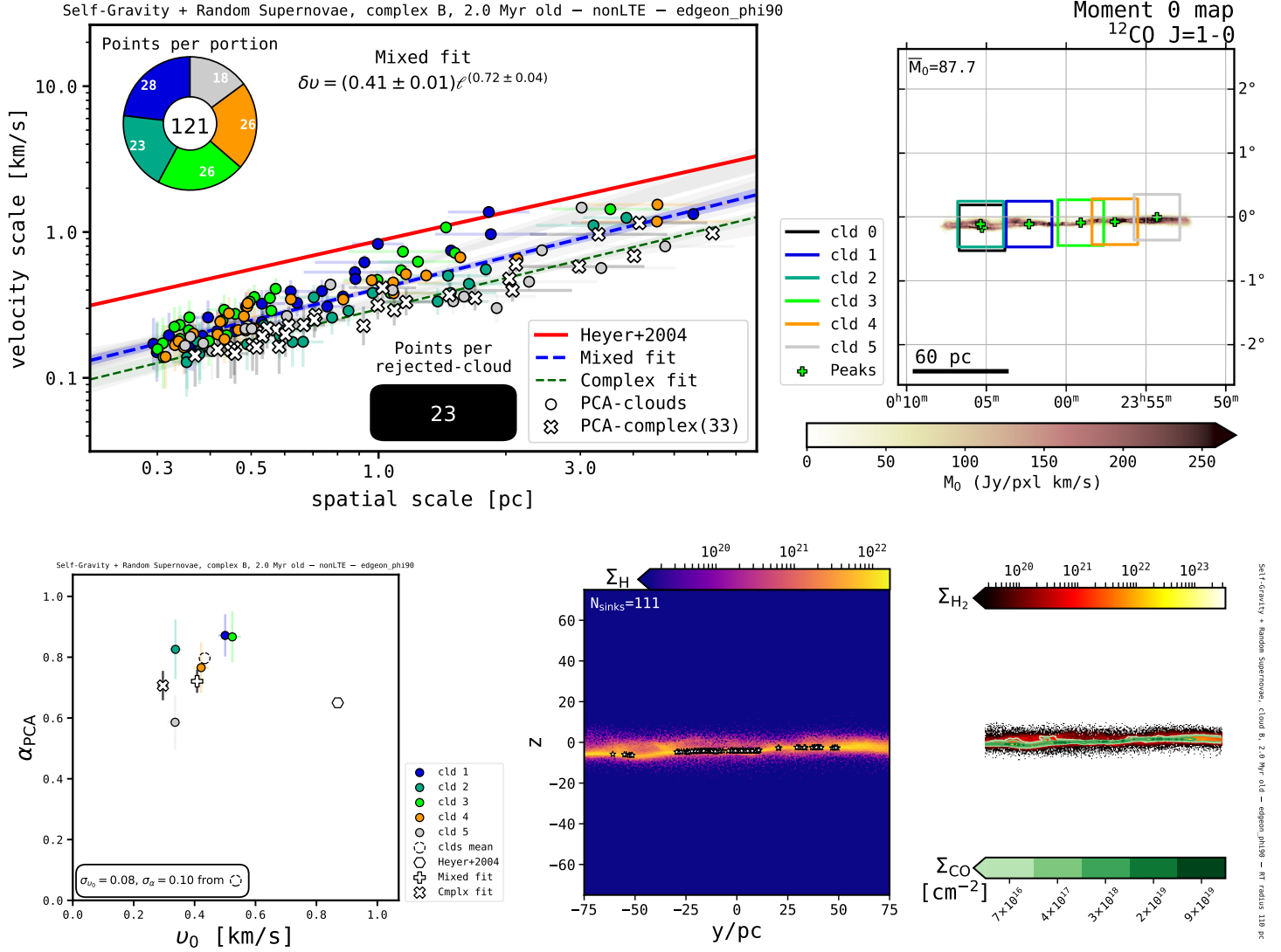


Figure 2.15: Principal component analysis and column densities from Cloud Complex: B; physical scenario: Potential-dominated → Galaxy Potential, Self-Gravity, Random Supernovae; snapshot time: 2.0 Myr; orientation: edge-on $_{\phi=90^{\circ}}$; RT mode: nonLTE. See full captions in figures on the main manuscript.

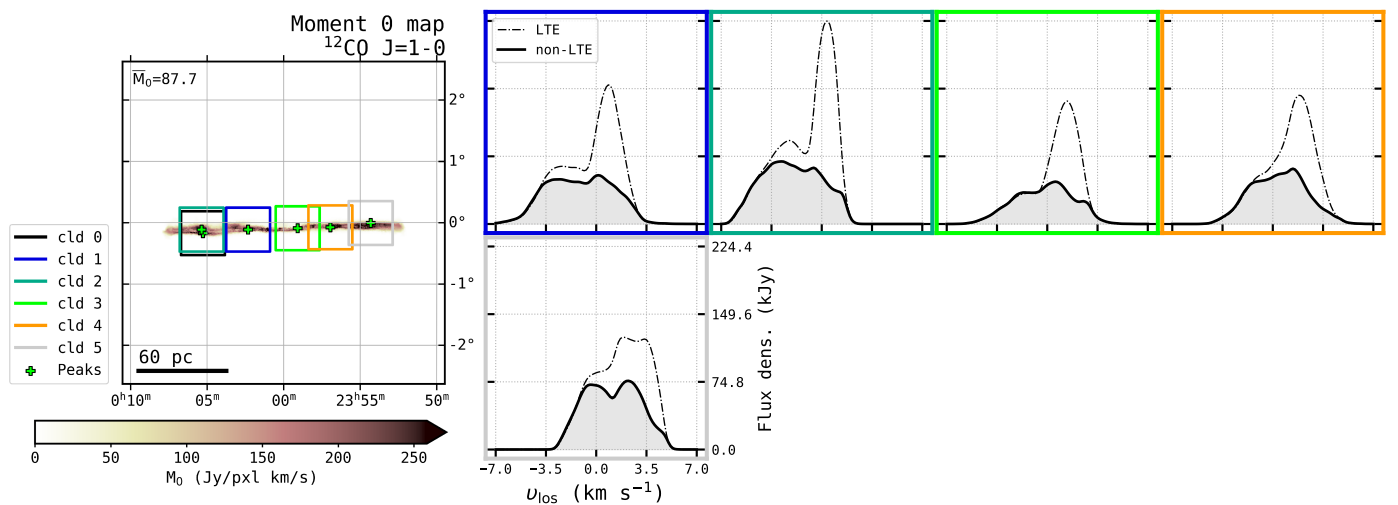


Figure 2.15: (continued) LTE (dashed) and non-LTE (solid) ^{12}CO $J=1-0$ line profiles from non-rejected molecular cloud portions.

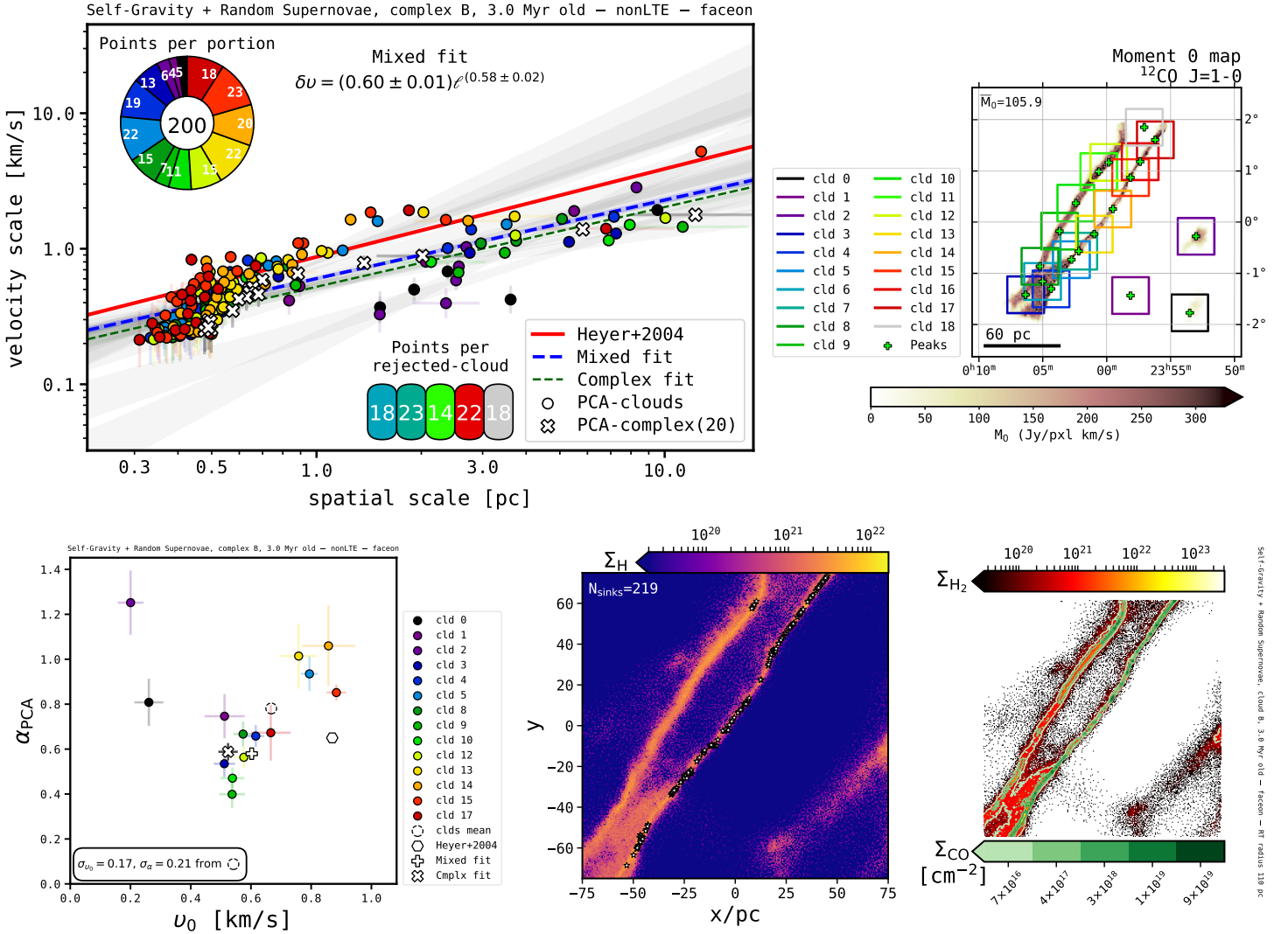


Figure 2.16: Principal component analysis and column densities from Cloud Complex: B; physical scenario: Potential-dominated → Galaxy Potential, Self-Gravity, Random Supernovae; snapshot time: 3.0 Myr; orientation: face-on; RT mode: nonLTE. See full captions in figures on the main manuscript.

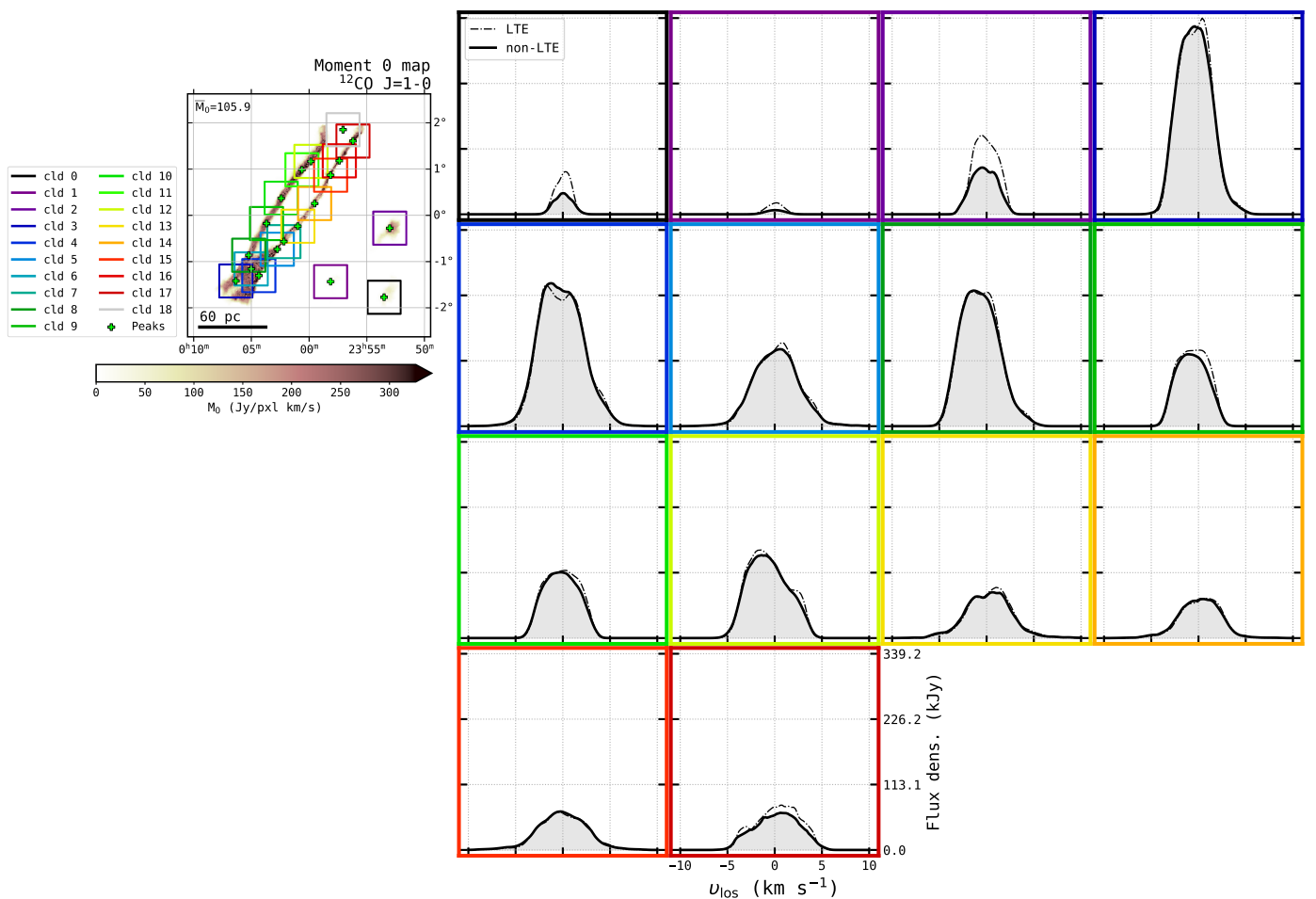


Figure 2.16: (continued) LTE (dashed) and non-LTE (solid) ^{12}CO $J=1-0$ line profiles from non-rejected molecular cloud portions.

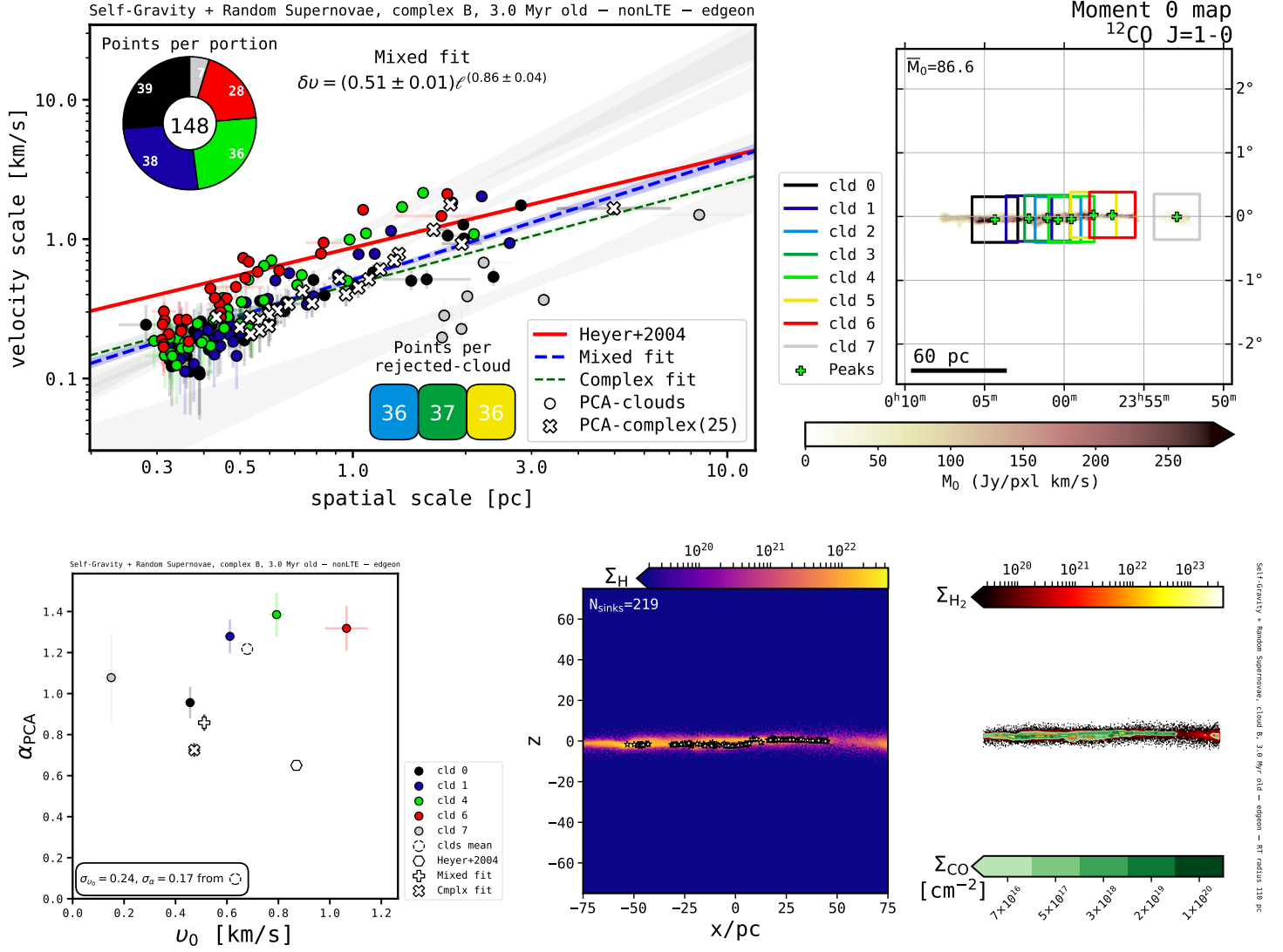


Figure 2.17: Principal component analysis and column densities from Cloud Complex: B; physical scenario: Potential-dominated → Galaxy Potential, Self-Gravity, Random Supernovae; snapshot time: 3.0 Myr; orientation: edge-on $\phi=0^\circ$; RT mode: nonLTE. See full captions in figures on the main manuscript.

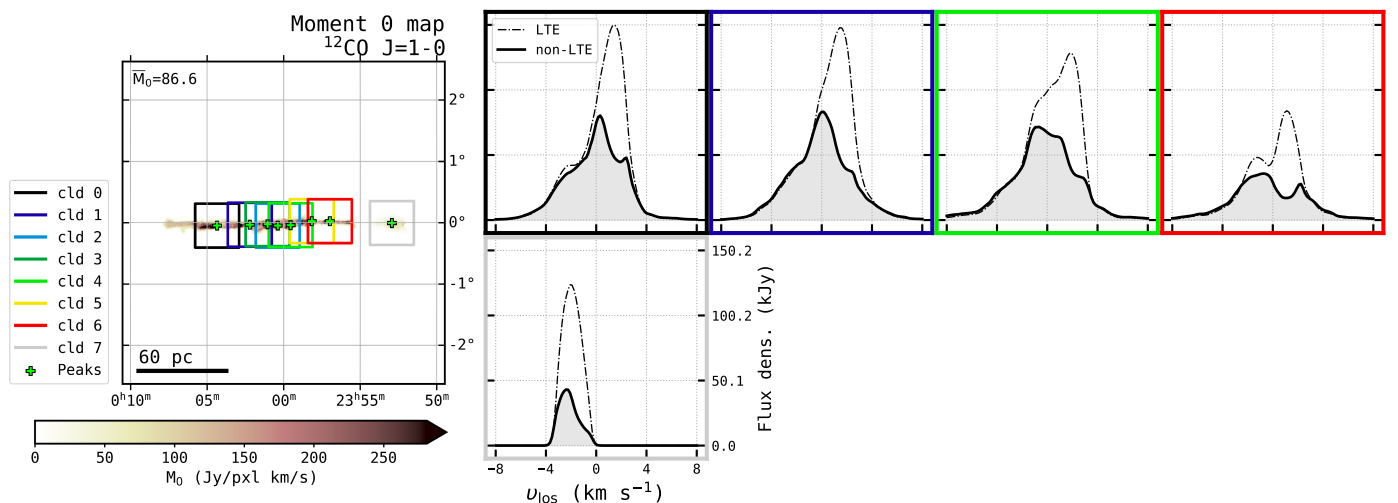


Figure 2.17: (continued) LTE (dashed) and non-LTE (solid) ^{12}CO $J=1-0$ line profiles from non-rejected molecular cloud portions.

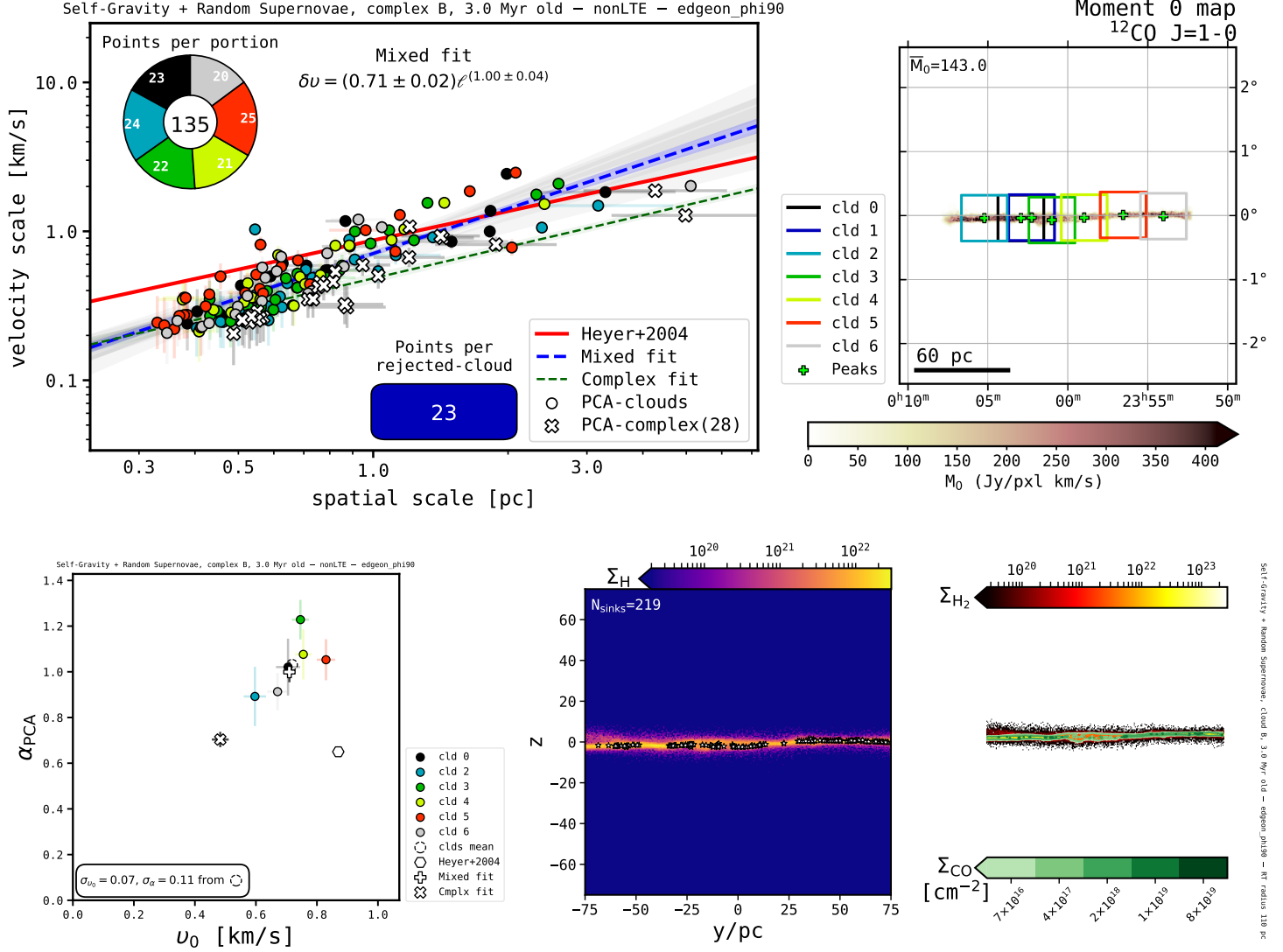


Figure 2.18: Principal component analysis and column densities from Cloud Complex: B; physical scenario: Potential-dominated → Galaxy Potential, Self-Gravity, Random Supernovae; snapshot time: 3.0 Myr; orientation: edge-on $_{\phi=90^\circ}$; RT mode: nonLTE. See full captions in figures on the main manuscript.

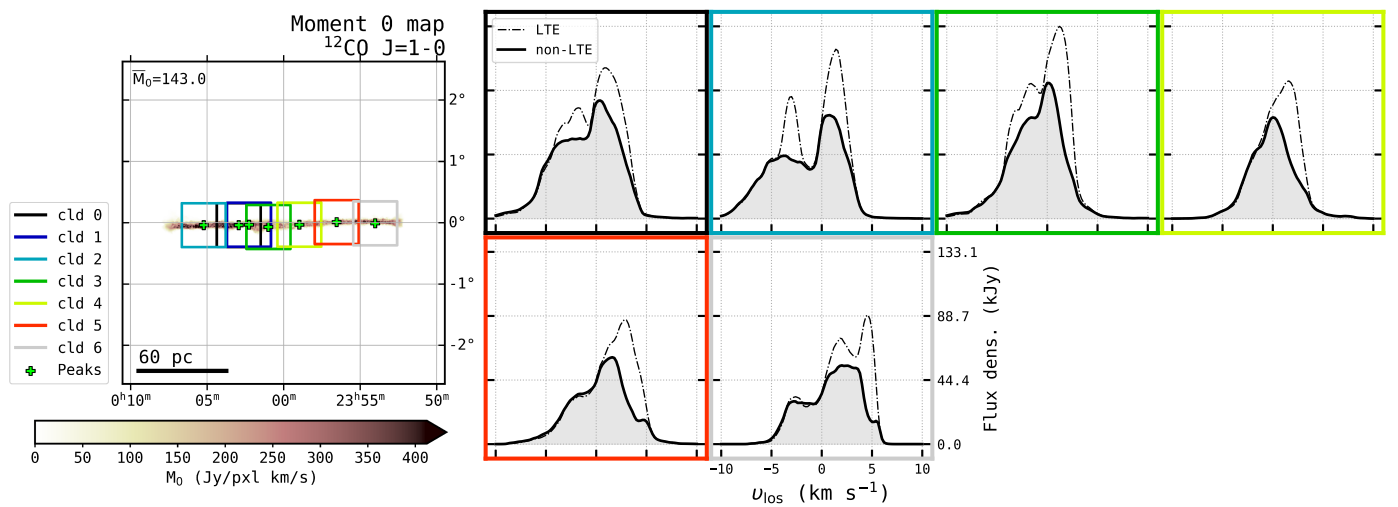


Figure 2.18: (continued) LTE (dashed) and non-LTE (solid) ^{12}CO $J=1-0$ line profiles from non-rejected molecular cloud portions.

Chapter 3

Feedback-dominated → Galaxy Potential, Self-Gravity, Mixed Supernovae

3.1 Cloud C

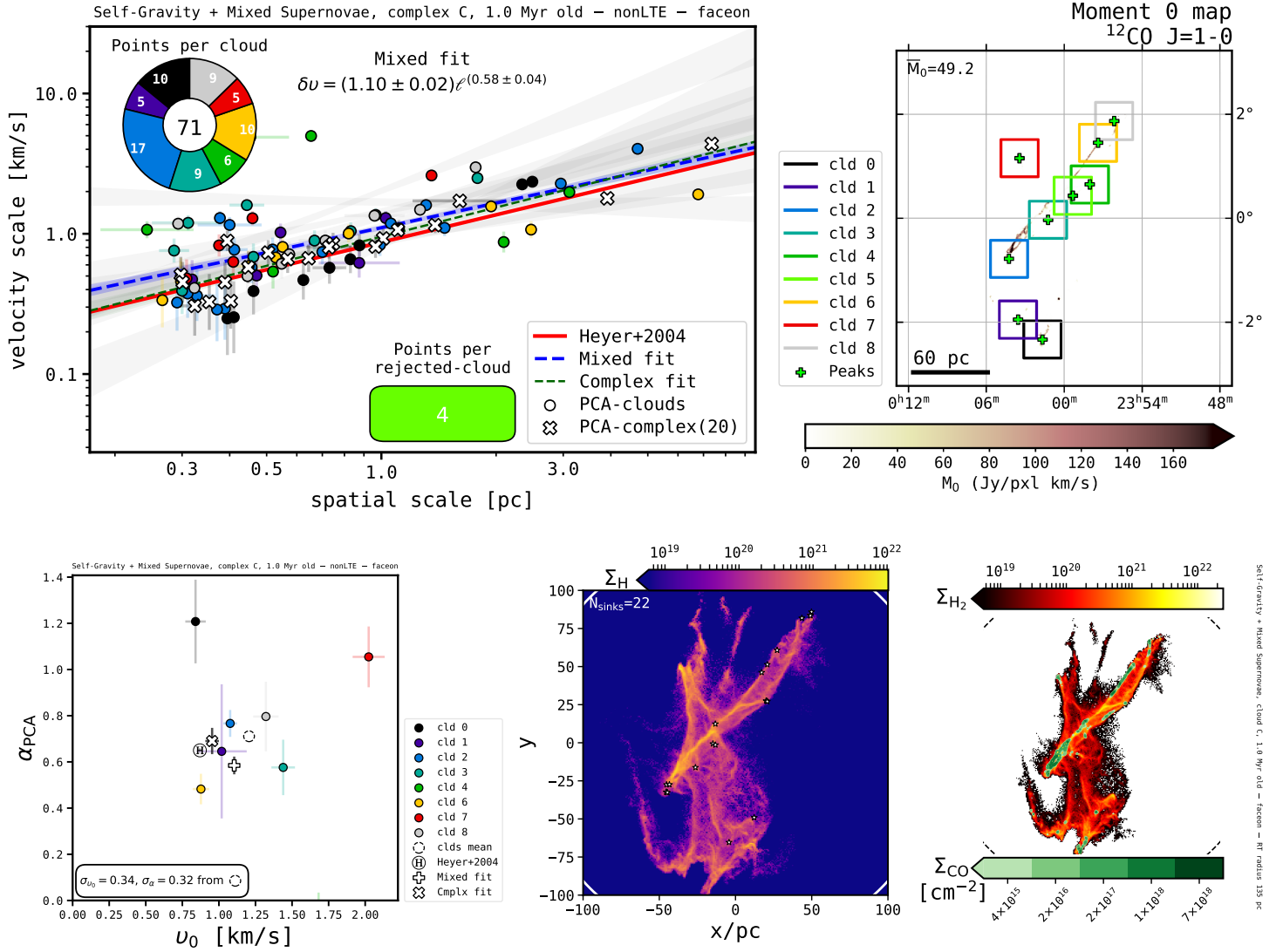


Figure 3.1: Principal component analysis and column densities from Cloud Complex C; physical scenario: Feedback-dominated → Galaxy Potential, Self-Gravity, Mixed Supernovae; snapshot time: 1.0 Myr; orientation: face-on; RT mode: nonLTE. See full captions in figures on the main manuscript.

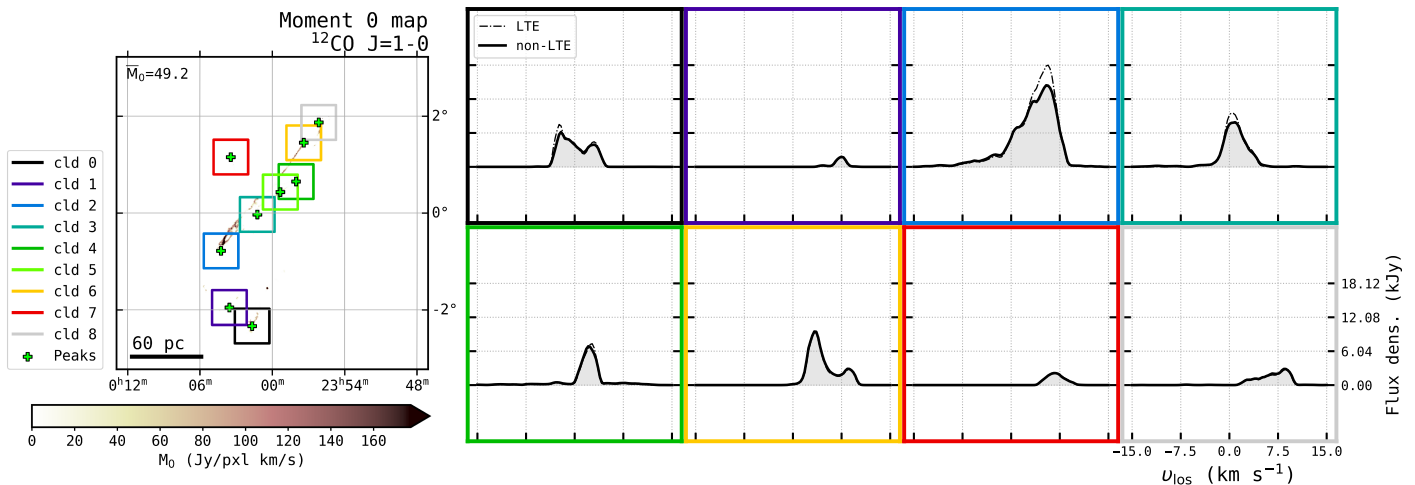


Figure 3.1: (continued) LTE (dashed) and non-LTE (solid) ^{12}CO $J=1-0$ line profiles from non-rejected molecular cloud portions.

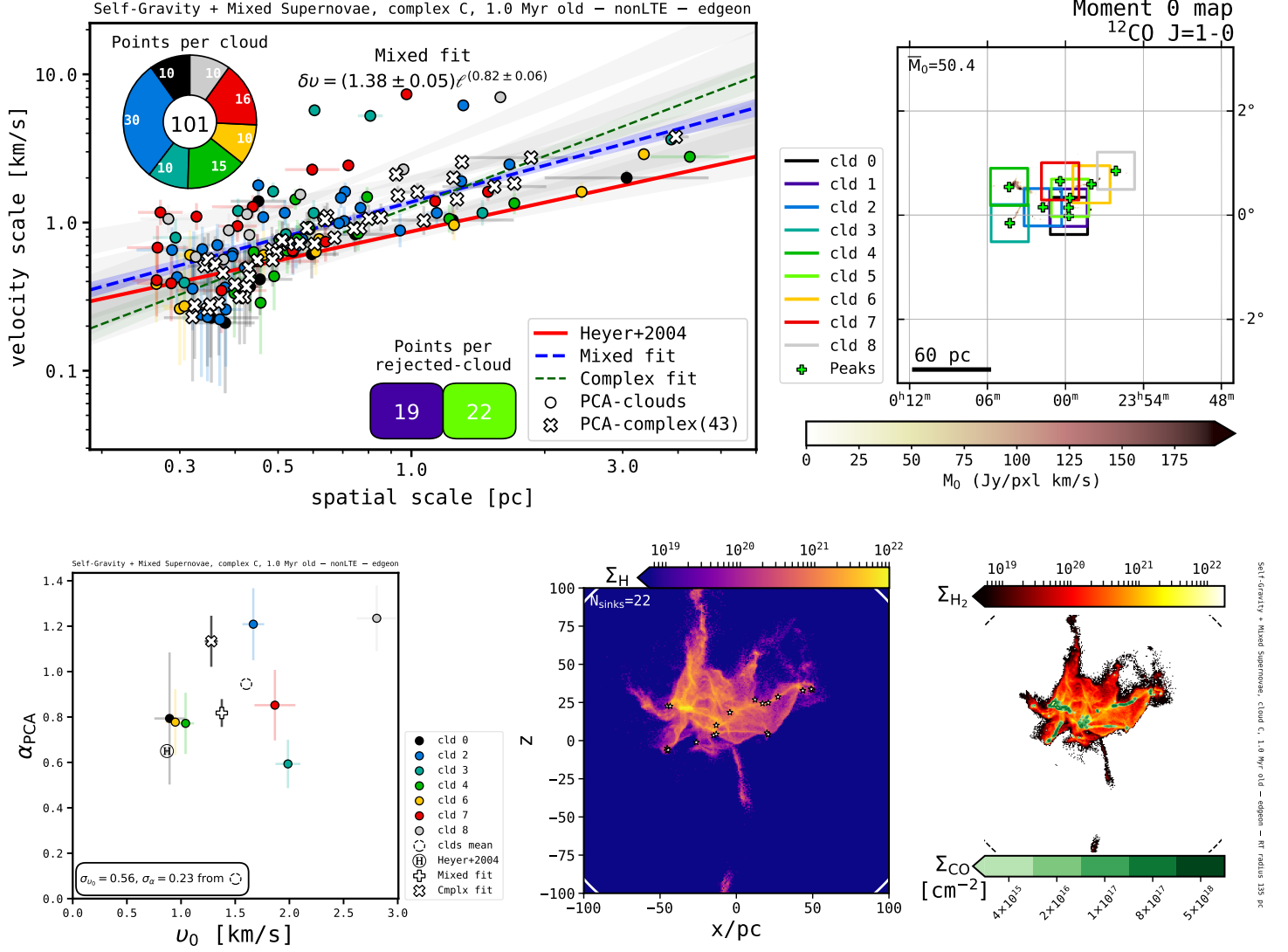


Figure 3.2: Principal component analysis and column densities from Cloud Complex: C; physical scenario: Feedback-dominated \rightarrow Galaxy Potential, Self-Gravity, Mixed Supernovae; snapshot time: 1.0 Myr; orientation: edge-on $\phi=0^\circ$; RT mode: nonLTE. See full captions in figures on the main manuscript.

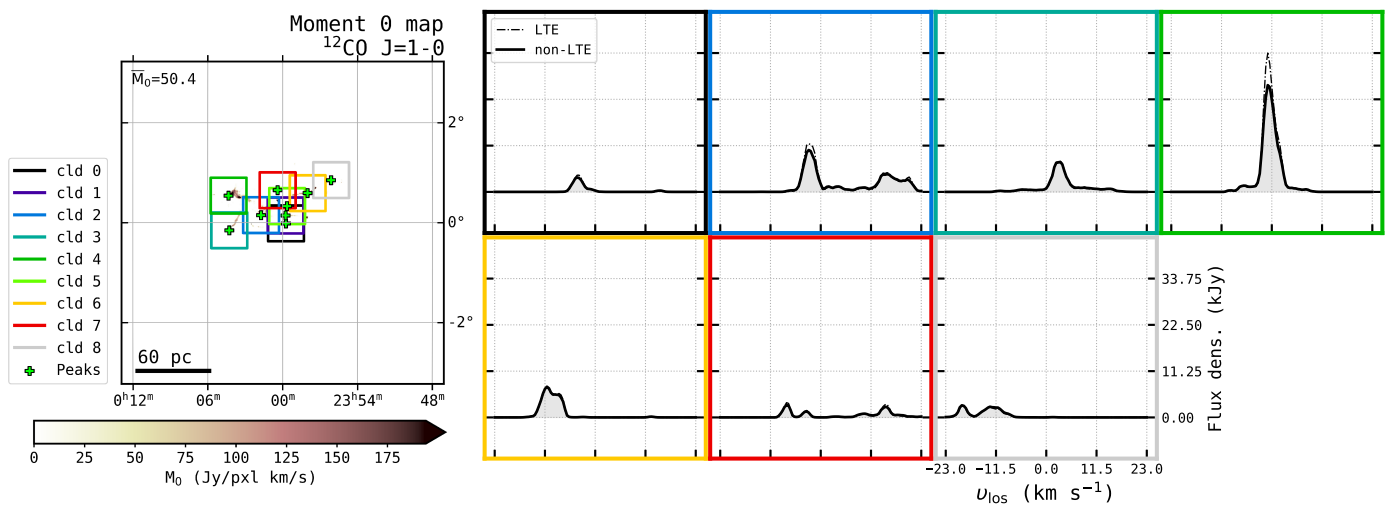


Figure 3.2: (continued) LTE (dashed) and non-LTE (solid) ^{12}CO $J=1-0$ line profiles from non-rejected molecular cloud portions.

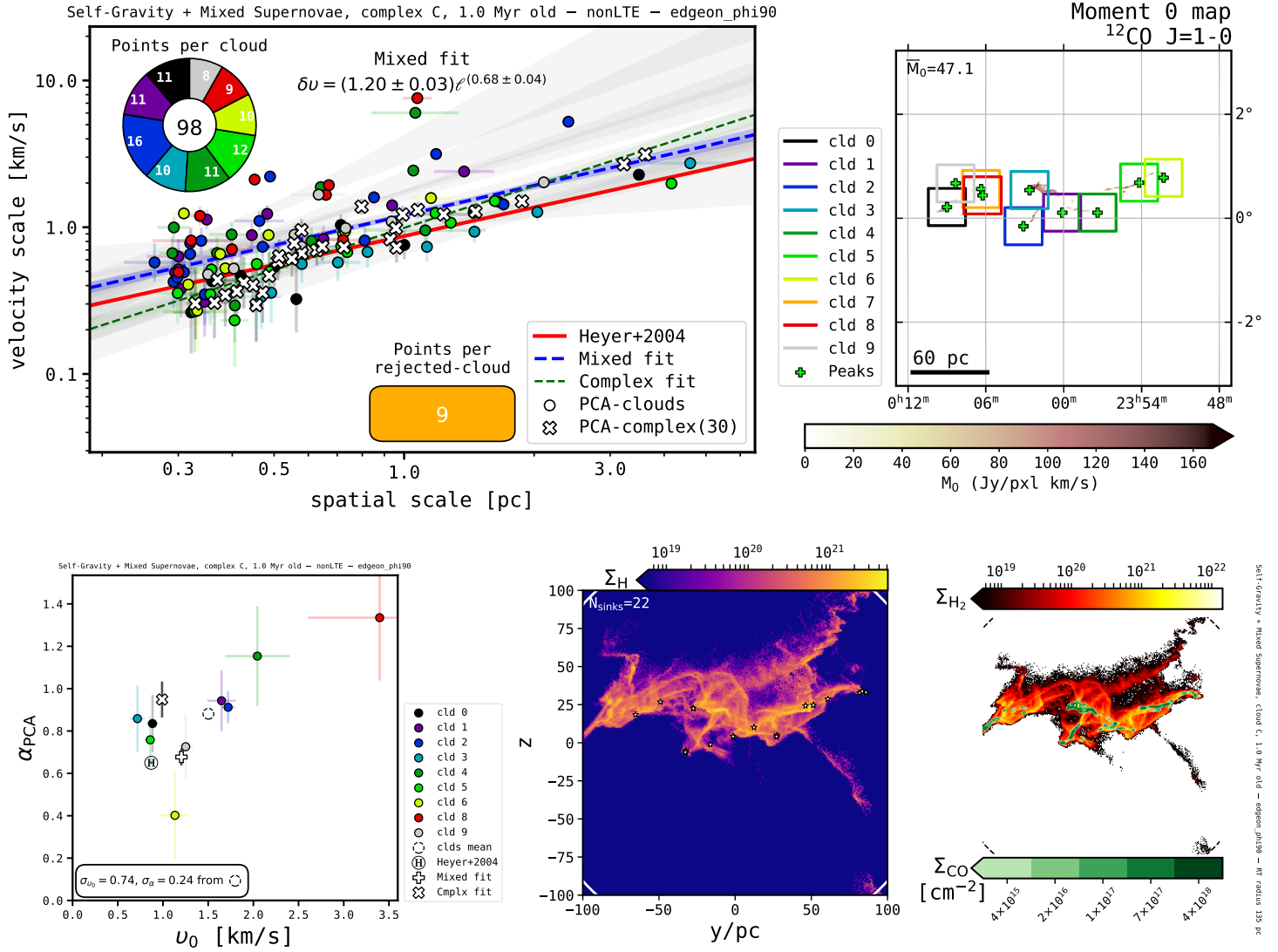


Figure 3.3: Principal component analysis and column densities from Cloud Complex: C; physical scenario: Feedback-dominated \rightarrow Galaxy Potential, Self-Gravity, Mixed Supernovae; snapshot time: 1.0 Myr; orientation: edge-on $\phi=90^\circ$; RT mode: nonLTE. See full captions in figures on the main manuscript.

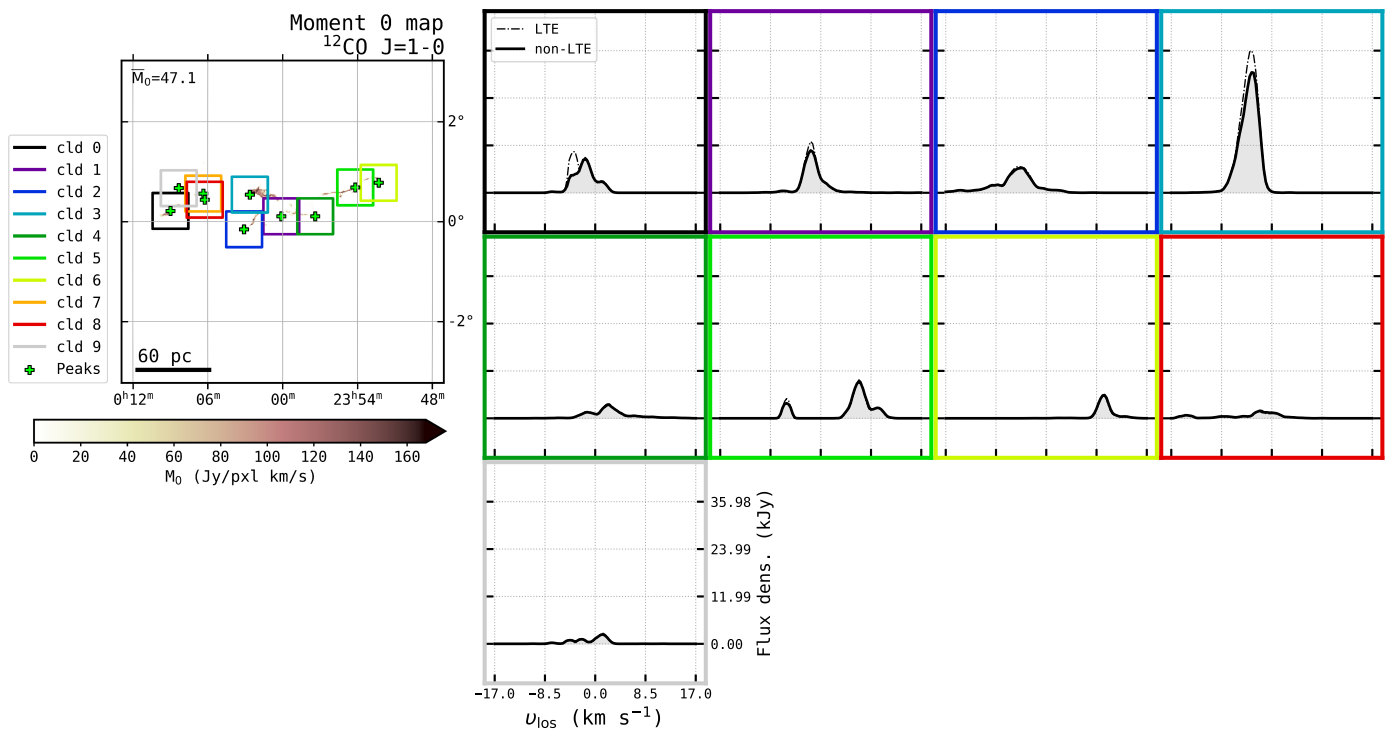


Figure 3.3: (continued) LTE (dashed) and non-LTE (solid) ^{12}CO $J=1-0$ line profiles from non-rejected molecular cloud portions.

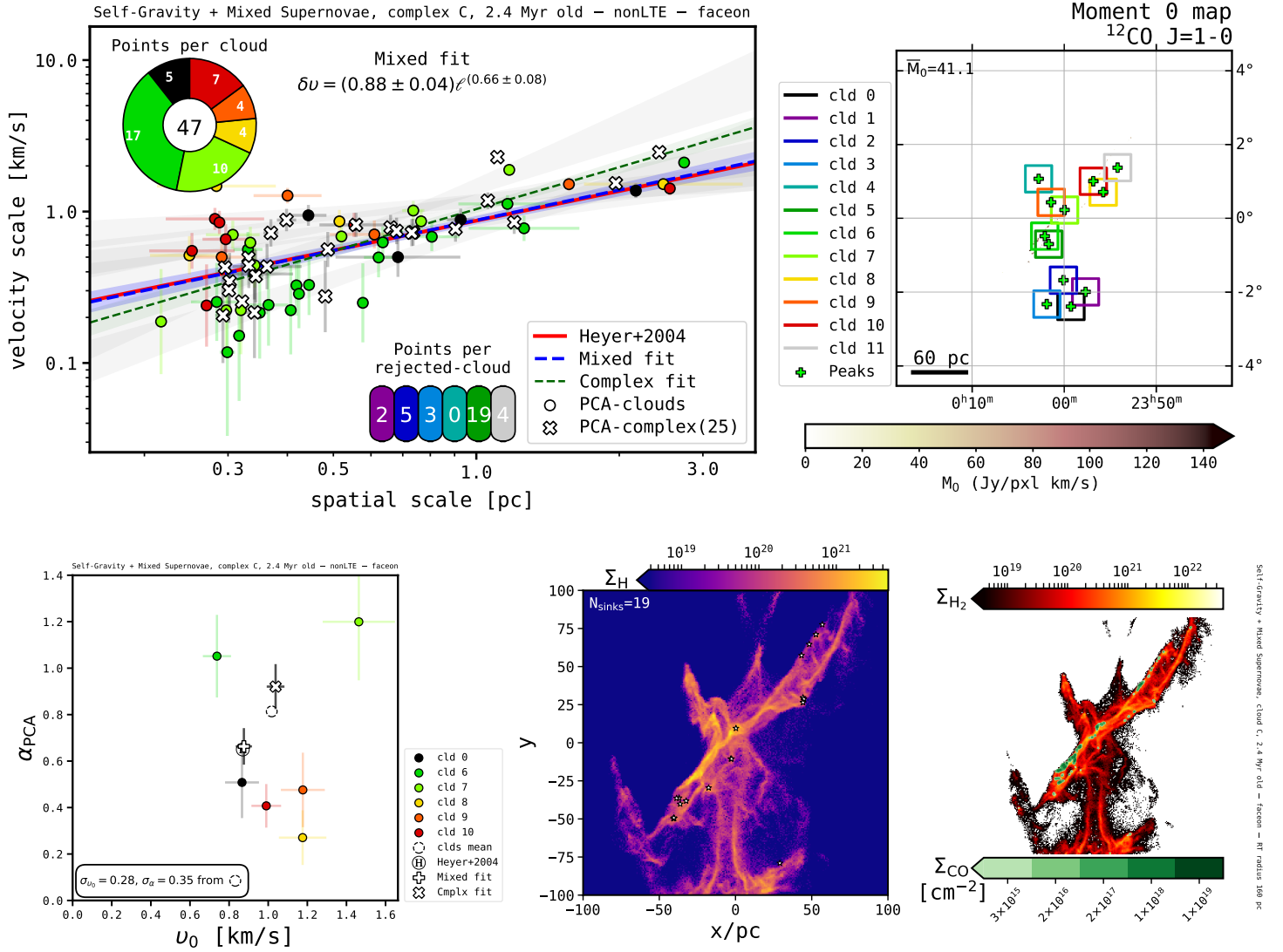


Figure 3.4: Principal component analysis and column densities from Cloud Complex: C; physical scenario: Feedback-dominated \rightarrow Galaxy Potential, Self-Gravity, Mixed Supernovae; snapshot time: 2.4 Myr; orientation: face-on; RT mode: nonLTE. See full captions in figures on the main manuscript.

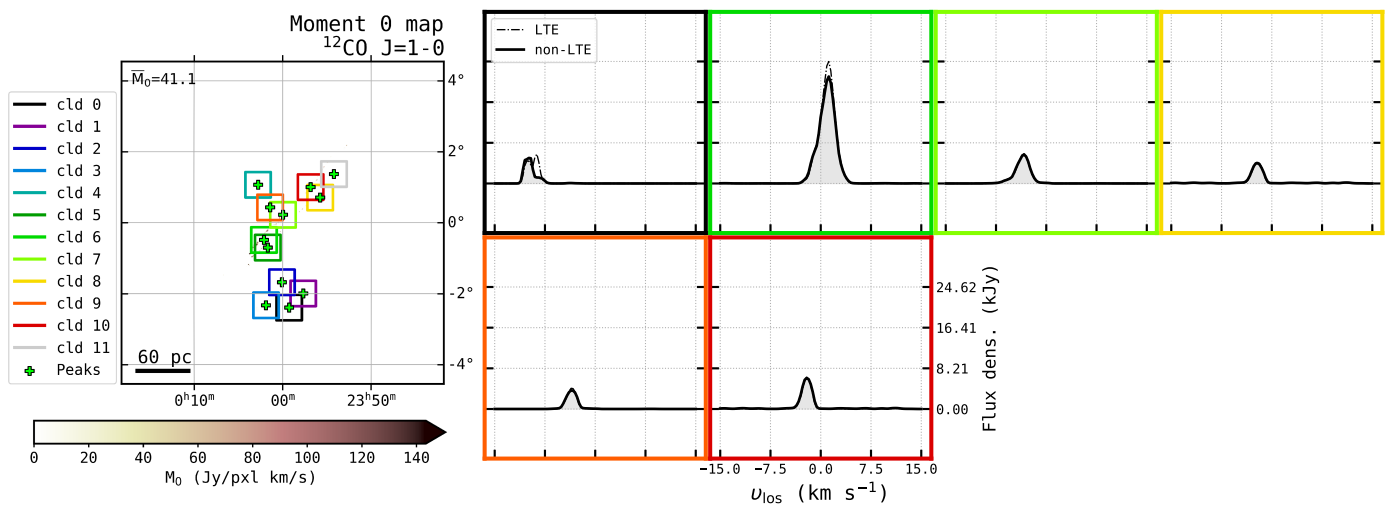


Figure 3.4: (continued) LTE (dashed) and non-LTE (solid) ^{12}CO $J=1-0$ line profiles from non-rejected molecular cloud portions.

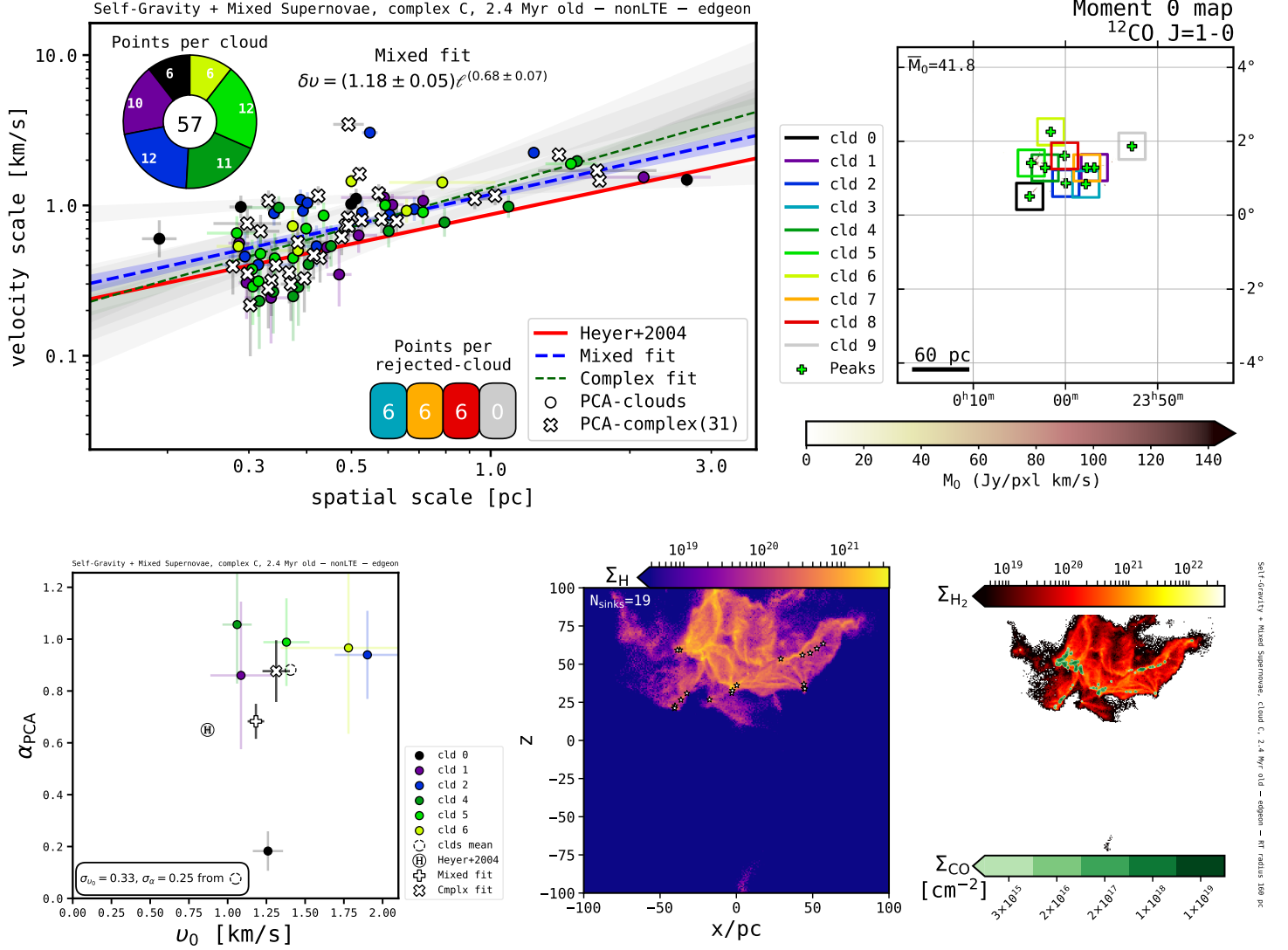


Figure 3.5: Principal component analysis and column densities from Cloud Complex: C; physical scenario: Feedback-dominated \rightarrow Galaxy Potential, Self-Gravity, Mixed Supernovae; snapshot time: 2.4 Myr; orientation: edge-on $\phi=0^\circ$; RT mode: nonLTE. See full captions in figures on the main manuscript.

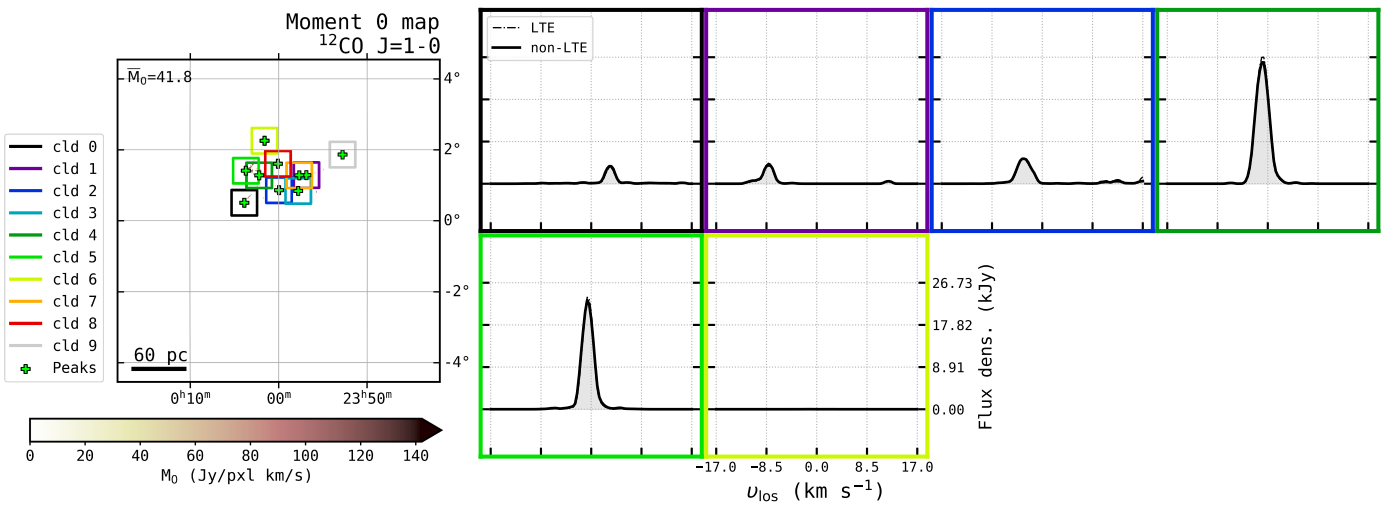


Figure 3.5: (continued) LTE (dashed) and non-LTE (solid) ^{12}CO $J=1-0$ line profiles from non-rejected molecular cloud portions.

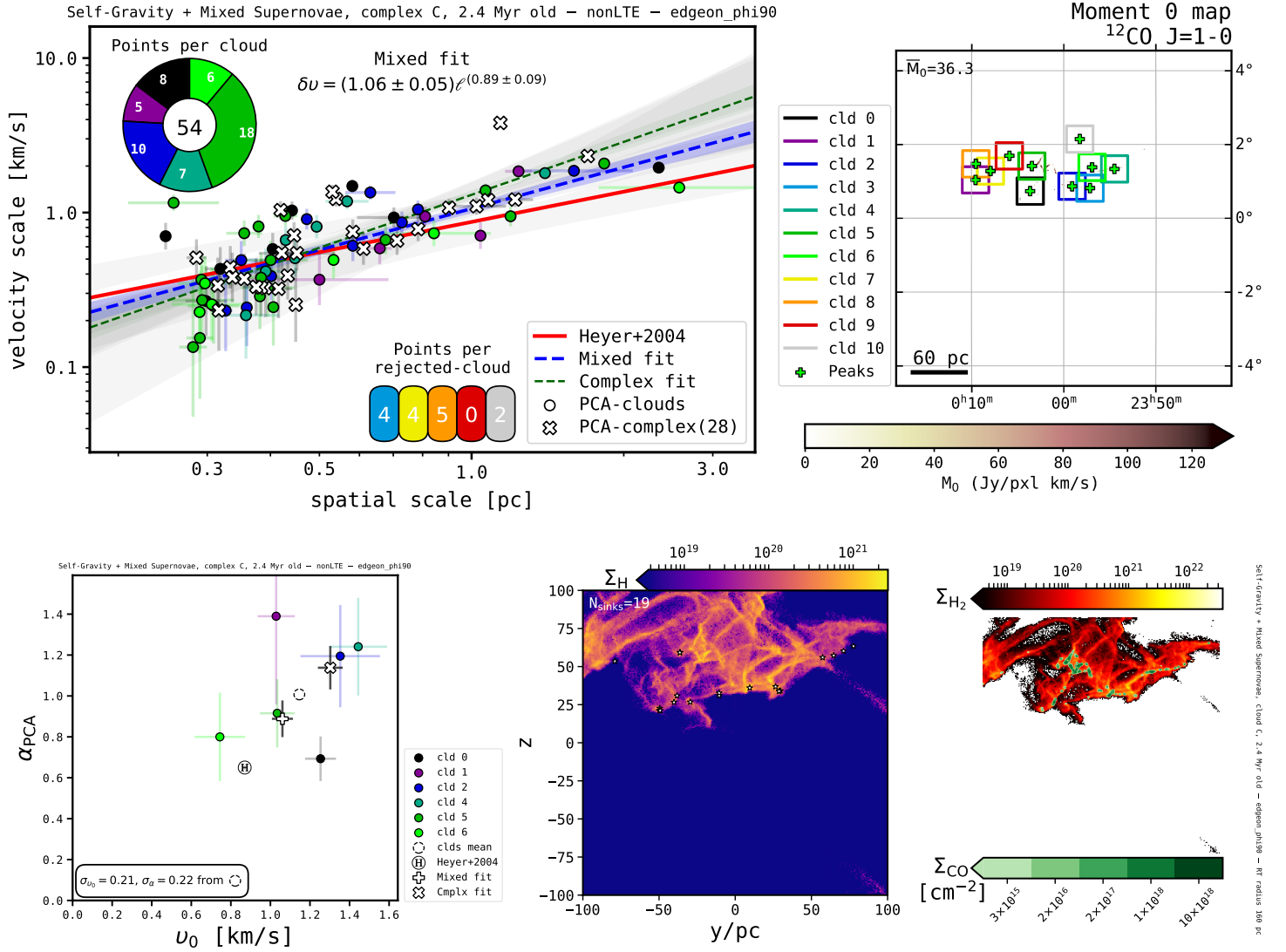


Figure 3.6: Principal component analysis and column densities from Cloud Complex: C; physical scenario: Feedback-dominated \rightarrow Galaxy Potential, Self-Gravity, Mixed Supernovae; snapshot time: 2.4 Myr; orientation: edge-on $\phi=90^\circ$; RT mode: nonLTE. See full captions in figures on the main manuscript.

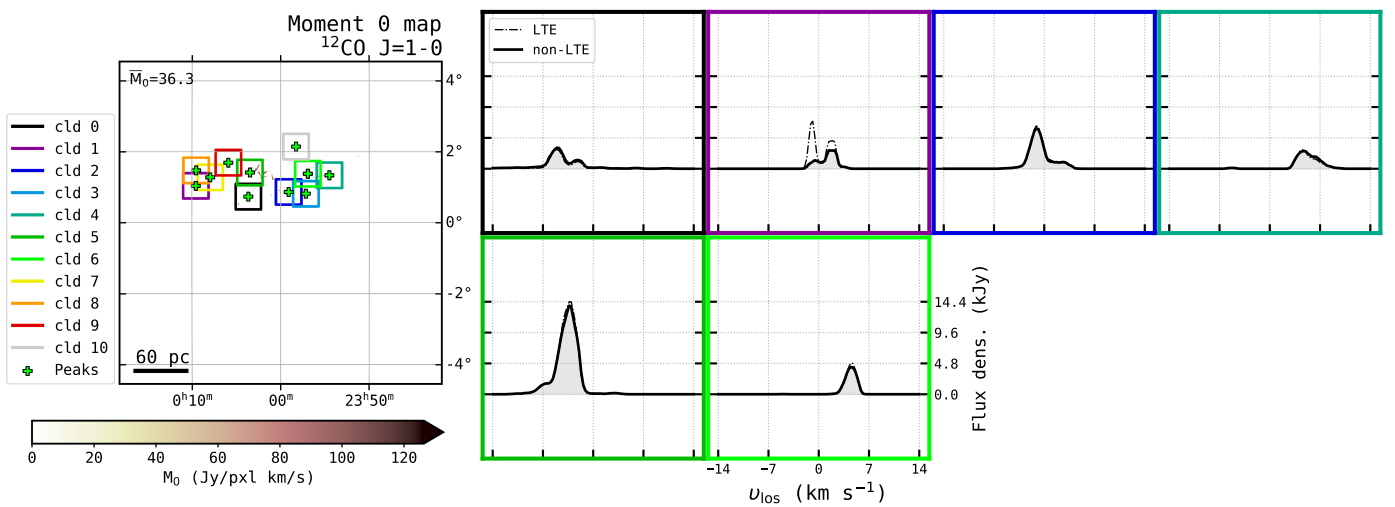


Figure 3.6: (continued) LTE (dashed) and non-LTE (solid) ^{12}CO $J=1-0$ line profiles from non-rejected molecular cloud portions.

3.2 Cloud D

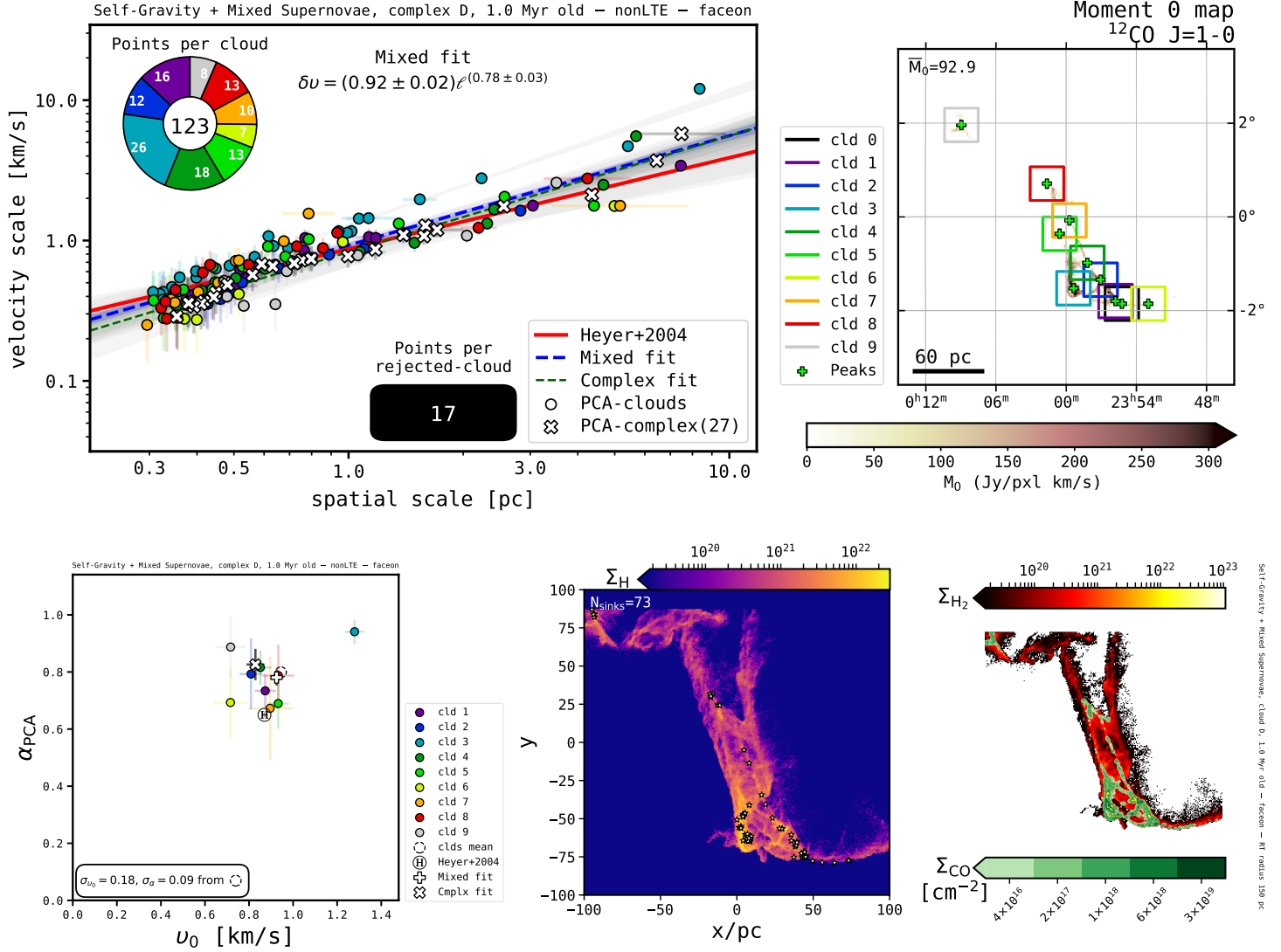


Figure 3.7: Principal component analysis and column densities from Cloud Complex D; physical scenario: Feedback-dominated → Galaxy Potential, Self-Gravity, Mixed Supernovae; snapshot time: 1.0 Myr; orientation: face-on; RT mode: nonLTE. See full captions in figures on the main manuscript.

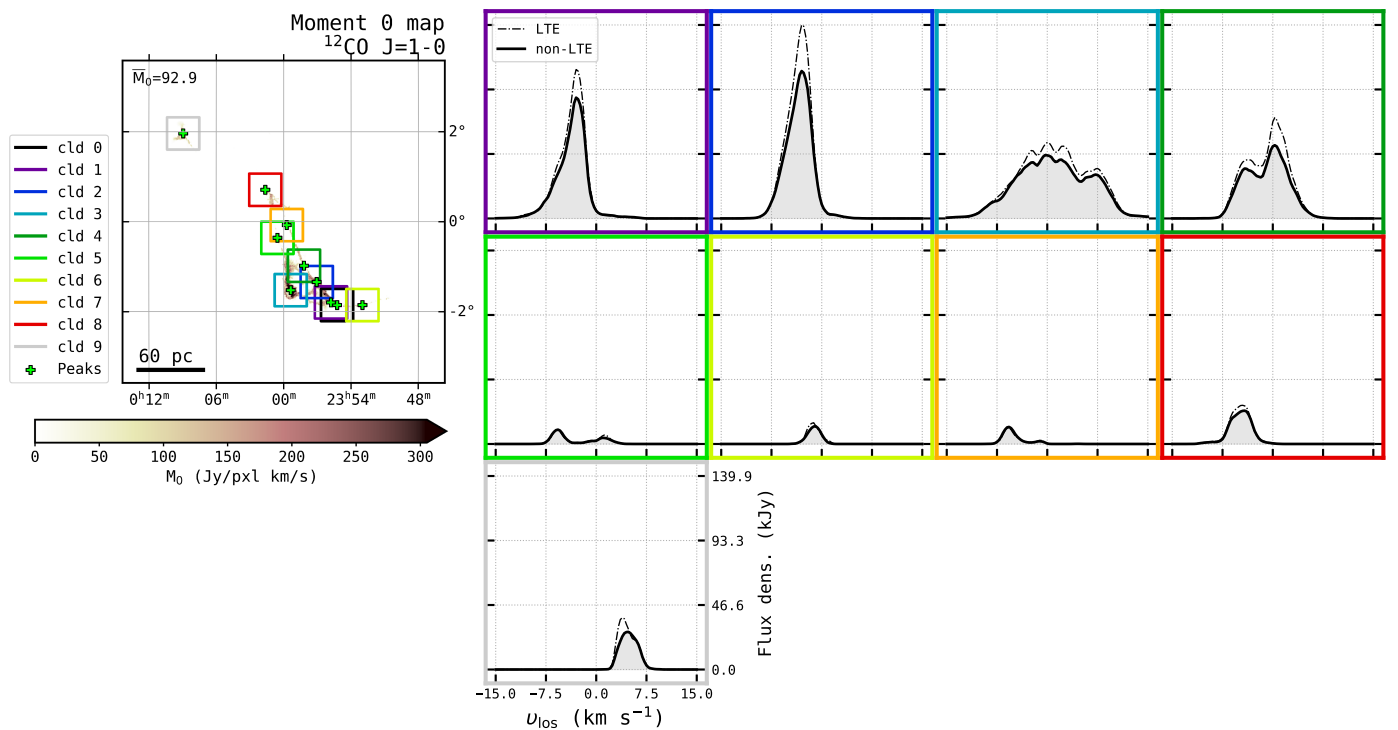


Figure 3.7: (continued) LTE (dashed) and non-LTE (solid) ^{12}CO $J=1-0$ line profiles from non-rejected molecular cloud portions.

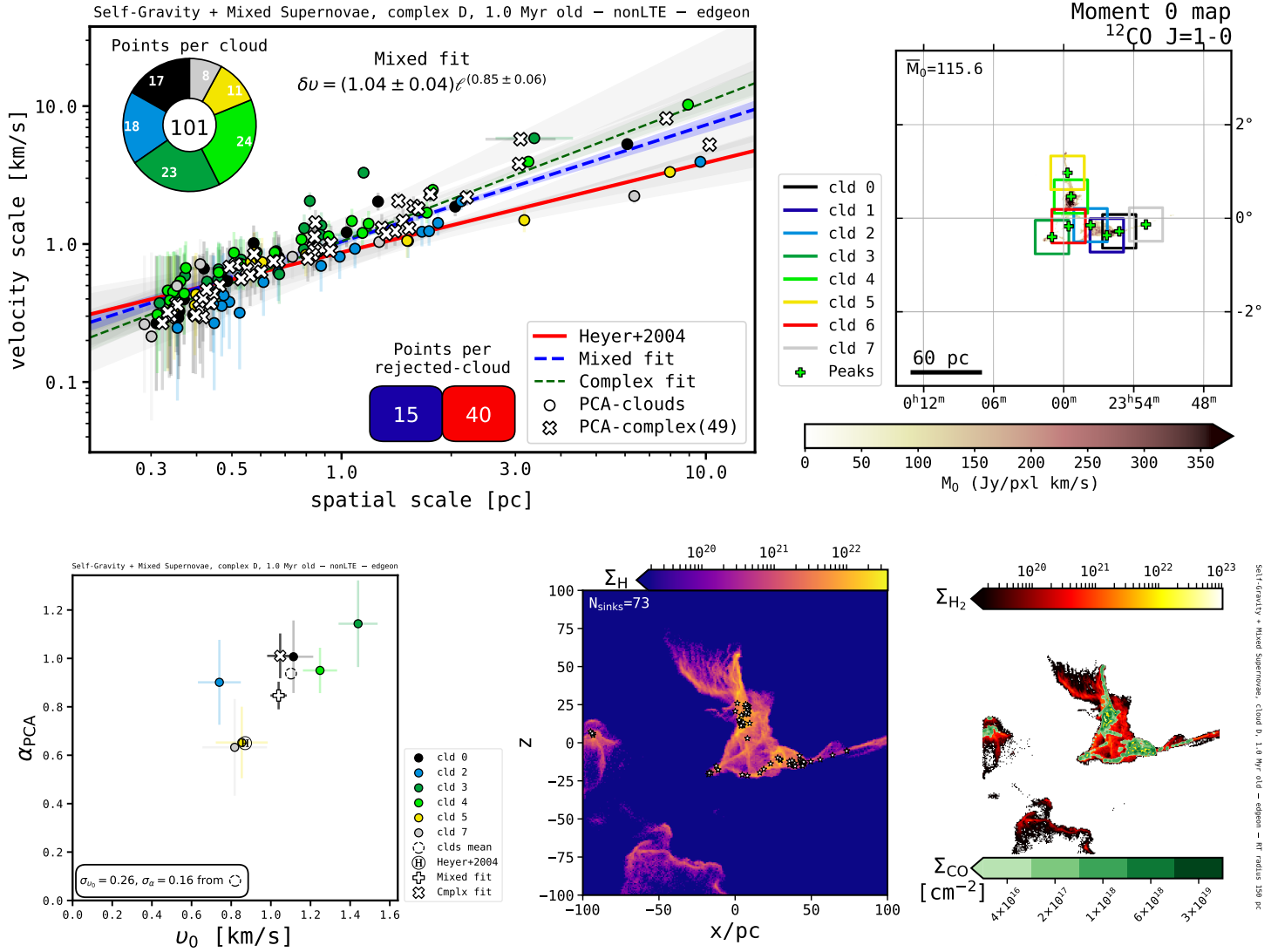


Figure 3.8: Principal component analysis and column densities from Cloud Complex: D; physical scenario: Feedback-dominated → Galaxy Potential, Self-Gravity, Mixed Supernovae; snapshot time: 1.0 Myr; orientation: edge-on $\phi=0^\circ$; RT mode: nonLTE. See full captions in figures on the main manuscript.

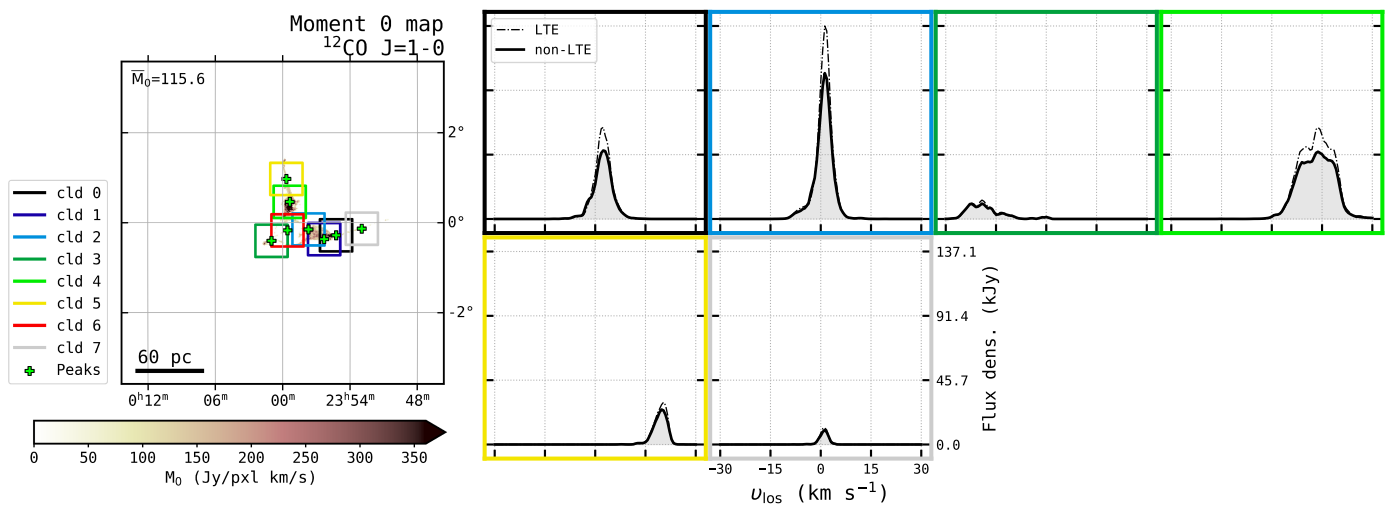


Figure 3.8: (continued) LTE (dashed) and non-LTE (solid) ^{12}CO $J=1-0$ line profiles from non-rejected molecular cloud portions.

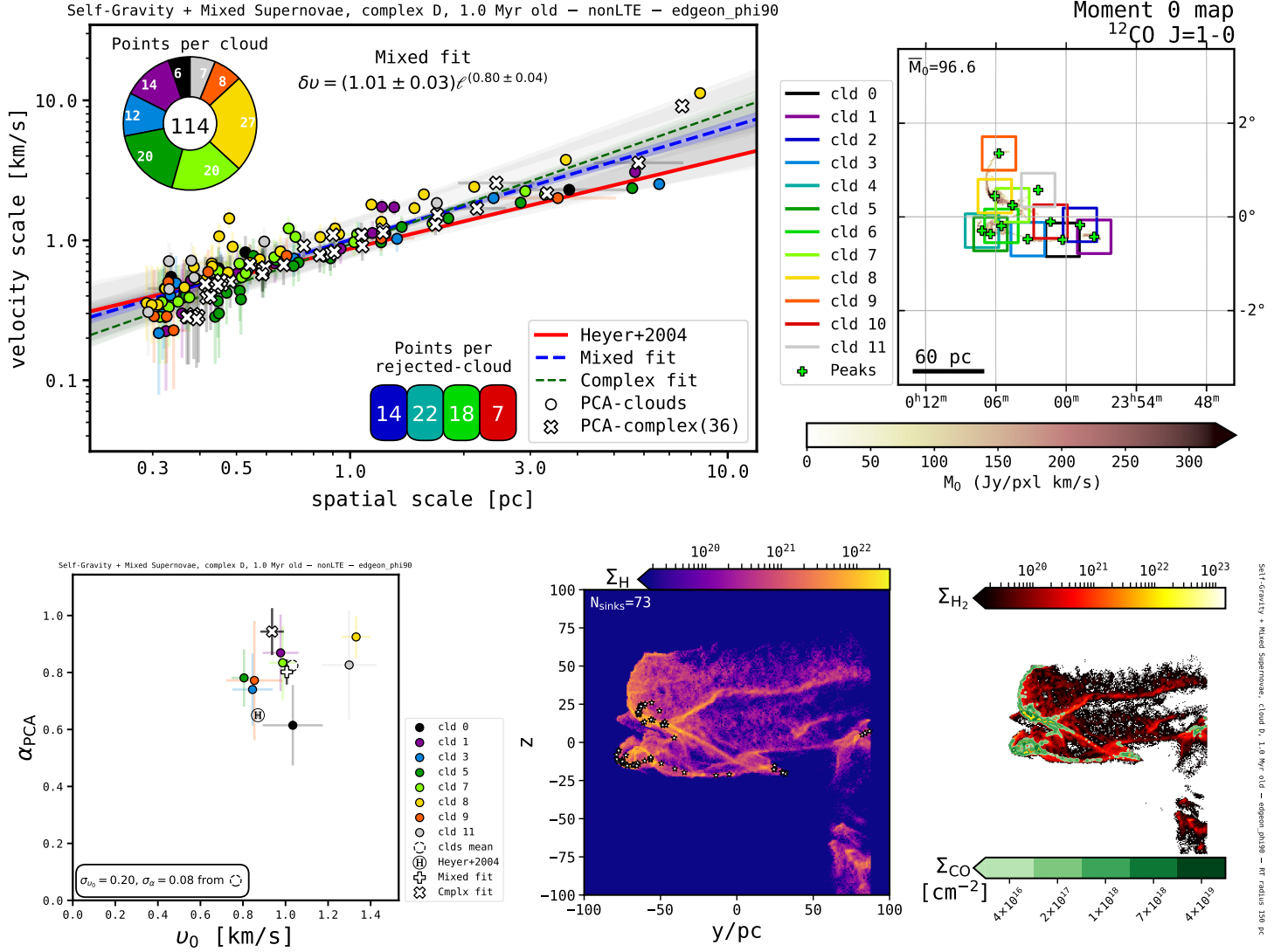


Figure 3.9: Principal component analysis and column densities from Cloud Complex D; physical scenario: Feedback-dominated → Galaxy Potential, Self-Gravity, Mixed Supernovae; snapshot time: 1.0 Myr; orientation: edge-on $_{\phi=90^\circ}$; RT mode: nonLTE. See full captions in figures on the main manuscript.

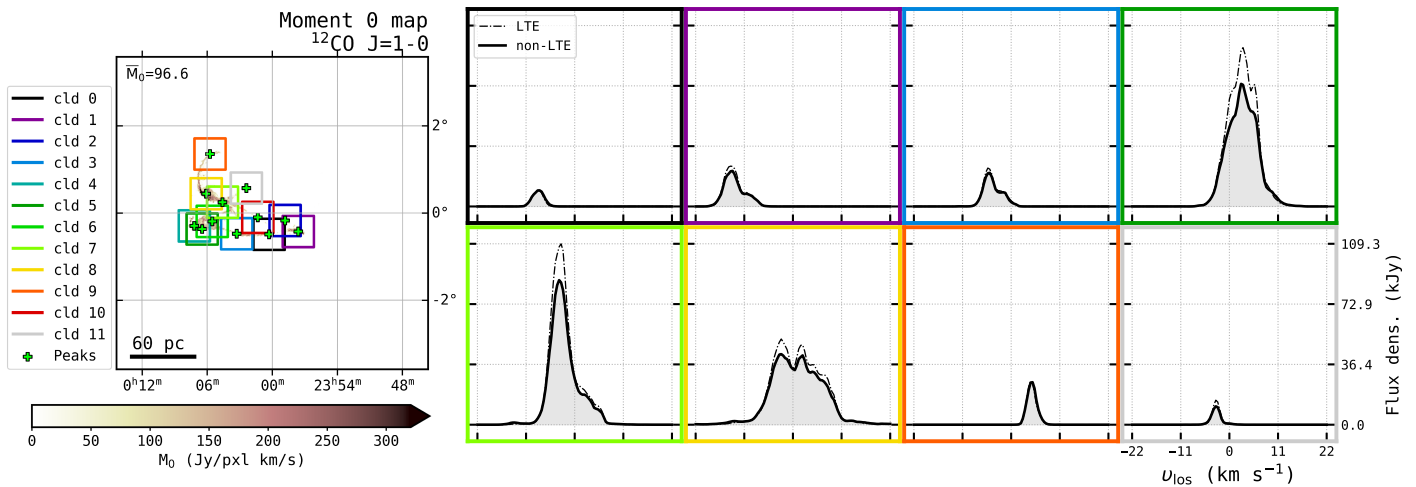


Figure 3.9: (continued) LTE (dashed) and non-LTE (solid) ^{12}CO $J=1-0$ line profiles from non-rejected molecular cloud portions.

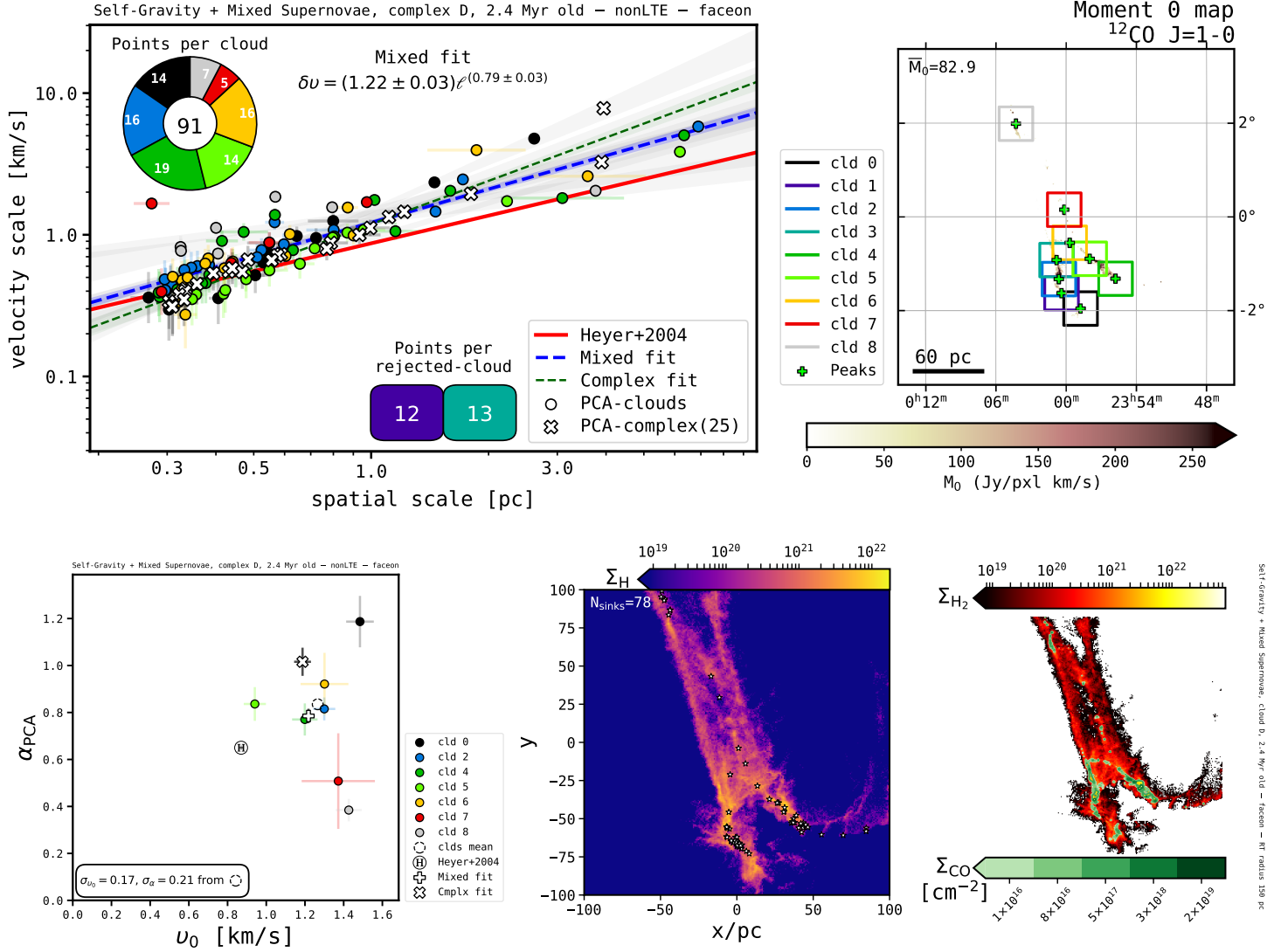


Figure 3.10: Principal component analysis and column densities from Cloud Complex: D; physical scenario: Feedback-dominated → Galaxy Potential, Self-Gravity, Mixed Supernovae; snapshot time: 2.4 Myr; orientation: face-on; RT mode: nonLTE. See full captions in figures on the main manuscript.

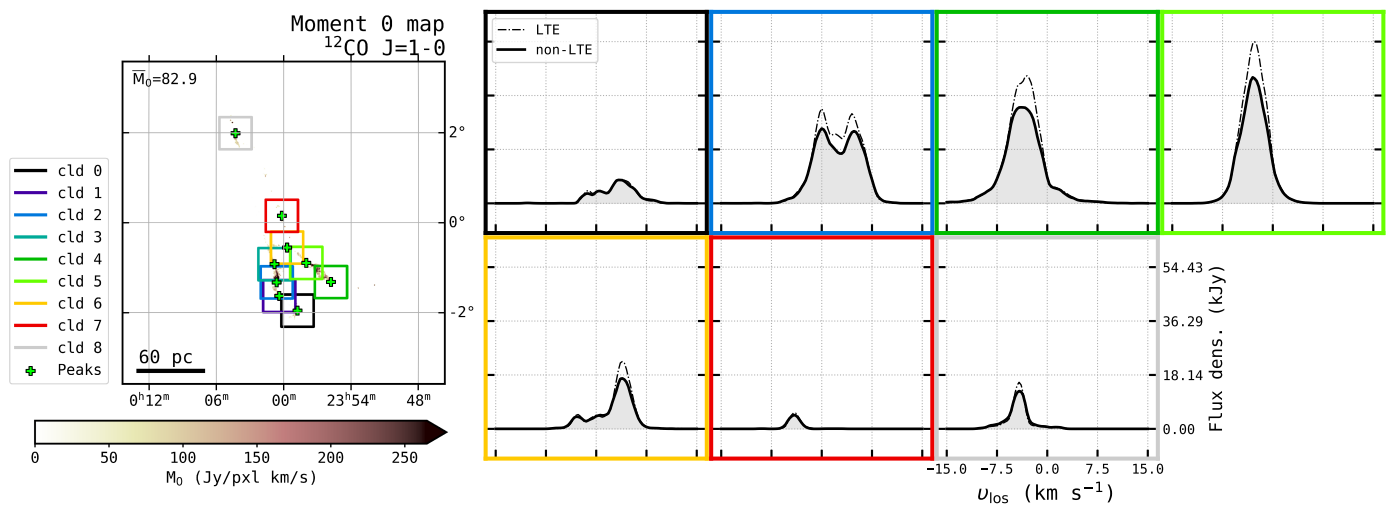


Figure 3.10: (continued) LTE (dashed) and non-LTE (solid) ^{12}CO $J=1-0$ line profiles from non-rejected molecular cloud portions.

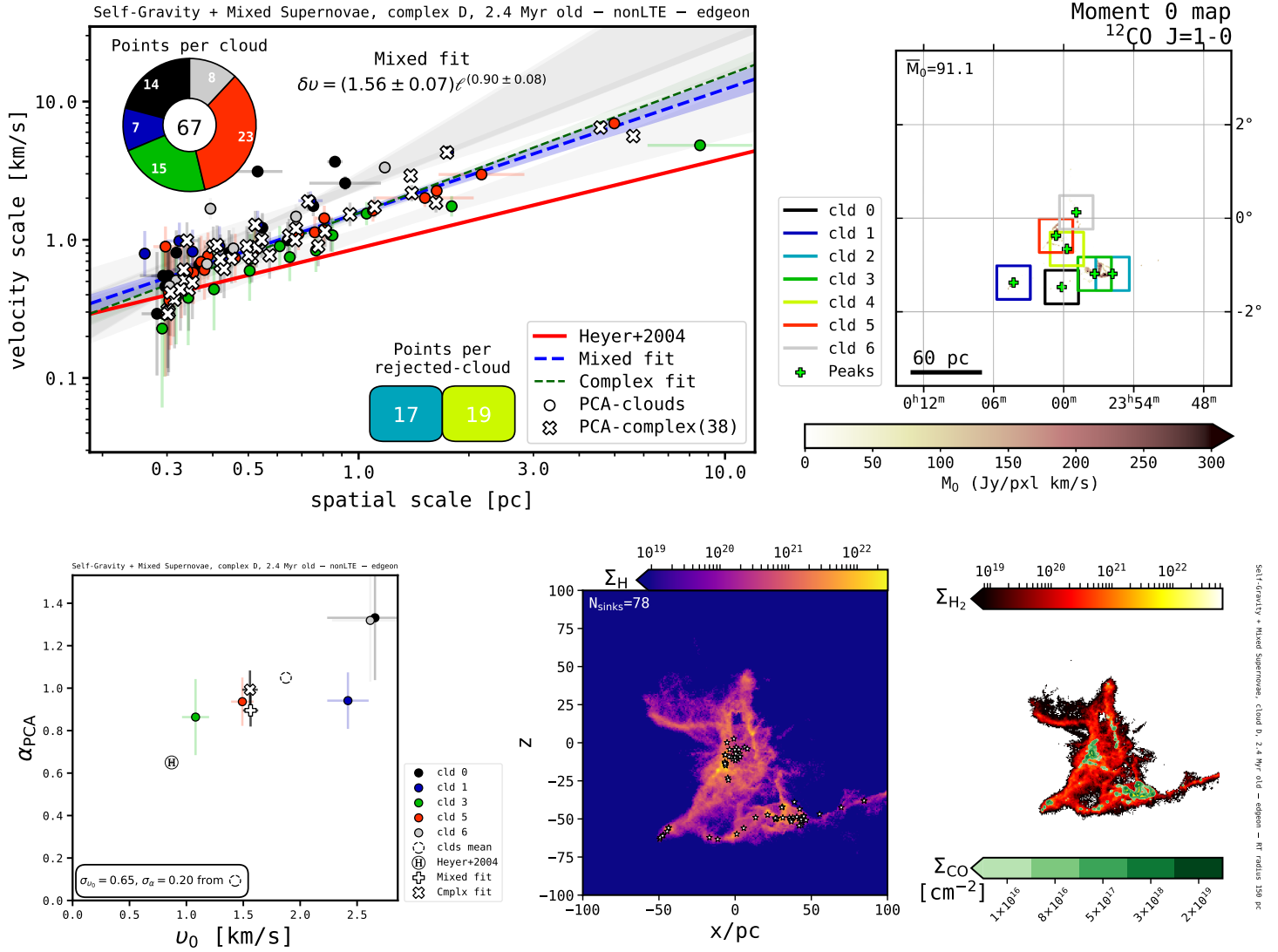


Figure 3.11: Principal component analysis and column densities from Cloud Complex: D; physical scenario: Feedback-dominated → Galaxy Potential, Self-Gravity, Mixed Supernovae; snapshot time: 2.4 Myr; orientation: edge-on $_{\phi=0^\circ}$; RT mode: nonLTE. See full captions in figures on the main manuscript.

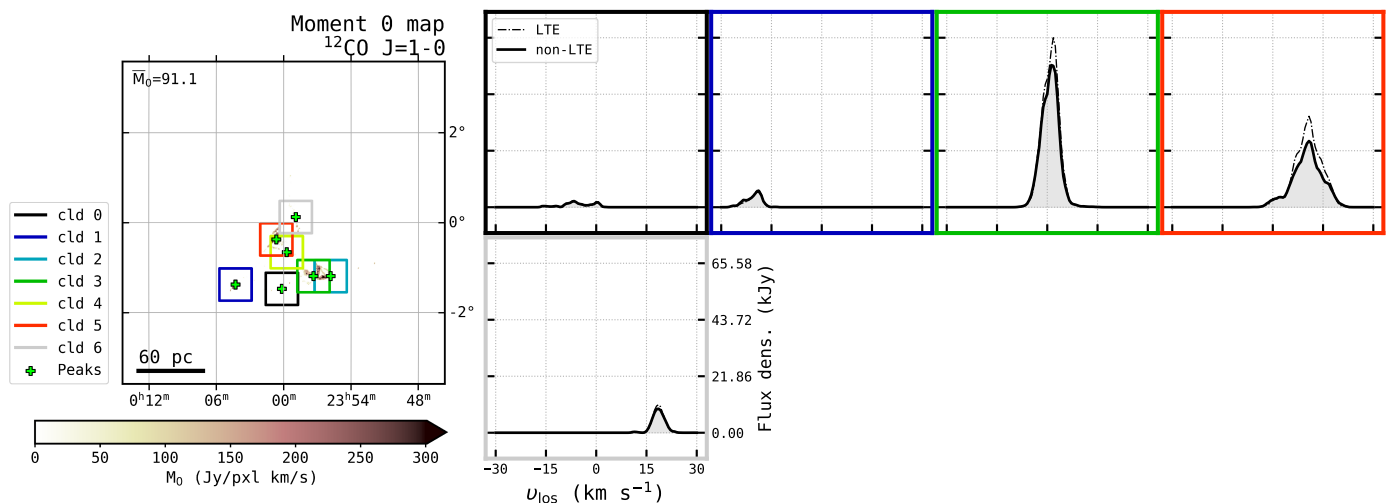


Figure 3.11: (continued) LTE (dashed) and non-LTE (solid) ^{12}CO $J=1-0$ line profiles from non-rejected molecular cloud portions.

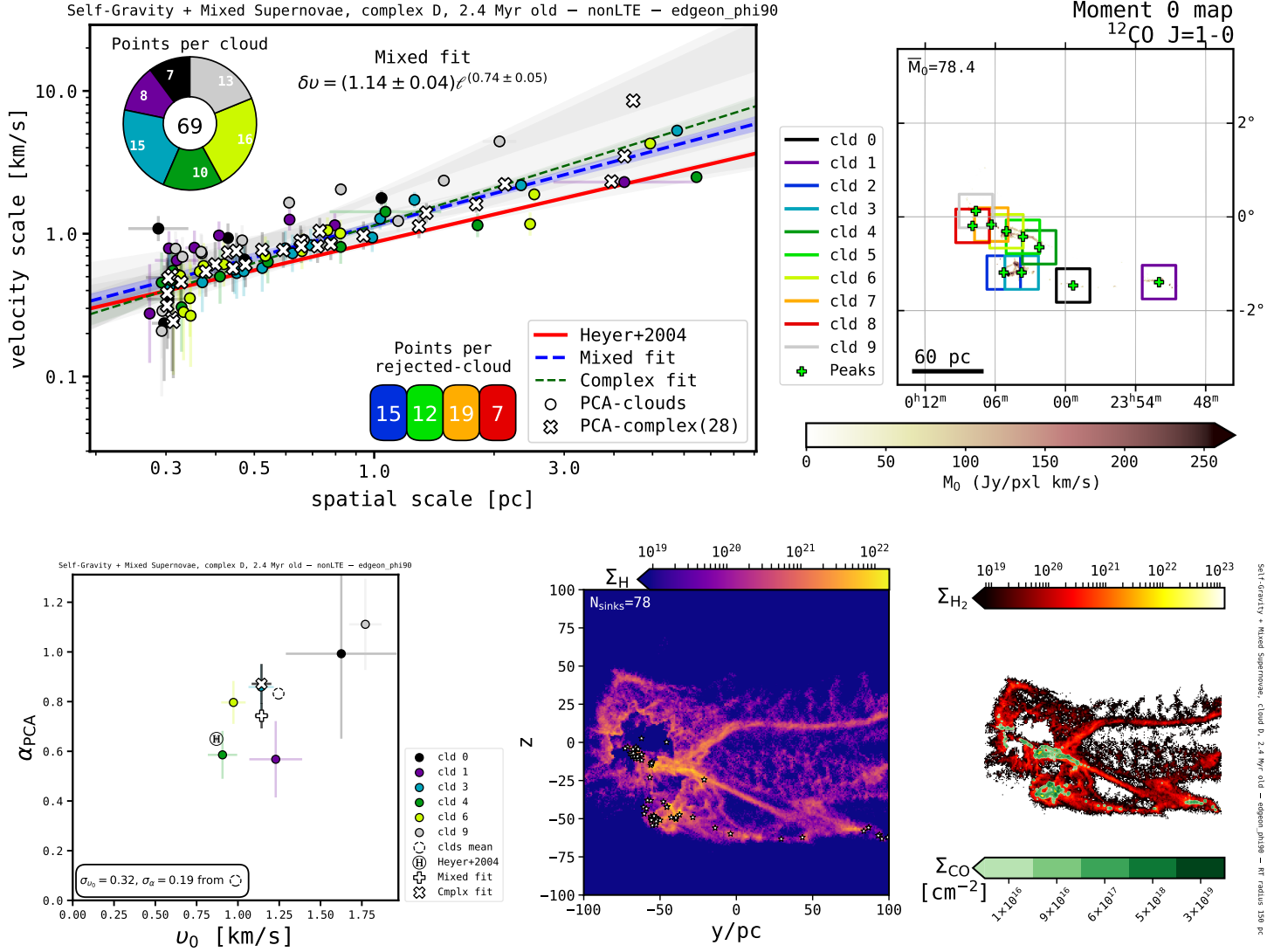


Figure 3.12: Principal component analysis and column densities from Cloud Complex: D; physical scenario: Feedback-dominated → Galaxy Potential, Self-Gravity, Mixed Supernovae; snapshot time: 2.4 Myr; orientation: edge-on $_{\phi=90^\circ}$; RT mode: nonLTE. See full captions in figures on the main manuscript.

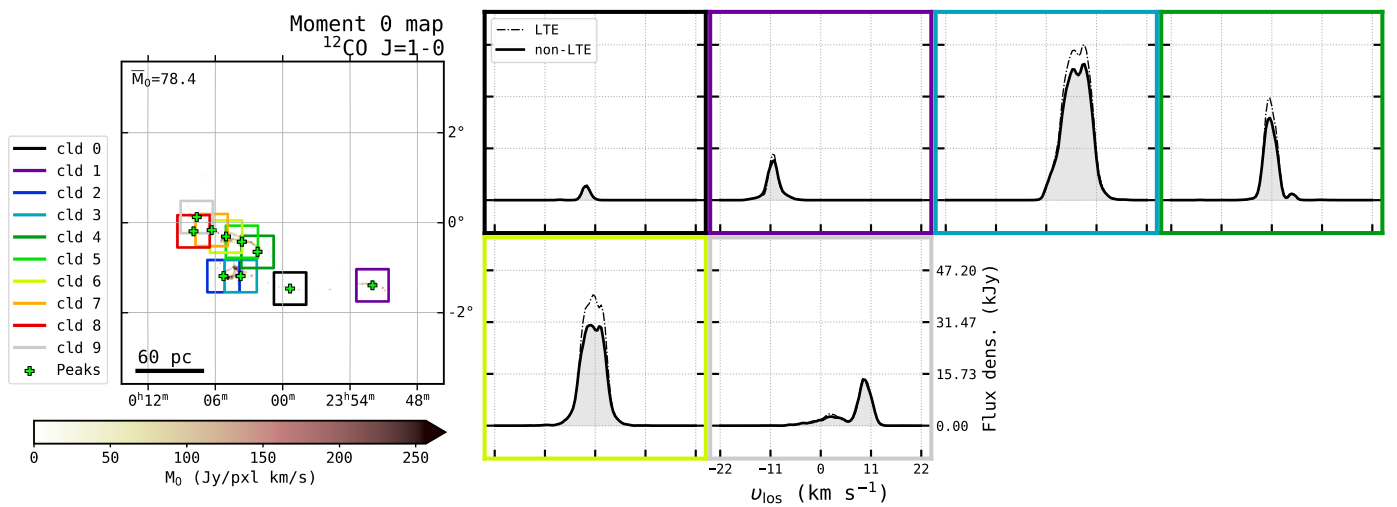


Figure 3.12: (continued) LTE (dashed) and non-LTE (solid) ^{12}CO $J=1-0$ line profiles from non-rejected molecular cloud portions.